UNIVERSITY OF CAMBRIDGE

Innate Sensing and Regulation During Enteric Caliciviruses Infections

by

Aminu Suleiman Jahun

Hughes Hall

This dissertation is submitted for the degree of

Doctor of Philosophy

January 2019

Division of Virology, Department of Pathology, University of Cambridge,

Addenbrooke's Hospital, Hills Road, Cambridge.

Declaration

This dissertation is the result of my own work and includes nothing which is the outcome of work done in collaboration except as declared in the Preface and specified in the text. It is not substantially the same as any that I have submitted, or, is being concurrently submitted for a degree or diploma or other qualification at the University of Cambridge or any other University or similar institution except as declared in the Preface and specified in the text. I further state that no substantial part of my dissertation has already been submitted, or, is being concurrently submitted for any such degree, diploma or other qualification at the University of Cambridge or any other University or similar institution except as declared in the Preface and specified in the text. It does not exceed the prescribed word limit for the relevant Degree Committee.

Title: Innate Sensing and Regulation During Enteric Caliciviruses Infections

Name: Aminu Suleiman Jahun

Abstract

Several decades after the discovery of the human norovirus, with thousands of lives and billions of dollars lost, the lack of a robust cell culture system still severely hampers development of vaccines and therapeutics. This is likely in large part as a result of our limited understanding of the immune responses against an infection with the virus. Here, the presence of a RIG-I/STING-dependent innate response pathway that restricts the replication of noroviruses is described, and an attempt by the murine norovirus to subvert it through expression of an accessory protein is demonstrated. We show that both RIG-I and STING are required for a robust interferon response to infection with MNV1 in primary BMDMs and RAW264.7 cells, with a significant increase in viral titres following infection in RIG-I- and STING-deficient cells. We also show that STING is non-canonically activated in MNV1-infected cells partly in a RIG-I dependent manner. Furthermore, our data indicate that the MNV VF1 protein binds to STING and can inhibit interferon induction downstream of RIG-I. Secondly, while exploring the mechanisms for the differential induction of interferon sub-types, we show that depletion of MED23 leads to a reduction in expression of both types I and III IFNs in human and mouse cell lines. We also show that *Med23* knockout cells undergo genetic compensation, suggesting a critical role for MED23 in this pathway. Mechanistically, we show that MED23 interacts with IRF3, and is required for recruitment of RNA Polymerase II to promoters of IRF3-dependent genes. Taken together, our data indicate that MED23 plays a central role in antiviral responses by coupling IRF3 activation and RNA Pol II recruitment.

Acknowledgements

I would like to extend my profound gratitude to my supervisor, Professor Ian Goodfellow, for guiding me throughout this arduous PhD journey, for all his help within and outside of the lab, and for tolerating my many eccentricities – I could not ask for a better mentor. I would also like to thank Dr Frederic Sorgeloos, for being an amazing guide and a good friend. He was a critical filter for my many bad ideas, for which I am truly grateful.

I would also like to extend my heartfelt appreciation to my mother, for always being there, for offering help even when I did not know I need it, and for being an amazing mother overall. Many thanks to my awesome family, especially Malam, Mamun, Zainab, Rahila, Umar, Abba, Badariyya, Aisha, Yaya Mama, Fatima, and my niece Amal. And last but not the least, I wish to express my sincere appreciation to all past and present members of the Goodfellow Lab, and the Division of Virology.

Table of contents

List of Figures

List of Tables

Abbreviations used

AIM2	-	Absent in melanoma 2
AP-1	-	Activator protein 1
BHK	-	Baby hamster kidney
BMDCs	-	Bone marrow-derived dendritic cells
BMDMs	-	Bone marrow-derived macrophages
CARD	-	Caspase activation and recruitment domain
CARDIF	-	Card adaptor inducing interferon-β
cGAMP	-	Cyclic guanosine monophosphate–adenosine monophosphate
cGAS	-	cGAMP synthase
Cyto-MAVS	-	Cytosolic MAVS
DAI	-	DNA-dependent activator of interferon
DMEM	-	Dulbecco's modified eagle medium
DNA-PK	-	DNA-dependent protein kinase
EMCV	-	Encephalomyocarditis virus
FCV	-	Feline calicivirus
GAS	-	Interferon-gamma-activated sequence
hAst	-	Human astrovirus
HEK	-	Human embryonic kidney
HOIL1	-	Heme-oxidized IRP2 ubiquitin ligase 1
HPV	-	Human papilloma virus

HRV	-	Human rhinovirus
IAV	-	Influenza A virus
IFIT	-	Interferon-induced protein with tetratricopeptide repeats
IFN	-	Interferon
IFNAR	-	Type I interferon receptor
IFNGR	-	Interferon-γ receptor
IFNLR	-	Interferon-λ receptor
IKK	-	Inhibitor of nuclear factor kappa-B kinase
IPS-1	-	Interferon-β promoter stimulator 1
IRF	-	Interferon regulatory factor
ISG	-	Interferon-stimulated gene
ISGF3	-	Interferon-stimulated genes factor 3
ISRE	-	Interferon-stimulated response elements
JAK	-	Janus kinase
LGP2	-	Laboratory of genetics and physiology 2
LPS	-	Lipopolysaccharide
MAM	-	Mitochondria-associated endoplasmic reticulum membrane
MAVS	-	Mitochondrial antiviral signalling
M-CSF	-	Macrophage colony-stimulating factor

MDA5	-	Melanoma differentiation-associated protein 5
MED23	-	Mediator of RNA polymerase II subunit 23
MEFs	-	Murine embryonic fibroblasts
Mito-MAVS	-	Mitochondrial MAVS
MLN	-	Mesenteric lymph nodes
MNV	-	Murine norovirus
Mx	-	Myxovirus resistance protein
NEMO	-	NF-kB essential modulator
NF-kB	-	Nuclear factor of kappa B
NLRP6	-	NOD-like receptor family pyrin domain containing 6
ORF	-	Open reading frame
PABP	-	Poly A-binding protein
PAMP	-	Pathogen-associated molecular pattern
PBS	-	Phosphate buffered saline
PBST	-	1x PBS with tween 20
Pex-MAVS	-	Peroxisomal MAVS
PKR	-	Protein kinase RNA-activated
PMA	-	Phorbol myristate acetate
PRR	-	Pathogen recognition receptors
PRR	-	Pattern recognition receptor
PVDF	-	Polyvinylidene difluoride
RdRp	-	RNA-dependent RNA polymerase

REAP	-	Rapid efficient and practical
RIG-I	-	Retinoic acid-inducible gene 1
RIP1	-	Receptor-interacting serine/threonine-protein 1
RIPA	-	Radioimmuno-precipitation assay buffer
RLR	-	RIG-I-like receptor
RLU	-	Relative luciferase unit
SeV	-	Sendai virus
SFV	-	Semliki forest virus
SHARPIN	-	Shank-associated RH31 domain-interacting protein
STAT	-	Signal transducer and activator of transcription
STING	-	Stimulator of interferon genes
TAK1	-	TGFβ-activated kinase 1
TANK	-	TRAF family member-associated NF-kB activator
TBK	-	Tank-binding kinase
TLR	-	Toll-like receptor
TMD	-	Trans-membrane domain
TNF	-	Tumour necrosis factor
TRAF	-	Tumour necrosis factor receptor-associated factor
TRIM	-	Tripartite motif-containing protein

TYK2	-	Tyrosine kinase 2
VF1	-	Virulence factor 1
VISA	-	Virus-induced signalling adaptor
VP	-	Viral protein
VPg	-	Viral protein genome-linked
VSV	-	Vesicular stomatitis virus

Chapter 1

Introduction

1.1. Enteric Caliciviruses

1.1.1. Introduction and classification

Caliciviridae is a family of positive-sense single-stranded non-enveloped RNA viruses with poly-adenylated RNA genomes ranging between 7.4-7.7kb, possessing 2-4 open reading frames (ORFs), and able to infect both humans and animals[1–3]. The family is composed of five genera, including *Norovirus, Sapovirus, Nebovirus, Lagovirus,* and *Vesivirus,* among which noroviruses and sapoviruses cause disease in humans. Following the introduction of the rotavirus vaccine, they are increasingly becoming the commonest causes of infectious gastroenteritis worldwide[4–7]. Due to a lack of robust culture systems for either of the two human viruses, the murine norovirus (MNV, genus *Norovirus*), porcine sapovirus (genus *Sapovirus*), and feline calicivirus (genus *Vesivirus*) have proven to be very useful tools in studying the biology of caliciviruses[3].

Their genomes contain a long 5' ORF that encodes a polyprotein that is subsequently processed into 6-7 non-structural (NS) proteins by the viral protease (NS6), a second ORF that encodes the major capsid protein VP1, and a short 3' ORF that encodes the minor capsid protein VP2[2,8] (figure 1.1). While both the non-structural proteins and VP1 in sapoviruses are encoded by the 5' ORF (ORF1), some human and bat stains have a third predicted yet uncharacterised alternate ORF that overlaps the VP1 sequence[9]. The MNV genome also has a similar alternate ORF overlapping the VP1 sequence and encoding an accessory protein called virulence factor 1 (VF1)[10]. Like those of picornaviruses, the genomes of calicivirus are covalently linked to a small

protein called Viral Protein genome-linked (VPg, NS5) at the 5' end that is involved in virus replication[1,2].

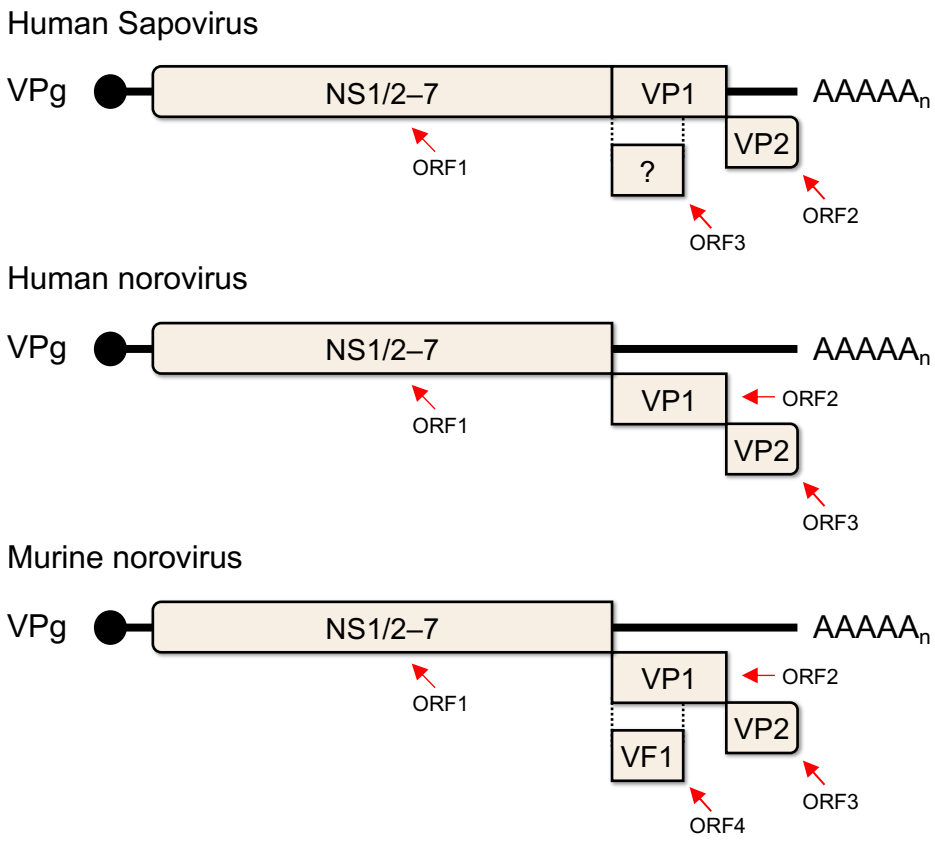

Figure 1.1. Schematic representation of the genome organisation of the human sapovirus, HuNoV, and MNV. (Adapted from Goodfellow, I. (2012) in Reverse Genet. RNA Viruses 91–112).

The NS1/2, NS3 (viral NTPase), and NS4 are thought to play central roles in the formation of viral replication complexes, the NS5 protein (VPg) mediates translation of viral proteins, and the NS6 and NS7 are the viral protease and RNA-dependent RNA polymerase (RdRp), respectively[3,9]. The VP1 protein forms the bulk of the

icosahedral viral capsid (90 dimers), and the VP2 represents a minor component of the capsid (up to 2 copies)[2]. Although a virion contains the VP1, VP2 and VPg, the functions of the latter 2 in the virions are not well understood. Inside infected cells, the MNV VP2 protein was shown to counteract immune responses by inhibiting antigen presentation[11,12]. Because noroviruses decidedly include the more clinically important and most studied human virus within the *Caliciviridae* family[3–5], all discussion beyond this point will be focused on them.

1.1.2. Disease burden and clinical features of noroviruses

The human norovirus has been implicated in 20% of all cases of diarrhoea, and causes up to 19 million illnesses every year[4,13]. It spreads primarily via the faeco-oral route and has an incubation period of 10-51 hrs[14]. The virus infects people of all ages, although the incidence is higher in children[4,14]. It is estimated that $4.2 billion (£3.3 billion) is spent on norovirus-related healthcare, and $60 billion (£46.9 billion) is lost by society annually due to norovirus-related productivity losses[15]. Worldwide, up to 200,000 thousand deaths have been reported, with severity of symptoms increasing significantly in young children, the elderly (>65 yrs.), organ transplant recipients, and people that are immunocompromised. An infectious dose as low as 18 is able to cause infection, and infected humans frequently present with diarrhoea (81%), vomiting (65%), abdominal cramps (68%), and occasionally fever (45%)[2,4,14]. Symptoms often resolve within 24-48 hrs in immunocompetent hosts[2]. Outbreaks often occur where there are large gatherings of people in confined spaces, such as nursing homes, cruise ships and day-care centres.

MNV has served as a surrogate model for studying the biology of noroviruses, owing to the lack of a robust culture system for the human norovirus[16,17] (the recent development of a human intestinal enteroids model for culturing human noroviruses[18], although remarkable, is currently still very expensive and difficult to establish). MNV can cause acute, lethal, or persistent infections in its natural host (mice), depending on the strain used and the genetic background of the host. For example, while infection with the acute strain of MNV in wild-type mice is asymptomatic, *Stat1*$^{-/-}$ and IFNαβγR$^{-/-}$ mice present with severe diarrhoea, weight loss, and death within 2 weeks of infection[10,19,20]. Therefore, in addition to providing a tool for the study of norovirus biology, MNV provides a robust experimental system to understand viral pathogenesis, as well as the contribution of viral and host factors to viral persistence.

1.1.3. Replication cycle of noroviruses

Due to the absence of a robust cell culture system to grow the human norovirus, much of what is known about norovirus replication came from studies in MNV[3,21]. Cell entry during an infection with noroviruses is thought to occur by receptor-mediated dynamin II- and cholesterol-dependent endocytosis, followed by uncoating to release the VPg-linked viral genome into the cytosol[2,22]. Translation of the viral genome occurs in a VPg-dependent manner, and the viral polyprotein is then cleaved into mature non-structural proteins[21]. The non-structural proteins recruit host membranes to form peri-nuclear replication complexes, and the viral RdRp uses VPg as a protein primer for genome replication, although replication can also occur *de novo*[21]. *De novo* transcription by the RdRp produces a negative-strand RNA that serves as a template for both the genomic RNA and a VPg-linked subgenomic RNA that encodes the VP1

and VP2 proteins (and VF1 in MNV). It is not known if the negative-strand RNA is VPg-linked. Infected cells undergo apoptosis to release mature virions.

1.1.4. Cell tropism

Both acute and persistent strains of MNV were shown to be able to infect macrophages and dendritic cells *in vitro* early on after the discovery of the virus, although the *in vivo* tropism was not known at the time[3,23]. The recent determination of the proteinaceous receptor for MNV[24,25], coupled with advances in *in situ* hybridisation assays allowed for the subsequent discovery of the *in vivo* tropism of MNV to myeloid cells, lymphocytes and tuft cells[26–28]. The human norovirus was also recently shown to infect a B-cell cell line (BJABs) and the enterocyte component of the human intestinal enteroids *in vitro*[18,29]. Its *in vivo* tropism is however not clear, although viral antigens have been detected in the intestinal epithelial cells of infected gnotobiotic pigs, lamina propria of a biopsy sample from an infected person, and dendritic cells of an infected chimpanzee[3].

1.2 Innate immune responses against RNA viruses

1.2.1. General overview – Interferons and other cytokines

Innate immunity encompasses an elaborate system of physical and chemical barriers, secreted and membrane proteins, as well as a myriad of effector cells that provide rapid non-specific protection from an invading pathogen. Central to innate immunity in a virus-infected host is the interferon (IFN) response, which includes a system of receptors that detect pathogens, a cascade mechanism that culminates in the induction

and expression of IFNs, and the generation of an antiviral state in the infected and nearby cells by the released IFNs (figure 1.2). IFNs induce expression of proteins that facilitate the resistance of host cells to viruses, activate immune cells recruited to the sites of infection and upregulate factors required for activation of adaptive immunity, all of which makes them critical in the control of viral infections. For this reason, and on account of the co-evolution of hosts and pathogens, any virus that is able to infect a host is also likely to have evolved mechanism(s) of counteracting IFN responses[30,31].

Other cytokines also play important roles in innate immune responses against RNA viruses. Chemokines and pro-inflammatory cytokines such as Tumour Necrosis Factor (TNF)α, interleukin (IL)-1β and IL-18 are also induced following detection of viruses by pattern recognition receptors (PRRs), largely following NF-kB activation, but also downstream of IFN receptors[32,33]. They complement IFN responses by recruiting macrophages, dendritic cells, natural killer cells and lymphocytes to sites of infection, and by mediating the inflammation response. While not as critical as IFN responses to individual infected cells, they contribute to the overall protection of the host and the subsequent return to homeostasis.

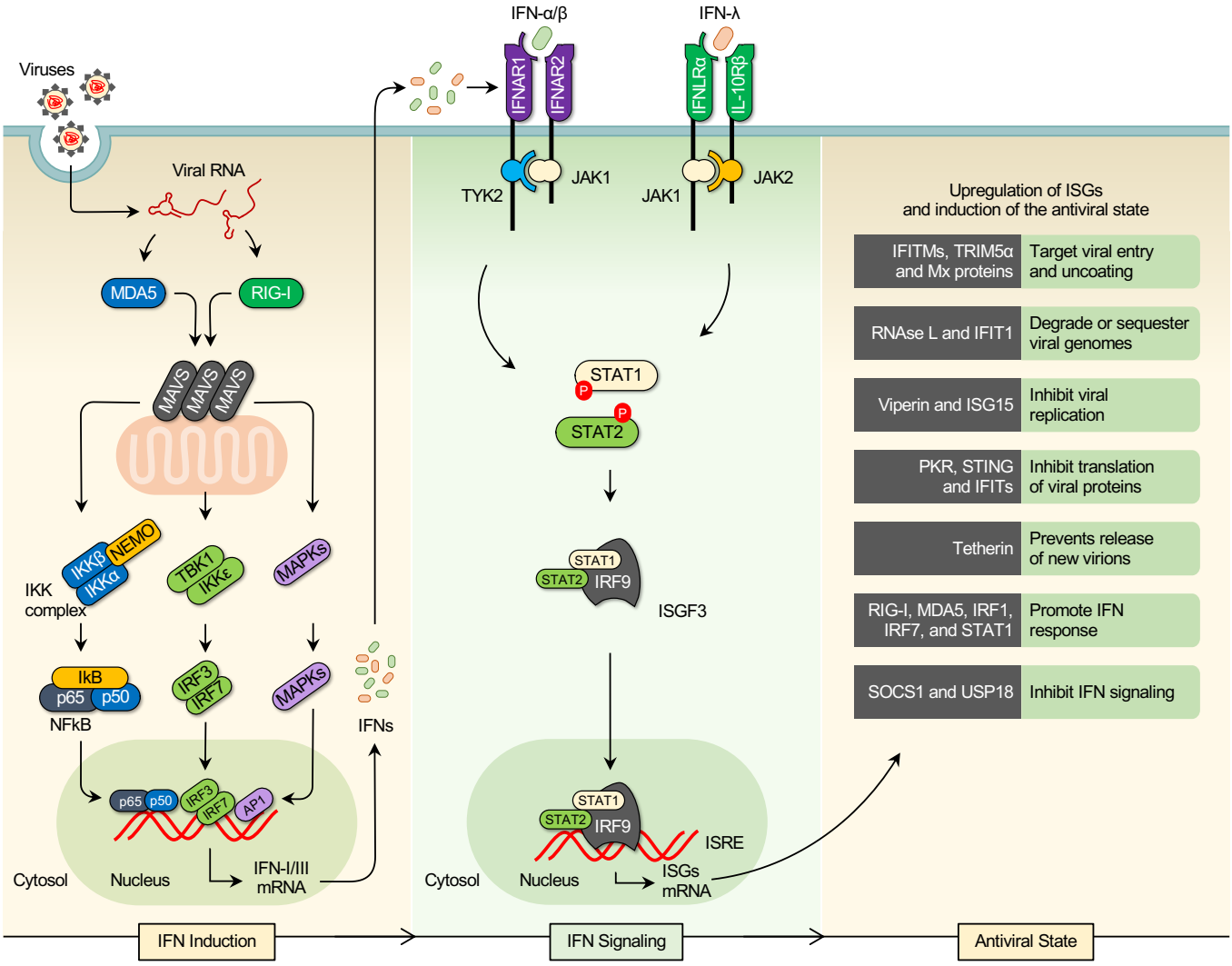

Figure 1.2. A simplified representation of the interferon response. (Adapted from Bowie & Unterholzner (2008), *Nature Reviews Immunology* **8**, 911-922).

1.2.2. Intracellular detection of RNA viruses

Viruses and other pathogens are detected by a myriad of receptors called pattern recognition receptors (reviewed by Iwasaki[34], and by Brubaker et al.[35]). These receptors are present in various compartments in the host cell where pathogens might traverse and thus increasing the likelihood of their detection, including on cell surfaces (such as toll-like receptors [TLR] and c-type lectin receptors), in endosomes (toll-like

receptors), and in the cytosol (such as the retinoic acid-inducible gene 1 [RIG-I]-like receptors, NOD-like receptors, etc). They are germline encoded and are able to detect pathogen-aasociated molecular patterns (PAMPs) which are general molecular patterns unique to pathogens (such as uncapped 5' tri-phosphorylated RNA), or common molecular signatures in aberrant conditions (such as the presence DNA in the cytosol). Activation of these sensors initiate signaling cascades that trigger the release of IFNs and other cytokines, and promote restriction of the invading pathogen.

Yoneyama *et al.* demonstrated, for the first time, the ability of RIG-I to induce a TLR3-independent type I IFN secretion through IRF3 and NF-κB activation, in the presence of intracellular RNA[36]. They did this by showing activation of both IRF3 and NF-κB in cells overexpressing a truncated RIG-I construct containing both its CARD domains, following transfection of synthetic or viral RNA into the cells, as well as inhibition of the type I IFN response following RNA silencing of RIG-I expression. At around the same time, a similar role was demonstrated by Andrejeva and her colleagues for melanoma differentiation-associated protein 5 (MDA5), another DExD/H box helicase containing two N-terminal CARD domains.[37] Together with LGP2, RIG-I and MDA5 form the RLR family and are implicated in the detection of the presence of most RNA viruses and some DNA viruses in an infected host cell.

RIG-I-like receptors typically sense viral replication intermediates in the cytoplasm. RIG-I is thought to sense uncapped 5'-tri- and di-phosphorylated single-stranded or short double-stranded RNA, while MDA5 detects longer double-stranded RNA, all typically seen in viral genomes or present as viral replication intermediates[34,38,39].

Activation of RIG-I or MDA5 by their cognate PAMPs triggers their oligomerization and recruitment to mitochondrial antiviral signalling protein (MAVS), which they activate via a homotypic CARD-CARD interaction. MAVS in turn recruits and activates downstream kinases, eventually leading to activation of transcription factors and expression of types I and III IFNs[38,40]. LGP2, although possessing an RNA-binding helicase domain, lacks a CARD domain and thus is unable to bind MAVS[38,41]. It is thought to mainly act as a positive regulator of RIG-I and a negative regulator of MDA5 through as yet poorly understood mechanisms.

1.2.3. Activation of MAVS, downstream kinases and transcription factors

Four groups published independent findings demonstrating the role of the Mitochondrial Antiviral Signaling protein (MAVS, also known as CARDIF, VISA, and IPS-1) in the activation of IRF3 and NF-kB mediated by RNA virus infection and transfection of synthetic dsRNA.[42–45] At the time, this discovery re-established the mitochondria as an essential organelle in innate immune responses, in addition to further elucidating the pathways of intracellular viral RNA recognition. MAVS is a membrane protein containing 540 amino acids and is abundantly expressed in all nucleated cells.[44–46] Although the precise mechanistic details are still being worked out, it is generally accepted that MAVS plays a central role as an adapter in the intracellular recognition of RNA, as well as in apoptotic and metabolic pathways. [40,47,48] It has an N-terminal CARD domain that is involved in homotypic CARD-CARD interactions with RIG-I and MDA5 during signal transduction. It also has a C-terminal trans-membrane (TM) domain that anchors it to the outer mitochondrial membrane, peroxisomes or the mitochondria-associated endoplasmic reticulum

membrane (MAM), and a proline-rich region through which it interacts with other proteins.[45,49,50] The CARD domain and the trans-membrane domains are both required for the canonical MAVS function. The proline-rich domain contains two TRAF-interacting motifs, and a third motif is present close to the C-terminal end of the protein. MAVS has a predicted molecular weight of 72kDa, although a smaller 50kDa truncated form devoid of the CARD domain (termed miniMAVS) is also expressed in cells, and is believed to regulate the functions of the full-length protein.[46]

Signaling via MAVS causes it to oligomerize on the outer mitochondrial membrane in a prion-like manner, and culminates in activation of IRF3 and NF-κB, through induction of IKKε/TBK1 by TRAF3/IKKγ/TANK, and IKKα/IKKβ/IKKγ by TRAF6/RIP1, respectively. The requirement for TRAF6 here is thought to be redundant, as both TRAF2 and TRAF3 are sufficient for MAVS signaling in its absence.[40,47] Activated IRF3 and NF-κB translocate into the nucleus to form an IFN 'enhanceasome' that facilitates production of type I and III IFNs, which in-turn further stimulate cells in an autocrine and paracrine fashion, and eventually lead to a wide range of antiviral innate immune responses via induction of IFN stimulated genes (ISGs).

The critical role played by MAVS in antiviral immunity was demonstrated in *Mavs* knockout mice. Murine embryonic fibroblasts (MEFs) from these mice had an impaired IFN and inflammatory cytokine secretion profile in response to transfected synthetic dsRNA (poly I:C) or following infection with *Sendai virus*, and showed a limited ability to restrict replication of *Vesicular stomatitis virus* (VSV).[51] MAVS-

deficient mice also showed significantly higher viral titers following intravenous injection of VSV or *Encephalomyocarditis virus* (EMCV) compared to wild-type mice, and increased mortality following intravenous injection of VSV.[51,52] These findings corroborate the essential role of MAVS in the innate antiviral response to RNA viruses.

The subcellular localization of MAVS was shown to be functionally critical. As alluded to earlier, the trans-membrane domain tethers the protein to the outer mitochondrial membrane, the peroxisomal membrane or the MAM, and absence of this localization leads to loss of function. One study in which the trans-membrane domain was modified so that MAVS was targeted only to the mitochondria (mitochondrial MAVS), the peroxisomes (peroxisomal MAVS) or has the trans-membrane domain truncated so that it is not targeted to any organelle (cytosolic MAVS), attempted to unraveled the functional significance of this subcellular localization.[50] A distinct immune response was seen with both the mitochondrial and peroxisomal MAVS, but not with cytosolic MAVS. Mitochondrial MAVS was seen to promote a delayed type I IFN-dependent induction of ISGs, while peroxisomal MAVS showed an early induction of ISGs in a type-I IFN-independent manner. This functional dichotomy was shown to be especially relevant in VSV infection where the virus evades immune responses by impairing transcription of type I IFNs. In this case, signaling via peroxisomal MAVS was shown to be essential in restricting viral replication. Further work by the same group showed this type I IFN-independent peroxisomal MAVS response in intestinal epithelial cells to be mediated by type III IFNs.[53] The mechanistic determinants of this differential localization of the subsets *in vivo* and differences in the downstream signaling events are yet to be understood, and

recent attempts at replication by a different lab proved challenging[54]. Nevertheless, these findings clearly point to an advantage in the functional differences of the MAVS subsets.

1.2.4. Intracellular sensing of DNA viruses

Several PRRs involved in recognising the presence of viral DNA in the host cell have been described (reviewed by Ma and Damania[55]). The best characterised among them is the cyclic GMP-AMP synthase (cGAS), which catalyses the formation of cyclic dinucleotides that activate the adapter protein Stimulator of IFN Genes (STING) following detection of viral DNA[56]. Like MAVS, activated STING in turn recruits and activate downstream kinases and transcription factors, and in the process mediates induction of IFNs and proinflammatory cytokines. Other receptors shown to be involved in the detection of foreign DNA include DNA-PK, TLR9, AIM2, DAI, IFI16, DHX9, DHX36, DDX60, and MRE11.

1.2.5. Crosstalk between MAVS and STING activation pathways

The RLR/MAVS pathway of RNA sensing and the cGAS/STING pathway that detects foreign or aberrant DNA extensively collaborate to coordinate innate immune responses against invading pathogens (recently reviewed by Zevini et al.[57]). First, RIG-I contributes to detection of viral DNA through sensing of a dsRNA intermediate transcribed by RNA polymerase III[58,59], while cGAS can detect DNA-RNA hybrids in the cytosol that are formed during the replication of retroviruses[60,61]. Additionally, infection with Dengue virus, a flavivirus, leads to leakage of mitochondrial DNA into the cytosol which is detected by cGAS[62,63]. Second, MDA5, RIG-I, STING, IRF1 and

IRF7 are all ISGs themselves, which means induction of IFNs by one pathway upregulates proteins that play central roles in the other, with the two pathways thereby potentiating activation of each other[57,64,65]. Third, STING, an adapter protein required for cytosolic DNA sensing, has been shown to promote IFN induction in cells infected with RNA viruses. For instance, it associates with both RIG-I and MAVS following activation of RIG-I in cells infected with SeV, and these interactions were found to promote induction of IFNs [40,66,67]. Importantly, this was observed to be restricted to RIG-I activation, but not MDA5[40,67]. It was also demonstrated that STING can facilitate a fusion-mediated IFN induction in IAV-infected cells, in a cGAS-independent manner, although the mechanistic details for this pathway are not yet known[68]. In cells infected with the Japanese Encephalitis virus (JEV), another flavivirus, STING is required for IFN induction downstream of RIG-I, and MAVS was seen to be dispensable in this case[69]. And lastly, STING was recently shown to inhibit translation in cells infected by a wide range of RNA viruses[70]. Altogether, these findings highlight an emerging theme of extensive crosstalk between the MAVS and STING pathways that underpins effective immediate and non-specific immune responses to a wide variety of invading pathogens.

1.2.6. IFN induction in the nucleus

Following virus-induced activation, the activated transcription factors translocate into the nucleus and bind to the IFN enhancer regions, composed of four positive regulatory domains (PRDs) in the case of IFN-β (reviewed by Ford and Thanos[71], and recently by Au-Yeung and Horvath[72]). Activated NF-kB binds to PRDII, IRF3/7 bind to PRDI and III, and AP-1 binds to PRDIV, forming the IFN-β enhanceosome.

Transcription of the IFN genes is tightly controlled, and involves collaborative recruitment of histone acetyl transferases, chromosome remodelers, and other transcriptional co-activators that eventually leads to formation of the RNA Pol II pre-initiation complex[72].

While the formation of the enhanceosome is required for a robust induction of type I and type III IFNs, recent studies suggest that activation of IRF3 preferentially promotes induction of IFN-β, while induction of type III IFNs is more dependent on activation of IRF7 and NF-kB[73–77]. The mechanistic details of this differential requirement of transcription factor activation is not yet known, considering the enhancers of both types I and III IFNs contain binding sites for both IRFs and NF-kB. One possible explanation is differential recruitment of co-activators by the different transcription factors. A recent paper described a function of MED23, a tail subunit of the Mediator complex, in triggering type III IFN-specific induction, following a genome-wide RNAi screen for host factors that inhibit replication of Herpes Simplex Virus type 1 (HSV1)[78]. Increased expression of type III IFNs was observed upon overexpression of MED23 in A549 cells, with a decrease in viral replication following infection with HSV1. Depletion of MED23 on the other hand, using a siRNA pool, lead to an increase in viral titres and a decrease in the induction of type III IFNs. The authors further demonstrated an interaction between MED23 and IRF7, but not between MED23 and other IRFs, concluding that MED23 specifically regulates induction of type III IFNs following infection with HSV1.

The Mediator is a large multi-subunit protein complex that plays an essential role in transcription by recruiting the RNA Pol II pre-initiation complex to sites of transcription, and is required for transcription of all eukaryotic genes[79,80]. It is divided into 4 distinct modules; the head and middle modules that form the core of the complex, a kinase module that is thought to form an autoinhibitory domain of the complex, and the tail module through which most gene-specific transcription factors interact with the complex. Several gene-specific transcription factors recruit RNA Pol II to promoter sites via interactions with specific tail subunits of Mediator[80–82]. It is therefore possible that another tail subunit mediates Mediator recruitment to activated IRF3.

1.2.7. IFN signalling and induction of ISGs

Released IFNs bind to their receptors on cell surfaces in an autocrine and paracrine manner. The IFN family in mammals consist of three groups; type I IFNs, including 13 IFN-α subtypes, IFN-β, IFN-κ, IFN-δ, IFN-ε , IFN-τ , IFN-ω , and IFN-ζ; type II IFN, IFN-γ; and type III IFNs which include the IFN-λs (reviewed by Fensterl et al.[30], and by Hoffmann et al.[31]). Human IFN-λs include IFN-λ1 (IL—29), IFN-λ2 (IL28A), IFN-λ3 (IL-28B), and IFN-λ4, but only IFN-λ2 and IFN-λ3 are functional in mice. Secretion of type II IFNs is restricted to specialized immune cells, whereas types I and III IFNs are ubiquitously expressed by all cell types, hence types I and III IFNs play larger more critical roles in innate responses against viruses[83]. While most cells can express IFN-α and IFN-β, plasmacytoid dendritic cells have the highest capacity of any cell type for expression of IFN-αs (except IFN-α4) as a result of a constitutive expression of IRF7[84,85].

All 3 classes of IFNs signal through multi-subunit class II helical cytokine receptors encoded by genes located within the same cluster (reviewed by de Weerd et al.[86]). The type I IFN receptor (IFNAR) consist of 2 subunits, IFNAR1 and IFNAR2, each composed of a cytoplasmic component that associates with Janus Kinases (JAKs), a transmembrane domain, and an extracellular immunoglobulin-like domain that remarkably recognises all the diverse members of the type I IFNs. IFNAR1 associates with TYK2 while IFNAR2 associates with JAK1, and these kinases compensate for their lack of an intrinsic kinase activity. Similarly, the type II IFN receptor is composed of 2 subunits, IFN-γ receptor (IFNGR)1 and IFNGR2, while type III IFNs are composed of IFN-λ receptor (IFNLR)α and Interleukin (IL)-10 receptor (IL10R)β. The IFNAR and IFNGR are ubiquitously expressed in all cell types, although expression of specific subunits may differ from one cell type to another. In contrast, IFNLRα expression is chiefly limited to epithelial cells, hepatocytes and select immune cells, therefore largely restricting the effects of type III IFNs to mucosal surfaces[73,74,87–91].

Ligand binding leads to receptor clustering and auto-phosphorylation of the receptor-associated JAK kinases – TYK-2/JAK1 in the case of IFNARs, JAK1/JAK2 for IFNGRs, and JAK1/JAK2 (or TYK-2/JAK1) for IFNLRs. This leads to phosphorylation of the receptors, and subsequently recruitment and phosphorylation of Signal transducer and activator of transcription proteins (STATs). Signalling downstream of both IFNAR and IFNLR leads to activation of STAT1/STAT2 heterodimers that form the IFN-stimulated genes factor 3 (ISGF3) complex together

with IRF9[30,31]. ISGF3 then translocates into the nucleus to induce expression of IFN-stimulated genes (ISGs) through binding to IFN-stimulated response elements (ISRE). On the other hand, binding of IFN-γ to the IFNGRs leads to activation of STAT1 homodimers that binds to IFN-γ-activated sequence (GAS) in the nucleus. While both types I and III binding to their respective receptors largely leads to formation of the ISGF3 complex and induction of the same genes, type III IFN-stimulated genes have been shown to be only a subset of type I IFN-dependent genes. In addition, STAT1 homodimers can form downstream of IFNAR-binding, which leads to induction of pro-inflammatory genes, in addition to ISGs[92].

Although both type I and type III Interferons ultimately induce expression of the same ISGs, and hence produce parallel responses[93], the specificity of type III Interferons lies in the differential expression of their receptors. Whereas the IFNAR receptors are abundantly expressed in most cell types, IFNLRα expression is limited to epithelial cells. This underpins the key roles of type III Interferons in innate immune responses, and is especially true against viruses that traverse mucosal surfaces where epithelial cells expressing the IFN-λ receptor are in abundance. A recent study showed that IFN-λ is required for clearance of persistent norovirus infection in the intestines, for example, with increased fecal shedding seen in IFN-λ receptor-deficient mice over 35 days of infection, but not in mice lacking type I interferon receptors.[94] A similar finding was reported for rotavirus, in which there was an impaired control of viral replication within intestinal epithelial cells of IFNLRα-deficient mice, but not in IFNAR-deficient mice.[95] In addition, recent work by Galani et al. showed that in mice infected with very low multiplicity of infection of influenza A virus (IAV) to mimic physiologic infection, an initial secretion of type III IFN was observed, characterized

by ISG induction with no pro-inflammatory cytokine expression and minimal inflammation[96,97]. It was only after this initial response was overcome by the viral infection that a second type I and III IFN response was observed, characterized by upregulation of both ISGs and pro-inflammatory cytokines, with significant inflammation and tissue damage. Altogether, these findings indicate the essential non-redundant roles of type I and type III IFNs in host restriction of viruses. Despite considerable interest, however, the mechanism for the host's ability to differentially induce type I and type III IFNs remains unclear (discussed in greater detail below)[74,97].

1.2.8. Outcomes of IFN responses – the antiviral state

The goal of the IFN response is to clear the infected cell of the pathogen, or if that fails, kill the one cell in order to save the whole organism and at the same time prepare neighbouring cells to resist infection. These goals are achieved by the upregulation of ISGs that induce a state of general resistance to all stages of the viral replication cycle via different mechanisms, termed 'the antiviral state'. Hundreds of ISGs have been reported, out of which only a small fraction have known functions (reviewed by Schneider et al.[98] and by Schoggins[83]). Among those already characterized are some of the central mediators of IFN induction, including RIG-I, MDA5, STING, IRF1, IRF7, and STAT1. Upregulation of these proteins provides a positive feedback loop that increases the efficiency of the IFN response. On the other hand, ISGs such as SOCS1 and USP18 are negative regulators of JAK/STAT signalling and act as brake systems that prevent development of immunopathology. Together, these opposing systems work in a balance that attempts to clear the cell of the infection while also limiting damage to the host. The majority of characterised ISGs are neither positive

nor negative regulators of the IFN response, however. Instead, they are mostly antiviral effectors that target different stages of the viral life cycle[64,98]. ISGs such as IFITMs, TRIM5α and the Mx proteins target viral entry and uncoating steps; RNAse L and IFIT1 degrade or sequester viral genomes; Viperin and ISG15 inhibit viral replication; PKR, STING and IFITs inhibit translation of viral proteins; and Tetherin prevents release of new virions[70,98–101]. Working together, these antiviral effectors ensure restriction of a broad range of viruses.

1.2.9. Regulation of IFN responses

Regulation of IFN responses ensures clearance of pathogens from infected cells while also minimizing immunopathology. This often occurs in the form of differential expression of protein isoforms, post-translational modifications (PTMs) or epigenetic changes relating to key proteins involved in the IFN response pathway (reviewed by Ivashkiv and Donlin[92]). For example, several mechanisms that regulate MAVS signaling have been described. A previous study characterized a shorter 50kDa variant of MAVS expressed from the MAVS gene via a complex interplay of leaky scanning events.[46] This 'miniMAVS' was shown to attenuate the interferon inducibility of the full length MAVS, which suggests that it plays a modulatory role. Post-translational regulation of MAVS signaling is achieved by various host and viral proteins and occurs in the form of both ubiquitination and phosphorylation. In virally infected cells, MAVS is negatively regulated through K48-linked ubiquitination and subsequent targeting for proteosomal degradation by various E3 ligases such as TRIM25, AIP4, RNF5, and RNF125.[102–105] Other negative regulators of MAVS, such as PLK1, bind to phosphorylated MAVS and prevent its binding to TRAF3.[106]

1.3. IFN responses to noroviruses

1.3.1 Restriction of Norovirus replication by IFNs

Data from both *in vivo* and *in vitro* studies have established the capacity of IFNs to restrict replication of noroviruses. First, MNV infection of wild type mice is largely asymptomatic, in contrast to *Stat1*$^{-/-}$ or IFNαβγR$^{-/-}$ mice in which infection is accompanied by a considerable increase in viral RNA and causes severe symptoms, significant multi-organ pathology, and death in all infected mice within 2 weeks of infection[19,20] – this increased susceptibility can be reversed by administration of IFN-λ[107]. Secondly, treatment of MNV-infected cells with recombinant IFN-β significantly inhibits viral replication, as is treatment of mice with IFN-λ[27,108,109]. Similarly, TLR7 agonists and plant extracts (Schizonepeta tenuifolia Briquet) were shown to significantly inhibit MNV replication by promoting IFN induction[110,111]. Likewise, over-expression of RIG-I and MDA5 was shown to inhibit MNV replication, likely by inducing IFN induction[112]. *In vivo* experiments in mice showed a context-dependent differential requirement of type I and type III IFNs in which type I IFNs protect against systemic spread via immune cells while type III IFNs restrict enteric persistence[94]. Lastly, selective knockout of *Ifnar1* in dendritic cells allows an otherwise acute strain of MNV (CW3) to persist, despite the presence of a functional adaptive immune system[113]. This was recently shown to occur due to an IL-1α-mediated recruitment of monocytes and neutrophils, in a manner dependent on lytic cell death induced by the viral capsid[114]. While there are no data on the restriction of human norovirus replication by IFNs in human subjects, gnotobiotic pigs infected with the human norovirus showed decrease faecal shedding following treatment with

IFN-α[115]. Treatment of human norovirus replicon-harbouring HG23 cells with IFN-α was shown to result in a reduction in viral genomes in a dose dependent-manner[116,117]. Moreover, treatment of cells with cell culture supernatant from poly (I:C)-transfected cells inhibited replication of human norovirus RNA in Huh-7 cells[118]. Overall, these studies show the capacity of IFNs to inhibit replication of noroviruses.

The specific ISGs responsible for inhibiting norovirus replication are not all known. Pre-treatment of cells with recombinant IFN-β or IFN-γ was shown to inhibit translation of viral proteins without affecting viral genome integrity[108]. This inhibition was shown to be independent of PKR and RNAse L for the IFN-β-pre-treated cells, but not in IFN-γ-pre-treated cells, indicating the presence of another ISG(s) that inhibits viral translation. Several ISGs have since been shown to generally inhibit translation of viral proteins via disparate mechanisms (reviewed by Li et al.[119]), but their functions have not been looked at in the context of a norovirus infection. ISG15 is among the few ISGs clearly implicated in restricting norovirus replication[109]. Higher viral titres were obtained from IFN-α-treated IS15-deficient bone marrow-derived macrophages (BMDMs) compared to wild-type cells, indicating a role for ISG15 in IFN-dependent control of MNV replication. This function was shown to be at the level of viral entry or uncoating, as replication in MEFs transfected with the MNV RNA was not affected by the absence of ISG15. Other ISGs shown to counteract norovirus replication include NLRP6, IRF1, IRF7, IFN-λs, STAT1, MHCII, and β2M[120]. It should be noted that limited levels of ISGs are seen in MNV-infected cells as the virus has been shown to inhibit ISG translation through at least 2 independent mechanisms[109,121] (discussed in greater detail below under '*Counteraction of IFN responses by Noroviruses*').

1.3.2. IFN induction during Norovirus infections

Robust induction of type I and type III IFNs are seen following infection with MNV both *in vivo* and *in vitro*[20,121–125]. In mice, IFN-β is detected in intestinal homogenates as early as 12 hrs following per-oral inoculation, and in the serum within 24 hrs of infection[20]. *In vitro*, while an increase in transcripts is seen early during infection, IFN release appears to be temporally different in cell lines compared to primary cells, with IFN-β secretion seen within 4 hrs of infection in BMDMs, and 20 hrs in RAW264.7 macrophage cell line[124]. This unexplained delay in IFN release is potentially responsible for the higher viral titres seen in macrophage cell lines compared to primary macrophages and dendritic cells.

In contrast to MNV, there was no evidence of IFN induction in Huh-7 and 293FT cells transfected with the human norovirus RNA[118,126]. Cell culture supernatant from poly (I:C)-transfected cells was able to inhibit replication of human norovirus in Huh-7 cells, but not that from norovirus RNA-transfected cells[118]. In 293FT cells, there was no IFN induction following transfection of human norovirus RNA compared to control RNA[126]. Replication of the human norovirus did not interfere with the IFN response pathway as secondary transfection of poly (I:C) and infection with Sendai virus (SeV) in the norovirus RNA-transfected cells led to a robust induction of IFN-β. Interestingly, siRNA depletion of MAVS and IRF3 did not affect levels of viral genome copies. This contrasts with data from work in gnotobiotic pigs, where an increase in IFN-α and IFN-γ were seen as early as 24-48 hrs after infection, with a second peak for IFN-α seen after 10 days in the serum and gut of infected animals[127].

One caveat with the *in vitro* experiments is that in both the Huh-7 and 293FT studies, purified RNA was used from stools of norovirus-infected humans which may contain other contaminating RNA. Also, virus replication seen in these cells was only marginal. Nevertheless, these preliminary studies offer the only available account of IFN responses to the human norovirus in cell lines, in the absence of a robust culture system, and highlight the increasing need for more work in this area.

In terms of the mechanism of IFN induction, MDA5 was shown to play a central role in the innate immune response to both acute and persistent strains of MNV[122,123] (figure 1.3). Near-baseline levels of IFN-α were seen in bone marrow-derived dendritic cells from MDA5-deficient (*Ifih1*$^{-/-}$) mice following infection with an acute strain of MNV (CW3) compared to the wild type, with a significant increase in viral titres seen in the spleen, mesenteric lymph nodes (MLN) and proximal intestines of *Ifih1*$^{-/-}$ mice. The role of MDA5 in restricting MNV replication was shown to be completely IFN-dependent, as similar viral titres were obtained from wild-type and *Ifih1*$^{-/-}$ cells following pre-treatment with IFN-α. Surprisingly, while higher viral titres were seen in *Ifih1*$^{-/-}$ mice infected with a persistent strain of MNV (CR6), there was no difference in wild-type and *Ifih1*$^{-/-}$ bone marrow-derived dendritic cells (BMDCs)[123]. The authors speculate that the inability of BMDCs to sense type III IFNs accounts for this disparity, although it could also indicate a strain-specific role for other PRRs. At the same time, the increase in viral titres observed in *Ifih1* knockout mice and BMDCs infected with acute strains of MNV are only moderate, and MNV infection is not lethal in *Ifih1* knockout mice in contrast to *Stat1* knockout mice[19,122], indicating the potential presence of other factors that restrict viral replication (reviewed by Karst[128]).

TLR3, TLR7, and presumably TLR8 (via Myd88) do not appear to play any role in IFN responses to noroviruses *in vitro*, although a marginal increase in viral titres was observed in the MLNs of *Tlr3*$^{-/-}$ mice[122,123]. Interestingly, no published study has examined MNV infection in RIG-I-deficient (*Ddx58*$^{-/-}$) cells. In a recent study looking at RIG-I inhibition by a bacterial quorum-sensing molecule, it was shown that while treating cells with the molecule led to a moderate increase in SeV titres in HEK293T cells, it did not appear to affect MNV titres in RAW264.7 cells[129]. It is however not clear whether there was any effect on IFN induction by the MNV infection or if the dose used was sufficient. Also, no statistically significant difference was observed in viral replication following transfection of the human norovirus RNA in Huh-7 and RIG-I-deficient Huh-7.5, although norovirus replication in these cell lines did not induce an IFN response, as discussed above.[118,130]

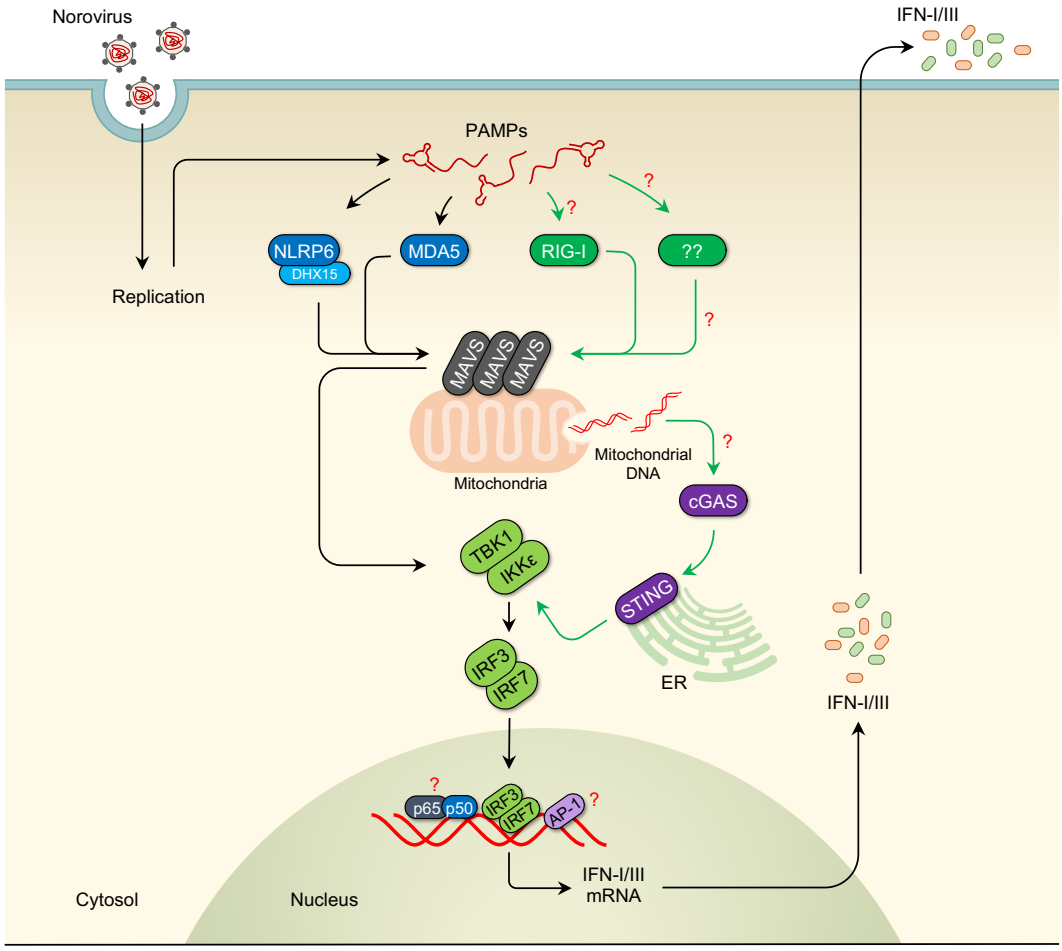

Figure 1.3. Mechanism of IFN induction in norovirus-infected cells. Pathogen-associated molecular patterns (PAMPs), generated from virus replication, are thought to be detected by MDA5 and NLRP6, leading to activation of MAVS at mitochondria and peroxisomes. Activated MAVS in turn activate downstream kinases, TBK1 and IKKε, which recruit and phosphorylate IRF3 and IRF7. This results in their dimerization and translocation into the nucleus, where they induce expression of type I and type III interferons. The interferons produced are then released to act on cells in an autocrine and paracrine manner. Although clear experimental evidence is lacking, it is likely that additional pattern recognition receptors, such as RIG-I, cGAS and/or others, contribute to the sensing of norovirus PAMPs.

The NOD-like receptor family pyrin domain containing 6 (NLRP6) protein was also shown to contribute to cytosolic detection of MNV, likely in a manner dependent on the RNA helicase DHX15[131]. Increased – though modest – viral titres were obtained in intestinal epithelial cells, spleen and faeces from *Nlrp6*$^{-/-}$ mice compared to wild-

type, with faecal shedding persisting beyond 8 days post-infection. The authors demonstrated an inverse relationship in the expression of MDA5 and Nlpr6 in intestinal epithelial cells and myeloid cells in the gut, with higher levels of MDA5 in myeloid cells and NLRP6 in intestinal epithelial cells, and posit that NLRP6 likely compliments MDA5 detection of viruses in epithelial cells.

The phenotypic differences between MNV-infected MDA5 and STAT1 knockout mice are unlikely to be explained solely by the contribution of NLRP6 in norovirus detection, indicating a role for other receptors (Figure 2). As discussed above, while the presence of VPg was always thought to protect the viral genome from RIG-I sensing[122,132], there is currently insufficient experimental evidence to rule it out as a sensor of noroviruses. Moreover, recent studies on picornaviruses and on the Tulane virus show that RIG-I can still detect viruses that have VPg-linked genomes[133–136]. Other PPRs can also potentially participate in the recognition of noroviruses. The DNA sensor cGAS, for example, was recently shown to indirectly recognise infection with dengue viruses by sensing leaked mitochondrial DNA[62,137]. The release of mitochondrial DNA into the cytosol was shown to occur downstream of IL-1β[137], a proinflammatory cytokine abundantly secreted by MNV-infected cells[138]. While this pathway is not present in cells infected with many other RNA viruses[70], whether it occurs in norovirus-infected cells remains to be explored. A recent study suggested that the capsid-detecting TLR2, expressed on cell surfaces, can bind HuNoV virus-like particles, although it is not known if this potential interaction leads to an IFN response[139]. The endosomal TLR10 was also recently shown to be able to recognise dsRNA in cells, and may therefore be involved in sensing noroviruses[140]. Taken together, these points highlight the need for more work in this area.

Downstream of the PRRs, MAVS, IRF3 and IRF7 have all been shown to play central roles in induction of IFN following infection with MNV[120,123]. Heme-oxidized IRP2 ubiquitin ligase 1 (HOIL1), a component of the linear ubiquitin assembly complex (LUBAC), was also recently shown to contribute to IFN induction in MNV-infected mice, and the authors speculated that it likely acts downstream of MDA5[123]. Like in MDA5-deficient mice, HOIL1-deficient (*Rbck1*$^{-/-}$) mice infected with a persistent strain of MNV (CR6) had higher viral titres in the stool, colon, ileum and MLN, and no difference in viral titres in BMDMs despite a significant reduction in IFN induction. However, direct mechanistic evidence connecting MDA5 and HOIL1 remains to be uncovered, and the levels of the SHANK-associated RH31 domain-interacting protein (SHARPIN) were also consistently reduced in the cells used indicating possible alternative explanations for the phenotypes observed. Moreover, the LUBAC complex has previously been shown to inhibit RLR signalling, while also activating NEMO and IRF3-dependent apoptosis[141–143]. Nevertheless, these studies indicate a complex role for linear ubiquitination in controlling infections with RNA viruses and more work is thus required to understand it.

IFN induction in norovirus-infected cells appears to be replication-dependent, as no IFNs were detected following infection with gamma-irradiated virus or transfection of proteinase K-treated MNV RNA in BMDCs[122]. No other published study has examined the cognate PAMP recognised by host PRRs in cells infected with noroviruses, although it has been shown that the MNV polymerase can transcribe RNA species that are detected by MDA5 and RIG-I, but not TLR3[144]. Potential

candidate PAMPs for MDA5 will include the dsRNA intermediates and VPg-linked subgenomic RNA produced during viral genome replication[145] (discussed above). Single-stranded negative sense RNA intermediate that is likely not VPg-linked is also produced, and could be a potential ligand for other host PRRs such as RIG-I.

1.3.3. Counteraction of IFN responses by Noroviruses

The virulence factor 1 (VF1) protein is the first norovirus protein shown to antagonize the IFN response[10,11,146]. It is a small 213-amino acid protein encoded by an alternate open reading frame overlapping the VP1 sequence. It is present only in MNV and is not encoded by human noroviruses. Much of its structure is not known, but data from our lab (Mcfadden et al.[10], and unpublished data generated by Dr. Frederic Sorgeloos and I) suggest that it is a multi-pass membrane protein with a free cytosolic amino-terminal end and a carboxyl-terminus largely embedded within the outer mitochondrial membrane. RAW264.7 cells infected with MNV1-M1, a VF1-deleted mutant, showed an increased induction of IFN-β and an impaired ability to activate apoptotic pathways compared to those infected with the wild-type virus[10]. Deletion of VF1 exacts a fitness cost on the virus in RAW264.7 cells and the M1 mutant reverted to wild-type virus after 3 passages. Although the mechanism is not clear, VF1 inhibited IFN induction after over-expression of RIG-I, MDA5, MAVS, and TBK1, indicating that it likely acts downstream of TBK1 activation[10,11]. Mice infected with MNV-M1 show decreased viral titres on days 3 and 5 in all tissues tested, including MLNs, spleen, liver, kidney, intestine, heart, lung and faeces, compared to those infected with the wild-type virus[10]. Infection with the MNV-M1 virus in *Stat1*$^{-/-}$ mice led to significant reduction in weight loss and intestinal pathology. Taken together,

these findings demonstrate a defined strategy by MNV to counteract IFN responses through expression of VF1, although the exact mechanism and target of this action have not been determined.

Limited levels of ISGs are seen in MNV-infected cells, as the virus inhibits ISG translation via at least 2 possible mechanisms[109,121]. First, the viral protease was shown to cause cleavage of poly A-binding protein PABP, required for cap-dependent, but not VPg-dependent, translation[121,147]. Cleavage occurs at position Q440 of PABP and allows for a disruption of host translation while translation of viral proteins occurs unimpeded. Secondly, MNV infection triggers apoptosis and caspase-dependent cleavage of eIF4E[121]. While the specific role of eIF4E in the replication of MNV is not clear, its depletion affects cap-dependent translation of host proteins, but does not seem to affect translation of viral proteins[148,149].

Although the mechanism still remains to be tested, the MNV NS1 protein mediates persistence of the CR6 strain of MNV in mouse intestinal epithelial cells, specifically the CD300lf+ Tuft cells[27,28,150–152]. Replacing the CR6 NS1 with that of CW3, the acute strain, led to clearance of the persistent virus, while replacing the CW3 NS1 with that of CR6 led to persistence of the acute strain in intestinal epithelial cells[27]. While the intestinal epithelial cells express the IFNLR1 and respond readily to type III IFNs, they show a minimal response to type I IFNs[153], and persistence in them therefore allows for escape from type I IFN responses. Interestingly, wild-type CW3 MNV was also shown to persist in the absence of the IFNLR1, indicating potential neutralisation of type III IFN responses by the CR6 NS1[27].

Other strategies deployed by noroviruses to evade IFN responses have been proposed (reviewed by Roth and Karst[146]). First, the human norovirus non-structural proteins p22 and p48 were implicated in Golgi disassembly and disruption of ER-Golgi trafficking of cellular proteins and thereby potentially impairing cellular secretory pathways utilized for release of IFNs[146]. The mechanism for this activity is still under investigation, and its direct effect on IFN responses in the context of a viral infection remains to be tested. Secondly, considering that no evidence of IFN induction was observed in Huh-7 and 293FT cells harbouring human norovirus RNA, it has been suggested that the viral genomes could be sequestered within replication complexes and away from the RLRs[118,126]. While both RIG-I and MDA5 can be recruited to stress granules in virus-infected cells, the presence of MDA5 in viral replication complexes has not been reported[154–156]. Further work is warranted to confirm these, and other potential strategies employed by noroviruses to evade IFN responses.

1.3.4. Outstanding questions

While MDA5 has been established as a bona fide PRR in MNV-infected cells, other PRRs likely contribute, considering MNV infection is lethal in *Stat1*$^{-/-}$ mice but not in *Ifih1*$^{-/-}$ mice. Current available data[129,130,144] provide support for and against RIG-I as a PRR in MNV-infected cells, and warrants future examination of its role in norovirus restriction. Additional work is also required to determine the cognate PAMPs recognised during infection with noroviruses.

Regulation of IFN responses by the MNV VF1 protein has been demonstrated, but the mechanism by which it executes this is still unclear. Preliminary mechanistic work by McFadden et al.[10] using protein over-expression assays indicate that it acts downstream of TBK1. As a transmembrane protein on the outer mitochondrial membrane, it could potentially interfere with the MAVS/TBK1/IRF3 complex either directly or by modulating the mitochondrial membrane potential. VF1 also appears to interact with TOM70 (Nora McFadden, unpublished PhD thesis) which itself participates in signalling downstream of MAVS[157,158], and may therefore interfere with the TOM70-dependent activation of MAVS. However, this potential interaction could also be unrelated to IFN signalling as most proteins on the outer mitochondrial membrane require TOM70 for membrane insertion[159]. Nevertheless, future studies are needed to further understand the function of VF1, and other potential strategies deployed by noroviruses to evade host innate immune responses.

1.4. Thesis objectives

This thesis aims to:

1. Define additional innate immune mechanisms employed in the detection of MNV1
2. Clarify the mechanism of VF1 antagonism of host IFN responses.
3. Explore other innate immune mechanisms at play in the restriction of RNA viruses

Chapter 2

Materials and Methods

Cells

RAW264.7, BV2, A549, HaCat, HEK293T, and HeLa M cells were maintained at 37ºC in complete Dulbecco's Modified Eagle Medium (DMEM, Sigma Aldrich) containing 4500mg/ml glucose, sodium bicarbonate, and sodium pyruvate, and supplemented with 10% heat-inactivated Fetal Bovine Serum (HyClone), 10U/ml of penicillin, 100 μg/ml of streptomycin, 2mM L-glutamine (Sigma Aldrich), and non-essential amino acids (Sigma Aldrich). A549 cells used in this work were a kind gift from Dr Rachel Ulferts (University of Cambridge) and the HaCat, HEK293T and HeLa M cells were generously provided by Dr Susanna M. Calaco (University of Cambridge). mCherry-PTS1 HeLa M cells expressing an mCherry protein engineered to localise to peroxisomes and HEK293T stably-transduced with mouse CD300lf were provided by Dr Frederick Sorgeloos (University of Cambridge UK and De Duve institute Belgium).

BSR-T7 cells, a kind gift from Karl-Klaus Conzelmann (Ludwid Maximillians University, Munich) derived from Baby Hamster Kidney (BHK) cells and expressing the T7 RNA polymerase, were maintained in complete DMEM supplemented with 0.5 mg/ml G418 (Invivogen).

Med23$^{+/+}$ and *Med23*$^{-/-}$ murine embryonic fibroblasts made from 8-week old embryos described in Stevens *et al.*[160] and Balamotis *et al.*[161], were maintained at 37ºC in Knockout DMEM (Gibco) supplemented with 15% Fetal Bovine Serum (HyClone), 2 mM L-Glutamine (Sigma Aldrich), 50 μg/μl Penicillin/Streptomycin, 0.1 mM non-essential amino acids (Sigma Aldrich) and 100 μM beta-mercaptoethanol (Gibco).

Both cell lines were kindly provided by Professor Arnold Berk (University of California, Los Angeles).

Bone marrow-derived macrophages (BMDMs) were differentiated from bone marrow cells of C57BL/6 mice as previously described[162]. Briefly, bone marrow cells were seeded on non-treated culture plates in complete DMEM supplemented with 10% CMG14 culture supernatant which contains M-CSF. Fresh medium was added every 3 days and cells were harvested and used for experiments on 9 or 10. *Ddx58*$^{+/+}$ and *Ddx58*$^{-/-}$ bone marrow cells were kindly provided by Adolfo Garcia-Sastre (Icahn School of Medicine at Mount Sinai in New York). All other bone marrow cells used were provided by Yasmin Goodfellow (University of Cambridge).

Plasmids

Plasmids used in this work are listed in Table 2.1.

Table 2.1: List of plasmids used

sn	Name	Insert/description	Source	Comments
1.	pT7:MNV-1_3'Rz	MNV1 WT cDNA clone	Chaudhry et al. 2007[163]	For generating wild type MNV1
2.	pT7:MNV-1_3'Rz_M1	MNV1 M1 cDNA clone	McFadden et al. 2011[10]	Similar to pT7:MNV-1_3'Rz, but with a T5118A mutation that introduces a stop codon 17 amino acids downstream of the VF1 start codon and a silent mutation in VP1
3.	pFS669IG	Mouse CD300lf	Frederic Sorgeloos	
4.	pAJ034IG	Bicistronic with MNV1 VF1 and mCherry	This work	Gateway cloning, codon-optimised

5.	pFS341	Bicistronic with EGFP and mCherry	Frederic Sorgeloos	
6.	pMDLg/pRRE	Encodes Gag and Pol; contains the rev response element	Frederic Sorgeloos	3rd generation lentiviral packaging plasmid
7.	pRSV-Rev	Encodes Rev	Frederic Sorgeloos	3rd generation lentiviral packaging plasmid
8.	pMD2G	VSV-G envelop plasmid	Frederic Sorgeloos	3rd generation lentiviral packaging plasmid
9.	shEGFP	shRNA sequence targeting EGFP	Sigma (SHC005)	MISSION pLKO.1-puro Control Plasmid
10.	shSTING-3	Mouse STING (TMEM173) shRNA	Sigma (SHCLNG-NM_028261)	MISSION shRNA plasmid TRCN0000346266
11.	shMED23-1	Mouse MED23 shRNA	Sigma (SHCLNG-NM_027347)	MISSION shRNA plasmid, TRCN0000341925
12.	shMED23-3	Mouse MED23 shRNA	Sigma (SHCLNG-NM_027347)	MISSION shRNA plasmid, TRCN0000341853
13.	shMED23-6	Human MED23 shRNA	Sigma (SHCLNG-NM_004830)	MISSION shRNA plasmid, TRCN0000218197
14.	shMED23-8	Human MED23 shRNA	Sigma (SHCLNG-NM_004830)	MISSION shRNA plasmid, TRCN0000229869
15.	shMED23-9	Human MED23 shRNA	Sigma (SHCLNG-NM_004830)	MISSION shRNA plasmid, TRCN0000229868
16.	pAJ118IG	HA-STING	This work	Cloned via digestion/ligation, cDNA template from MEFs; N-terminal tag; mouse
17.	pAJ116IG-	HA-EGFP	This work	Gateway cloning; N-terminal tag
18.	pAJ025IG	HA-VF1	This work	Gateway cloning, codon-optimised; N-terminal tag
19.	pAJ182IG	HA-MED23	This work	Gateway cloning, cDNA template from HeLa M cells; N-terminal tag, human
20.	pAJ093IG	FLAG-EGFP	This work	Gateway cloning; N-terminal tag

21.	pAJ117IG	FLAG-STING	This work	Cloned via digestion/ligation, cDNA template from MEFs; N-terminal tag; mouse
22.	pAJ024IG	FLAG-VF1	This work	Gateway cloning, codon-optimised; N-terminal tag
23.	pAJ111IG	FLAG-IRF3-5D	This work	Constitutively active IRF3 mutant (S388D, S390D, S394D, T396D, and S397D); Gateway and Overlap extension PCR cloning, cDNA template from MEFs; N-terminal tag, mouse
24.	pAJ175IG	EGFP-MED23 isoform 1	This work	Cloned via digestion/ligation, cDNA template from HeLa M cells; N-terminal tag, human
25.	pAJ176IG	EGFP-MED23 isoform 2	This work	Cloned via digestion/ligation, cDNA template from HeLa M cells; N-terminal tag, human
26.	pAJ177IG	EGFP-MED23 isoform 6	This work	Cloned via digestion/ligation, cDNA template from HeLa M cells; N-terminal tag, human
27.	IFN-β-luc	IFN-β promoter-driven firefly luciferase	Andrew Bowie	
28.	IFN-λ1-luc	IFN-λ1 promoter-driven firefly luciferase	Jurgen Haas	
29.	NF-kB-luc	Firefly luciferase under the control of an NF-kB-dependent promoter	Andrew Bowie	
30.	pRL-TK	TK promoter-driven renilla luciferase	Andrew Bowie	
31.	pAJ120IG	Flag-p65	This work	Cloned via digestion/ligation, cDNA template from MEFs; N-terminal tag, mouse
32.	p65-HA	Human p65	Irina Udalova	C-terminal tag
33.	pBent2	Empty vector	Irina Udalova	control vector for p65-HA
34.	pTM942	Empty vector	Frederic Sorgeloos	Bicistronic with MCS and mCherry; control vector for pAJ168IG

35.	pFS420	Empty vector	Frederic Sorgeloos	control vector for all plasmids used except pAJ168IG, p65-HA, and pCR3-IRF7
36.	pAJ007IG	Flag-MAVS	This work	Gateway cloning, cDNA template provided by Jonathan C Kagan; N-terminal tag, otherwise wild type, human
37.	pAJ014IG	Flag-mito-MAVS	This work	MAVS with its TMD replaced by the targeting sequence of Bcl-xl; Gateway cloning, cDNA template provided by Jonathan C Kagan
38.	pAJ010IG	Flag-cyto-MAVS	This work	MAVS with its TMD deleted; Gateway cloning, cDNA template provided by Jonathan C Kagan
39.	pAJ008IG	Flag-pex-MAVS	This work	MAVS with its TMD replaced by the targeting sequence of Pex13; Gateway cloning, cDNA template provided by Jonathan C Kagan
40.	pAJ168IG	Human MED23	This work	Bicistronic with mCherry; Gateway cloning, cDNA template from HeLa M cells
41.	pCR3-IRF7	Human IRF7	Jurgen Haas	N-terminal HA tag
42.	pCR3	Empty vector	Jurgen Haas	control vector for pCR3-IRF7

SiRNA transfection

SiRNA transfections were carried out using Lipofectamine RNAiMAX (Invitrogen) according to the manufacturer's protocol. Briefly, cells were seeded in 10cm dishes overnight. On day 2, 30µ Lipofectamine RNAiMAX and 150pmol siRNA were each diluted in 500µl Opti-MEM reduced serum media (ThermoFisher Scientific), following which the two were mixed and incubated at room temperature for 5 minutes, and then added dropwise onto the cells. The cells were then incubated at 37oC for 48hrs and then assessed for knockdown or were re-seeded for downstream

experiments. The siRNA used in this work include siMED23-1 <5′-aggcaaagaagttgggaat-3′> (previously reported[164,165]) and siGFP <5′-gcagcacgacuucuucaagtt-3′>.

Lentivirus transduction

For shRNA transduction, Mission shRNA plasmids (Sigma Aldrich) were transfected together with pMDL g/p RRE, pRSV-Rev, and pMD2G plasmids into HEK293T cells using Lipofectamine 2000. Pooled lentiviral supernatants harvested on days 2 and 3 were used to infect RAW264.7 cells, HeLa M cells, HaCat cells, HEK293T cells, A549 cells, and *Med23*$^{+/+}$ and *Med23*$^{-/-}$ MEFs. Puromycin (Invitrogen) selection was started 72 hrs post-infection. The MEFs and RAW264.7 cells were cultured in 2 μg/ml puromycin until all the control cells were dead and was then maintained in 5 μg/ml puromycin. All the other cell lines were cultured in 1.5 μg/ml puromycin until all the control cells were dead and was then maintained in 5 μg/ml puromycin.

For CD300lf, VF1, and EGFP lentiviral transduction, the pFS669IG, pAJ034IG and pFS341 plasmids, respectively, were transfected together with pMDL g/p RRE, pRSV-Rev, and pMD2G plasmids into HEK293T cells using Lipofectamine 2000. Pooled lentiviral supernatants harvested on days 2 and 3 were used to infect HeLa M cells. CD300lf-transduced HeLa were subsequently selected using 100 μg/ml Hygromycin (Invitrogen), starting 72 hrs post-infection.

Reverse genetics

The MNV1 virus was prepared via reverse genetics as previously described[145,163]. Briefly, $1.5x10^6$ BSR-T7 cells were seeded in a 6-well plate and incubated at 37°C for 3 hrs. The cells were then infected with Fowl pox virus (FPV)-T7 at an MOI of 0.5 pfu/cell in 700µl of cell culture media and incubated at 37°C for 2 hrs (2ml of antibiotic-free media was added 1 hr into the infection). Then, 1µg of the pT7:MNV-1_3'Rz or the pT7:MNV-1_3'Rz_M1 MNV cDNA clones (for the wild type or VF1-deficient M1 mutant, respectively) were transfected using Lipofectamine 2000, according to the manufacturer's instructions. The plate was incubated at 37°C for 2 days, freeze-thawed once (at -80°C overnight or longer), and titred by TCID50.

TCID50

TCID50 by cytopathic effect (CPE) was carried out as previously described[145]. Briefly, 1:10 serial dilutions of the virus preparations were made in cell culture media and aliquoted into wells of a 96-well plate, each in 4 replicates of 50µl. Then, $2x10^4$ RAW264.7 cells in 100µl of cell culture media was added to each well and the plate was incubated at 37°C for 5 days. The cells were subsequently assessed for CPE, and TCID50/ml was calculated using the Spearman & Kärber algorithm[166].

Cell stimulation and infection

Poly (I:C) (P1530, Sigma) and poly (dA:dT) (P1537, Sigma) transfections were carried out on cells seeded in 24-well plates overnight using Lipofectamine 2000, according to the manufacturer's protocol. For the MNV and EMCV infection experiments for RT-qPCR, cells seeded in 24-well plates overnight were incubated in 500 µl of prewarmed fresh media alone or media containing the appropriate amount

of virus at 37°C. The media was changed after 1 hr and the cells were incubated at 37°C for 12 hrs before harvesting for downstream experiments. Infections for western blotting were carried out in the same way but often scaled up to 10cm dishes or T150 flasks. The EMCV is a kind gift from Dr Frederick Sorgeloos (University of Cambridge UK and De Duve institute Belgium).

For experiments involving STING inhibition, cells were pre-treated in DMSO (Sigma), C-176 (Focus Biomolecules), or H-151 (Focus Biomolecules) for 2 hrs before infection or transfection with poly (I:C) or poly (dA:dT), and the drugs are supplemented in the media onwards until the cells are harvested for end-point assays. For experiments involving cGAS inhibition using RU.521 (Invivogen), cells were pre-treated for 3 hrs before infection or transfection, and the drug is supplemented in the media onwards until the cells are harvested for end-point assays.

Luciferase assay

Cells seeded in 24-well plates overnight were transfected with 180ng of the indicated firefly luciferase plasmid and 20ng of the renilla control plasmid, in addition to the expression or empty vectors, using Lipofectamine 2000 and according to the manufacturer's protocol. The media was changed 6 hrs after transfection and the cells were harvested after 24 hrs. For assays involving poly (I:C), cells were either mock transfected or transfected with the indicated amounts poly (I:C) 24hrs after the initial transfection and were harvested after 6 hrs. Cells were harvested in 100 µl of passive lysis buffer, and the samples were analysed in a Glomax luminometer. To calculate the fold induction, the raw relative luciferase unit (RLU) values of the firefly

luciferase were initially normalised to those of the renilla luciferase, and the results were divided by the average of the mock control (empty vector).

Cell fractionation

Cell fractionation was carried out based on a modified REAP protocol[167]. Briefly, the cells were washed in 1 ml of ice-cold PBS twice by centrifuging at 10,000 xg for 10 seconds at 4°C. The cells were then resuspended in 500 µl CF1 lysis buffer (50 mM Tris pH8, 2 mM EDTA, 1% NP-40) supplemented with a protease inhibitors cocktail by pipetting up and down 5 times and 50 µl was aliquoted into a new tube as the whole cell fraction. The remaining sample was centrifuged immediately at 10,000 xg for 10 seconds at 4°C, and 50 µl of the supernatant was aliquoted into a new tube as the cytoplasmic fraction. The remaining supernatant was discarded, and the pellet was resuspended in 500 µl of CF1 buffer and was centrifuged immediately at 10,000 xg for 10 seconds at 4°C. The supernatant was discarded, and the pellet was resuspended in 60 µl CF2 buffer (50 mM Tris pH8, 2 mM EDTA, 1% NP-40, 250 mM NaCl), kept on ice for 10 minutes, and centrifuged at 10,000 xg for 10 minutes at 4°C. The supernatant was transferred into a new tube as the nuclear fraction. To adjust the final NaCl concentration to 150 mM, 75 µl of CF2 was added each to the whole cell and cytoplasmic fractions, and 20 µl of CF1 buffer to the nuclear fraction. The samples were mixed with western blotting buffer (2% SDS, 10% glycerol, 0.002% bromophenol blue, 0.0625M Tris-Cl pH 6.8, 5% 2-mercaptoethanol), heated at 95°C for 5-10 minutes, and kept at -20°C or used immediately for western blotting.

Western blotting

Cells were washed in ice-cold PBS twice, resuspended in CF2 buffer and supplemented with a protease inhibitors cocktail (and a phosphatase inhibitors cocktail when phospho-proteins were of interest), and kept on ice for 20 minutes. The sample was pipetted up and down several times and was centrifuged immediately at 10,000 xg for 10 minutes at 4°C. The supernatant was transferred to a new tube and the pellet was discarded. The NaCl concentration was adjusted to 150 mM by adding appropriate amounts of the CF1 buffer, the sample was quantified using the BCA assay (Thermo Scientific) according to the manufacturer's recommendations. The sample was then mixed with SDS polyacrylamide gel electrophoresis (PAGE) sample buffer (2% SDS, 10% glycerol, 0.002% bromophenol blue, 0.0625M Tris-Cl pH 6.8, 5% 2-mercaptoethanol), heated at 95°C for 5 minutes, and kept at -20°C or used immediately for SDS PAGE. Transfers were made onto 0.45µm nitrocellulose membranes. The membranes were blocked in 5% milk PBST for 1 hr at room temperature, and the primary and secondary antibodies were incubated at 4°C overnight and 1hr at room temperature respectively, with three 5-minute washes in between incubations. The membranes were subsequently scanned on an Odyssey CLx imager (LI-COR) and the results were analysed using the Image Studio Lite software version 5.2.5 (LI-COR). Antibodies used in this work are listed in Table 2.2. Note that all western blotting for MED23 was done using the BD biosciences anti-MED23 antibody, unless otherwise stated.

Table 2.2: List of antibodies used for western blots and Co-IP

sn	Target	Supplier	Catalogue Number	Dilution
1.	Mouse MAVS	Cell signalling	#4983	1:500
2.	Human MAVS	Santa Cruz	sc-166583	1:100
3.	IkBα	Cell signalling	#4814S	1:500

4.	IKKα	Santa Cruz	sc-7218	1:100
5.	NF-κB p65	Santa Cruz	sc-8008	1:250
6.	Mouse GAPDH	Ambion	AM4300	1:20000
7.	Human GAPDH	Protein Tech	10494-1-AP	1:20000
8.	HA	Biolegend	901503	1:500
9.	Flag M2	Sigma	F1804	1:2000
10.	Human IRF3	Abclonal	A11373	1:250
11.	Human pIRF3	Abcam	ab138449	1:500
12.	Mouse IRF3	Cell signalling	#4302S	1:500
13.	Mouse pIRF3	Cell signalling	#4947	1:500
14.	TBK1	Cell signalling	#3013S	1:500
15.	STAT1	Abcam	ab92506	1:500
16.	pSTAT1	Cell signalling	9167S	1:500
17.	ISG56	Pierce	PA3-848	1:500
18.	RIG-I	Santa Cruz	sc-376845	1:100
19.	STING (D2P2F)	Cell signalling	#13647	1:500
20.	Mouse pSTING	Cell signalling	#72971S	1:500
21.	VF1	Abmart	4K5	1:100
22.	NS7	Non-commercial	-	1:500
23.	mCherry	Source BioScience	LS-C204825	1:2000
24.	GFP	Sigma	G1544	1:2000
25.	MED23 (HPA)	Sigma (HPA)	HPA070341	1:500
26.	MED23 (BD)	BD biosciences	550429	1:500
27.	hnRNPI	Santa Cruz	sc-16547	1:250

Co-immunoprecipitation

Co-immunoprecipitation was carried out based on a protocol modified from van Essen *et al.*[168] Briefly, the cells were washed in 1 ml of ice-cold PBS twice by centrifuging at 10,000 xg for 10 seconds at 4ºC. The cells were then resuspended in 600 µl L2 lysis buffer (50 mM Tris pH8, 2 mM EDTA, 0.1% NP-40, 10% glycerol, 250 mM NaCl) supplemented with a protease inhibitors cocktail and kept on ice for 20 minutes. The sample was pipetted up and down several times and was centrifuged at 10,000 xg for

10 minutes at 4°C. The supernatant was transferred to a new tube and the pellet was discarded. To adjust the NaCl concentration to 150 mM, 200 µl L1 lysis buffer (50 mM Tris pH8, 2 mM EDTA, 0.1% NP-40, 10% glycerol) was added, and 80 µl of this adjusted sample was transferred to a new tube as the whole cell lysate. To the remaining sample, 60 µl of resuspended 50% slurry of anti-FLAG M2 antibodies conjugated agarose beads were added and the samples were incubated on a rotator at 4°C for 2 hrs. The sample was centrifuged at 300 xg for 1 minute at 4°C, 80 µl of the supernatant was transferred to a new tube as the flow through and the rest was discarded. The pellet was washed in 1 ml of L3 buffer (50 mM Tris pH8, 2 mM EDTA, 0.1% NP-40, 10% glycerol, 150 mM NaCl) 4 times by centrifuging at 300 xg for 1 minute at 894°C and resuspended in 80 µl of L3 buffer. The samples were then mixed with western blotting buffer (2% SDS, 10% glycerol, 0.002% bromophenol blue, 0.0625M Tris-Cl pH 6.8, 5% 2-mercaptoethanol), heated at 95°C for 5 minutes, and kept at -20°C or used immediately for western blotting.

Chromatin immunoprecipitation

Chromatin immunoprecipitation was carried out using the Go-ChIP Protein G Enzymatic Kit (Biolegend), according to the manufacturer's protocol. Briefly, following cell stimulation with poly (I:C), the cells were trypsinised and washed in PBS. Crosslinking was carried out by incubating the cells in serum-free DMEM containing 1% formaldehyde (Sigma) for 10 minutes at room temperature, and the reaction was quenched by incubating the cells in 0.65M glycine at room temperature for 5 minutes. The cells were lysed in the hypotonic buffer, followed by incubation of the nuclei in digestion buffer. After a quick DNA quantification, 1U of shearing

cocktail was added for every 5µg of chromatin and the sample was incubated on the heat block at 37°C for 5 minutes. The cells were then lysed in lysis buffer and the chromatin was aliquoted and stored at -80°C while shearing efficiency analysis is performed.

After assessing shearing efficiency, 1µg of antibodies per 3µg of chromatin and the sample was incubated on a rotator at 4°C overnight. Immunoprecipitation was carried out with the protein G spin columns provided, followed by reverse crosslinking with NaHCO3 and NaCl at 65°C for 2 hrs. The sample was treated with proteinase K at 37°C for 1 hr, and the DNA was column-purified after which it was kept at -20°C or used immediately for qPCR.

The antibodies used include anti-RNA Polymerase II Antibody (Biolegend, 904003) and the IgG1 κ Isotype Ctrl Antibody (Biolegend, 401401). The primers used are listed in Table 2.3.

Table 2.3: List of ChIP-qPCR primers

sn	**Target**	**Sequence (FWD, REV)**	**Reference**
1.	*IFNB1* promoter	TGGCACAACAGGTAGTAGGCGACA, TGGAGAAGCACAACAGGAGAGCA	Freaney et al., 2013[169]
2.	*IFNL1* promoter	CTTCCTCTCTGCCACTCAGG, ACTGCTTCCCCAGCGGCATG	Lee et al., 2014[170]
3.	*IFIT1* promoter	ACCACCTTTACAGCAACCATGG, TCCTTGTTCCCCATCAGCAGTA	Atianand et. al., 2016[171]
4.	*RSDA2* promoter	CCTGTTCTGCTGGCTGAGAATA, GAGTGCTGTTCCCATCTTCCTG	Atianand et. al., 2016[171]
5.	*IL6* promoter	AGACTTCCATCCAGTTGCCT, CAGGTCTGTTGGGAGTGGTA	Atianand et. al., 2016[171]

6.	*CXCL10* promoter	CCGTCATTTTCTGCCTCATC, CTGCAAGCTGAAGGGATTTC	Atianand et. al., 2016[171]
7.	*GAPDH* promoter	TAGGACTGGATAAGCAGGGC, GAACAGGGAGGAGCAGAGAG	Atianand et. al., 2016[171]

Relative qPCR

RNA extraction with on-column DNAse treatment were done using the GenElute Mammalian Total RNA Miniprep Kit (Sigma-Aldrich) according to the manufacturer's protocol. Briefly, sample was lysed in 250µl of lysis buffer and kept on a rocker for 5 minutes. 250µl of 70% ethanol was added and mixed well, before transferring into the binding column. The column was centrifuged at maximum speed for 30 seconds and the flow through was discarded. 250µl of Wash Solution 1 was added and the column was centrifuged at maximum speed for 30 seconds. 50µl of master mix containing 1x DNAse I buffer and 1U of RNAse-free DNAse I was added to the column and incubated at 37^{o}C for 20 minutes. 250µl of Wash Solution 1 was then added and the column was centrifuged at maximum speed for 30 seconds. The flow through was discarded and 250µl of Wash Solution 2 was added and the column was centrifuged at maximum speed for 30 seconds. This was repeated once, after which the column was placed onto a new collection tube and centrifuged at maximum speed for 1 minute. The column was then re-fitted with a new collection tube, and RNA was eluted in 50µl of PCR-grade water. RNA was quantified using the Nanodrop 1000 (ThermoFisher Scientific) and was used immediately for downstream experiments or stored at -80^{o}C.

cDNA was synthesized using the M-MLV Reverse Transcriptase (Promega), according to the manufacturer's protocol. Briefly, 5µl of RNA (0.5-2µg) was mixed with 5µl of 50µM random hexamers (Roche) and heated at 70°Cfor 5 minutes. The tube was chilled on ice for 1 minute, and 1µl of 10µM dNTPs, 5µl of 5x M-MLV buffer (250mM Tris-HCl (pH 8.3 at 25°C), 375mM KCl, 15mM MgCl2, 50mM DTT), 0.5µl of RNAseOUT (20U, Invitrogen), 0.5µl of M-MLV enzyme (100U) and 8µl of PCR-grade water. The tube was centrifuged briefly to collect the contents at the bottom, incubated at 37°C for 1 hr and then 95°C for 5 minutes. The sample was then diluted to 90µl with PCR-grade water.

qPCR was carried out using the SYBR Green mastermix containing 2.5mM $MgCl_2$, 400µM dNTPs, 1/10,000 SybrGreen (Molecular Probes), 1M Betaine (Sigma), 0.05U/µl of Gold Star polymerase (Eurogentec), 1/5 10X Reaction buffer (750 mM Tris-HCl pH 8.8, 200 mM [NH4]2SO4, 0.1 % [v/v] Tween 20, Without MgCl2), and 28/10,000 ROX Passive Reference buffer (Eurogentec). 5µl of sample from the cDNA synthesis or from the ChIP experiment was added to 0.25µl each of the forward and reverse primers (2.5pmol/µl final concentration), 12.5µl of the master mix and 7µl of PCR-grade water. Plate was centrifuged briefly to collect the contents at the bottom and ran on a ViiA 7 Real-Time PCR System (ThermoFisher Scientific), with a 15-second 95°C denaturation step and a 1-minute 60°C annealing/extension step for 40 cycles. Relative gene expression was calculated using the Livak method (ΔΔCt) relative to mock-transfected conditions,[172] and normalized to a house keeping gene (*Gapdh* for all the mouse samples, and β-actin for the human samples). Primers used in this work are listed in Table 2.4.

Table 2.4: List of qPCR Primers used

sn	**Target**	**Lab no.**	**Sequence (FWD, REV)**	**Ref.**
1.	Mouse *Ifnb1*	IGUC0339 IGUC0340	ATGAACAACAGGTGGATCCTCC AGGAGCTCCTGACATTTCCGAA	Petro 2005[173]
2.	Mouse *Ifnl2*	IGUC1998 IGUC1999	GGATGCCATCGAGAAGAGGCTG CTGTGTACAGGTCTGCAGCTGG	This work
3.	Mouse *Rsad2*	IGUC1898 IGUC1899	GGTTCAAGGACTATGGGGAGTATTTGGAC GAAATCTTTCTGCTTCCCTCAGGGCATC	This work
4.	Mouse *Isg15*	IGUC1902 IGUC1903	GGTAACGATTTCCTGGTGTCCG GCTCAGCCAGAACTGGTCTTCG	This work
5.	Mouse *Il6*	IGUC1904 IGUC1905	GAAGTTCCTCTCTGCAAGAGACTTCCATC CAACTCTTTTCTCATTTCCACGATTTCCC	This work
6.	Mouse *Gapdh*	IGUC0945 IGUC0946	CATGGCCTTCCGTGTTCCTA GCGGCACGTCAGATCCA	-
7.	Mouse *Med23*	IGUC4053 IGUC4055 IGUC4054	AATTAGCTGCTTGGCGGC (FWD) GGGCTGTGTTGGCCATGA (Rev. for qPCR) TCATTGCAAAGGCGTGCG (Rev. for PCR)	This work
8.	Mouse *Irf3*	IGUC4051 IGUC4052	CTGGGTGCCTCTCCTGAC GCCCCAAGATCAGGCCAT	This work
9.	Mouse *p65*	IGUC4056 IGUC4057	GACTGCCGGGATGGCTAC ACACACTGGATCCCCAGG	This work
10.	Mouse *Ikkb*	IGUC4060 IGUC4061	AGCCTGCTACTCAGTGCA TTCCGCTTGGGCTCCTGA	This work
11.	Mouse *Tbk1*	IGUC4058 IGUC4059	GCCTGCAGAACTGCCAGT CCGTCTTCTTGTGGACGG	This work
12.	Mouse *Mavs*	IGUC4062 IGUC4063	CAGGCTCTCAGCCCTCAG CGGTTGGAGACACAGGTC	This work
13.	Mouse *Sting*	IGUC4112 IGUC4113	GTCCAGTCCAGGTACCAGG CCATACAGTGGATGGGGCA	This work
14.	Human β-actin	IGUC0784 IGUC0785	TTCTACAATGAGCTGCGTGTG GGGGTGTTGAAGGTCTCAAA	-
15.	Human *IFNB1*	IGUC0772 IGUC0773	CAGAAGGAGGACGCCGCATTGAC CCAGGCACAGTGACTGTACTCC	-
16.	Human *IFNL1*	IGUC2600 IGUC2601	GAAGCCTCAGGTCCCAATTC CGCCTTGGAAGAGTCACTCA	-

17.	Human *IFNL2*	IGUC2602 IGUC2603	GAACCGGTACAGCCAATGGT AGTTCCGGGCCTGTATCCAG	-
18.	Human *IFNL3*	IGUC2604 IGUC2650	TAAGAGGGCCAAAGATGCCTT CTGGTCCAAGACATCCCCC	-
19.	Human *RSAD2*	IGUC2411 IGUC2412	CCTGTCCGCTGGAAAGTGTT GACACTTCTTTGTGGCGCTC	This work
20.	Human *ISG15*	IGUC2409 IGUC2410	GTGGACAAATGCGACGAAC CGAAGGTCAGCCAGAACAG	This work
21.	Human *IL6*	IGUC1231 IGUC1232	ACTCACCTCTTCAGAACGAATTG CCATCTTTGGAAGGTTCAGGTTG	-
22.	Human *TNFA*	IGUC1225 IGUC1226	CCTCTCTCTAATCAGCCCTCTG GAGGACCTGGGAGTAGATGAG	-
23.	EMCV	IGUC2043 IGUC2044	GCCGAAAGCCACGTGTGTAA AGATCCCAGCCAGTGGGGTA	-

Confocal microscopy

The cells were seeded on cover slips overnight and were either mock transfected or transfected with 1 μg/ml of poly (I:C) using Lipofectamine 2000, according to the manufacturer's protocol. The cells were fixed in 4% paraformaldehyde for 15 minutes, washed twice with PBS, and blocked in 5% normal goat serum in PBST for 1 hr. The cells were then incubated with the primary antibody diluted in blocking buffer at room temperature for 1hr, washed 3 times with PBST for 5 minutes each, incubated with the secondary antibody diluted in blocking buffer at room temperature for 1hr, washed 3 times with PBST for 5 minutes each, and then washed twice in PBS. The cover slips were then mounted on slides with Mowiol (Sigma) containing the DAPI nuclear stain. The cells were visualised on the Leica SP5 confocal microscope, and data were analysed with Image J.

Statistical analysis and software

Prism 6.0 (Graph Pad) was used for all statistical analysis, and one-way repeated measures ANOVA with Bonferroni multiple comparisons tests was applied to determine statistical significance, unless where indicated otherwise. In all cases, 'ns', *, **, ***, and **** are used to denote $p>0.05$, $p\leq0.05$, $p\leq0.01$, $p\leq0.001$ and $p\leq0.0001$ respectively. The Image J software was used for all confocal micrograph preparation and Image Studio Lite 5.2 was used for western blot quantification. Clustal Omega was used for all sequence alignments, and Snapgene 4.2 was used for primer design and cloning strategies.

Chapter 3

A RIG-I/STING-dependent innate immune response pathway restricts replication of Noroviruses

Background

MDA5 (IFIH1) was shown to play a central role in IFN induction following infection with both acute and persistent murine noroviruses[122,123]. However, the increase in viral titres observed in MNV-infected *Ifih1* knockout mice and BMDCs are only moderate, and MNV infection is not lethal in *Ifih1* knockout mice in contrast to *Stat1* knockout mice[19,122], indicating the potential presence of other factors that restrict viral replication. While studying the MNV VF1 protein, we observed that it inhibits IFN induction only in STING-competent cells, and we therefore hypothesized that STING plays a role in IFN responses against MNV. This chapter aims to (1) define the function of STING in the restriction of MNV1, (2) determine the receptor responsible for STING activation in MNV1-infected cells, and (3) clarify the mechanism of VF1 antagonism of host IFN responses. We show that both RIG-I and STING contribute to a robust IFN response to infection with MNV1 in primary BMDMs and RAW264.7 cells, with a significant increase in viral titres following infection in RIG-I- and STING-deficient cells. We also show that STING is non-canonically activated in MNV1 infected cells, in a manner that may be partly, but not completely, RIG-I-dependent. Furthermore, our data indicate that the MNV VF1 protein binds to STING and can inhibit IFN induction downstream of RIG-I. Taken together, our data demonstrate the presence of a RIG-I/STING-dependent innate response pathway that restricts the replication of noroviruses, and an attempt by the murine norovirus to subvert it through expression of an accessory protein.

Results

3.1. VF1 inhibits IFN induction only in STING-competent cells

The MNV VF1 protein counteracts induction of type I IFNs through an as yet unknown mechanism[10,11]. A common and considerable challenge in studying the functions of MNV proteins, including VF1, is that primary murine macrophages and cell lines are often difficult to transfect[174,175], and the transfection process itself can lead to induction of IFNs in them. To circumvent these limitations, we transduced two easy-to-transfect cell lines, HeLa M and HEK293T, with the MNV receptor CD300lf[24,25]. To examine whether VF1 inhibits IFN induction in human cells, the CD300lf-expressing HeLa M and HEK293T cells were infected with wild-type MNV1 or the previously described VF1-deleted mutant M1 in which a stop codon was introduced at position 17 of VF1 without affecting the underlying VP1 sequence[10]. Interestingly, whereas RAW264.7 and HeLa M cells infected with the M1 virus induced higher levels of IFN-β compared to cells that were infected with wild type MNV1, there was no significant difference in IFN-β induction in HEK293T cells infected with either the wild type virus or M1 (figure 3.1a). These findings suggest that a factor or pathway present in HeLa M and RAW264.7 cells, but absent in HEK293T is required for the phenotypic differences observed between cells infected with the wild type and M1 viruses.

Both being epithelial-like cell lines, HeLa M and HEK293T cells likely express the same repertoire of components of the IFN response pathway, with an exception of the adapter protein STING that is only marginally expressed in HEK293T cells, compared to HeLa M cells (Burdette *et al.*[176], and figure 3.1b). To further examine IFN induction in HeLa M and HEK293T cells following infection with MNV, the cells were either

mock-infected, or infected with wild type MNV1 or M1 at a high multiplicity of infection. The cells were then harvested 10 hrs post infection and the lysates were assessed using western blotting. As shown in figure 3.1c (right panel), there was no difference in the levels of phospho-IRF3 and phospho-STAT1 between the mock-infected cells and cells infected with either wild type or M1 MNV1 in HEK293T cells. This contrasts with infection in HeLa cells (figure 3.1c, left panel) where a significant increase is seen in the levels of both phospho-IRF3 and phospho-STAT1 following infection with MNV1. The HEK293T cells have an intact RNA sensing pathway as they are able to phosphorylate IRF3 and STAT1 in response to poly (I:C) transfection (figure 3.1d). Taken together, these data demonstrate an attenuation of the IFN response to MNV1 in HEK293T cells, compared to HeLa M and RAW264.7 cells, and suggest a role for STING in the IFN response against noroviruses.

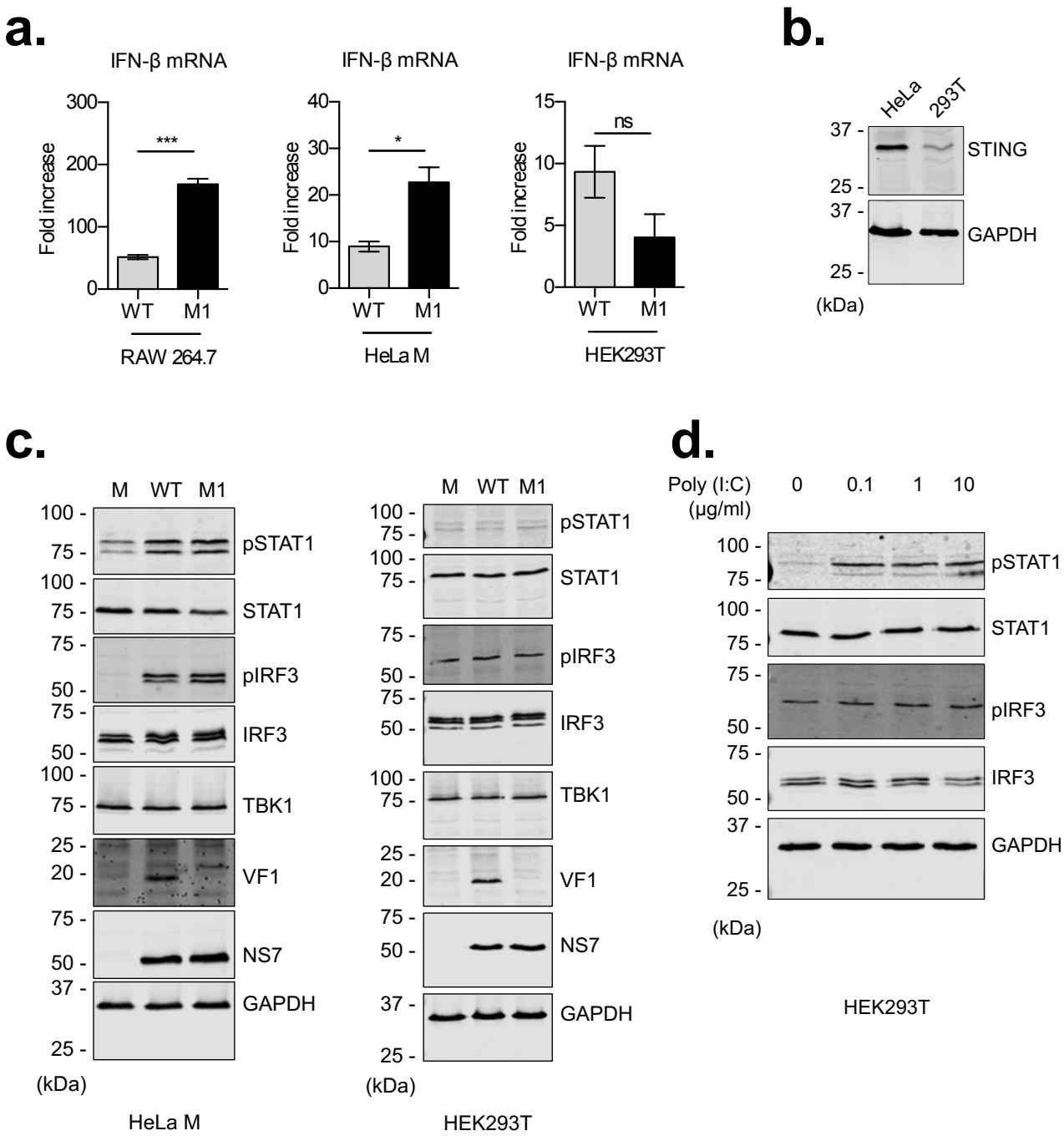

Figure 3.1. VF1 inhibits IFN induction only in STING-competent cells

(a) RAW264.7 were infected with MNV1 at an MOI of 0.01 and harvested 24hrs post-infection, while HeLa M and HEK293T cells were infected at an MOI of 10 and harvested 10hrs after infection. RNA from these samples were subjected to RT-qPCR. Data represent experiments done in triplicates, and is shown relative to mock-infected cells and normalised to mouse *Gapdh* for the RAW264.7 cells, and human β-actin for the HeLa M and HEK293T cells.

(b) Lysates from HeLa M and HEK293T cells were assessed by western blotting for MAVS, STING and GAPDH.

(c) HeLa M and HEK293T cells were either mock-infected, or infected at an MOI of 10 with either wild-type MNV1 or the VF1-deleted M1 mutant. The cells were harvested 10hrs after infection and assessed by western blotting for the indicated proteins.

(d) HEK293T cells were transfected with indicated amounts of poly (I:C). The cells were harvested 6hrs after transfection and assessed by western blotting for the indicated proteins.

3.2. Small-molecule inhibitors of STING reduce type I IFN induction in MNV1 infected RAW264.7 cells and BMDMs

To explore the role of STING in the antiviral response against MNV, we made use of the recently described covalent small-molecule inhibitors of STING; C-176 and H-151[177]. As shown in figure 3.2a, both drugs are able to inhibit induction of IFN-β following transfection of poly (dA:dT) in RAW264.7 cells, but not poly (I:C), consistent with previously published results. To determine whether STING is required for induction of IFNs following infection with MNV, RAW264.7 cells were pre-treated with DMSO or titrated doses of C-176 or H-151, and then infected with wild type MNV1 at a high MOI. The cells were harvested 9 hrs post infection and subjected to RT-qPCR. As shown in figure 3.2b, there is a significant dose-dependent decrease in IFN-β induction in cells treated with either C-176 or H-151, compared to DMSO. These data indicate that STING is required for a robust induction of IFNs in RAW264.7 cells infected with MNV1.

To examine the role of STING in primary macrophages, bone marrow cells from C57BL/6 mice were differentiated into bone marrow-derived macrophages (BMDMs), pre-treated with either DMSO or titrated doses of C-176 or H-151 for 2 hrs, and subsequently infected with MNV1 at a high MOI. The cells were harvested 12 hrs post infection and subjected to RT-qPCR. As shown in figure 3.2c, and consistent with data from assays in RAW264.7 cells, there is a significant decrease in IFN-β induction in MNV-infected BMDMs following treatment with the small-molecule inhibitors of STING in a dose-dependent manner. To determine the role of STING in restricting MNV1 replication, BMDMs were pre-treated with DMSO or titrated doses of C-176 or H-151, and then infected with MNV1. The samples were harvested at different time points post infection and infectious viral titres were determined using TCID50 in RAW264.7 cells. As shown in figure 3.2d, there is a significant increase in viral titres following treatment with STING inhibitors in a dose-dependent manner. Altogether, these data indicate that STING plays an important role in the antiviral responses to MNV1 in both primary macrophages and cell lines.

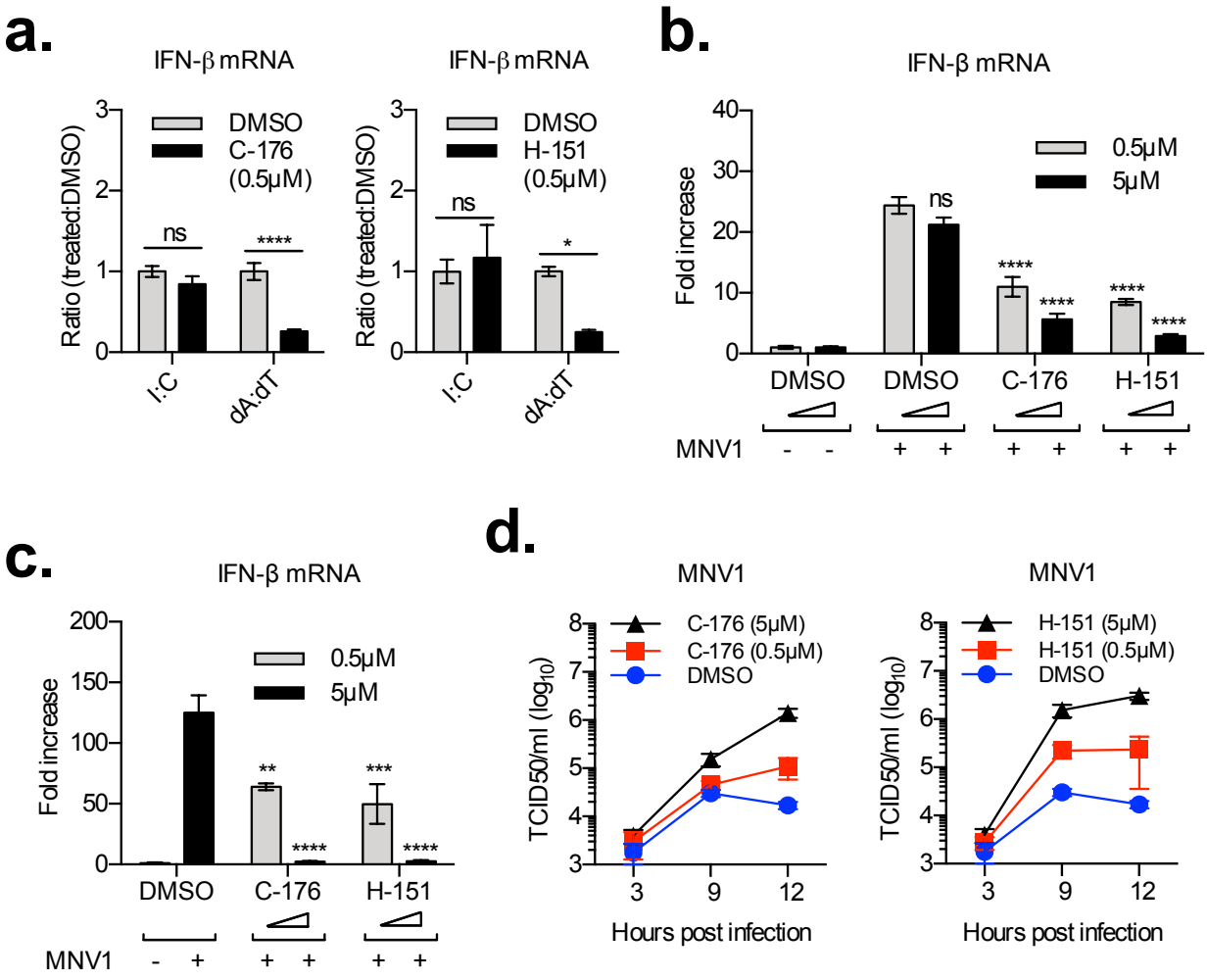

Figure 3.2. Small-molecule inhibitors of STING reduce type I IFN induction in MNV1-infected RAW264.7 cells and BMDMs

(a) RAW267.4 cells pre-treated with DMSO, 0.5μM C-176 or 0.5μM H-151 for 2 hrs, were either mock-transfected, or transfected with 1μg poly (I:C) or poly (dA:dT). The cells were harvested after 2 hrs and subjected to RT-qPCR. Data represent experiments done in triplicates, and is shown relative to mock-transfected cells, and normalised to mouse *Gapdh*

(b) RAW267.4 cells pre-treated with DMSO, or indicated amounts of C-176 or H-151 for 2 hrs, were either mock-infected or infected with wild-type MNV1 at an MOI of 10. The cells were harvested 9 hrs post-infection and subjected to RT-qPCR. Data represent two independent experiments done in triplicates, and is shown relative to mock-infected cells, and normalised to mouse *Gapdh*

(c) BMDM cells pre-treated with DMSO, or indicated amounts of C-176 or H-151 for 2 hrs, were either mock-infected or infected with wild-type MNV1 at an MOI of 10. The cells were harvested 12 hrs post-infection and subjected to RT-qPCR. Data represent two independent experiments done in triplicates, and is shown relative to mock-transfected cells, and normalised to mouse *Gapdh*

(d) BMDM cells pre-treated with DMSO, or indicated amounts of C-176 (left panel) or H-151 (right panel) for 2 hrs, were either mock-infected or infected with wild-type MNV1 at an MOI of 10. The samples were harvested 12 hrs post infection and infectious viral titres were determined using TCID50 in RAW267.4 cells. Data represent two independent experiments, each done in triplicates.

3.3. STING depletion impairs induction of type I IFNs in MNV1-infected RAW264.7 cells

To confirm the requirement for STING in the restriction of MNV, RAW264.7 cells were transduced with either a control shRNA (shEGFP) or shRNA targeting mouse STING (shSTING-3). STING knockdown was assessed by RT-qPCR and western blotting (figure 3.3a). The cells were then either mock transfected or transfected with poly (I:C) or poly (dA:dT) for 3hrs, and assessed by RT-qPCR. As shown in figure 3.3b, the cells expressing shRNA targeting STING showed a significant reduction in IFN-β induction following poly (dA:dT) transfection, but not poly (I:C) as expected. The cells expressing shRNA targeting STING showed a significant decrease in IFN-β induction following infection with MNV1 (figure 3.3c) at both high and low MOI, in keeping with data from the small-molecule inhibition experiments, with a corresponding increase in viral titres (figure 3.3d). Overall, these data confirm a role for STING in the antiviral responses to MNV1 infection.

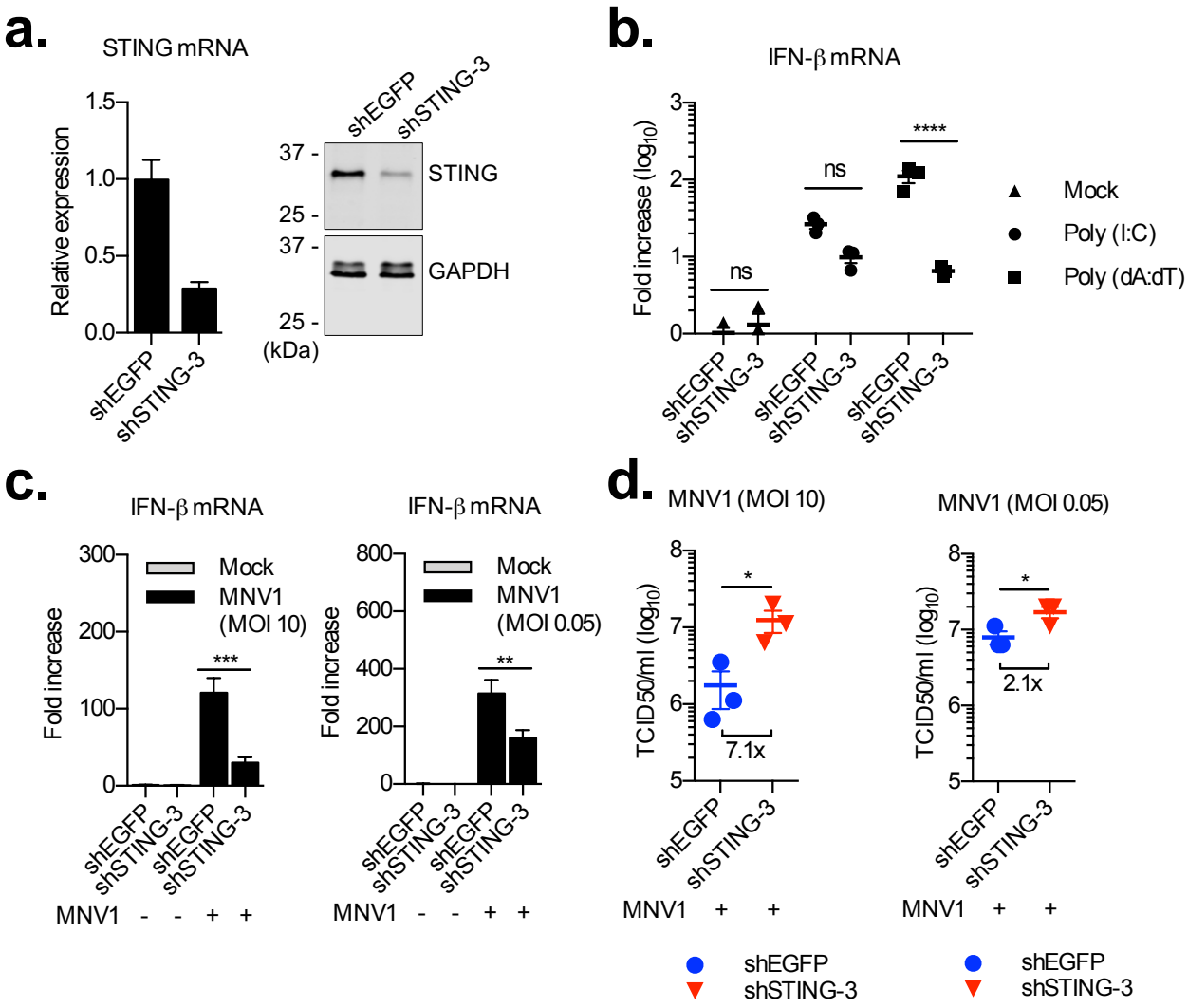

Figure 3.3. STING knockdown impairs induction of type I IFNs in MNV1-infected RAW264.7 cells

(a) RAW264.7 cells stably transduced with control shRNA (shEGFP) or shRNA targeting mouse STING (shSTING-3) were lysed and assessed for STING mRNA via RT-qPCR (left panel) or analysed via western blotting (right panel). Data in the left panel is presented relative to control and normalised to *Gapdh* (n=3).

(b) RAW264.7 cells stably transduced with control shRNA (shEGFP) or shRNA targeting mouse STING (shSTING-3), were mock transfected, transfected with 1µg/ml of Poly (I:C), or with 1µg/ml of Poly (dA:dT) for 6hrs, and were subsequently harvested and assessed for IFN-β mRNA using RT-qPCR. Data is expressed relative to control and normalised to *Gapdh* (n=3).

(c) and (d) RAW264.7 cells stably transduced with control shRNA (shEGFP) or shRNA targeting mouse STING (shSTING-3), were mock infected or infected with wild-type MNV1 at an MOI of 10 and 0.05, and harvested at 9 hrs and 24 hrs post infection, respectively. Samples were assessed for IFN-β mRNA via RT-qPCR (c), or infectious viral titres were determined using TCID50 in RAW264.7 cells (d). Data in (c) is presented relative to control and normalised to *Gapdh* (n=3 in both panels).

3.4. STING is non-canonically activated in MNV1 infected cells partly in a RIG-I-dependent manner

Canonical activation of STING following sensing of foreign or mis-localised DNA is marked by its dimerization and phosphorylation by TBK1 (figure 3.4a), followed by translocation from the ER to perinuclear vesicles[57,178]. A recent study that explored the role of STING in the restriction of a broad range of RNA viruses noted that neither phosphorylation nor translocation of STING occurs following infection with VSV, SINV, SeV, ISVP and IAV[70]. However, in that study, even though STING was shown to play an important role in controlling viral infections, it did so in an IFN-independent manner. Studies that showed a role for STING in IFN induction following infection with RNA viruses, including IAV and JEV, also demonstrated STING dimerization and translocation[68,69]. To assess STING activation in cells infected with MNV, HeLa M cells expressing the MNV receptor CD300lf and BMDMs were infected with MNV1 at a high MOI and probed for STING phosphorylation by western blotting. As shown in figures 3.4b and 3.4c, there was no increase in phosphorylation of STING in HeLa M cells and BMDMs infected with MNV1 compared to mock-infected cells, suggesting that STING activation in MNV-infected cells is likely to occur in a non-canonical manner, akin to that seen in infection with other RNA viruses as reported by Franz *et al*.[70], or similar to the recently described cGAS-independent IFI16-STING-TRAF6 pathway that induces gene expression via NF-kB following etoposide-induced nuclear DNA damage[179].

Next, the upstream receptor that mediates STING activation in MNV-infected cells was examined. Several studies in the past have linked RIG-I detection of viral RNA to activation of STING in cells infected with RNA viruses[66,67,69,70]. To examine the

role of RIG-I in IFN induction in MNV-infected cells, wild type and RIG-I-deficient BMDMs (figure 3.4d) were infected with MNV1 at a high MOI and harvested 12 hrs post infection. A significant decrease in induction of both type I and III IFNs was seen in the *Ddx58*$^{-/-}$ cells following MNV infection compared to *Ddx58*$^{+/+}$ cells (figure 3.4e), with a corresponding decrease in induction of ISGs (figure 3.4f). To determine if RIG-I is required for activation of STING, wild type and RIG-I-deficient BMDMs were infected with MNV1 following pre-treatment with either DMSO or H-151. Infectious viral titres were then obtained via TCID50 in RAW264.7 cells. As shown in figure 3.4g, there was an increase in viral titres in *Ddx58* knockout cells compared to the wild type. Interestingly, although there was generally more virus following STING inhibition than there was in the wild type or *Ddx58* knockout cells treated with DMSO, there was no difference between wild type and *Ddx58* knockout cells treated with H-151, suggesting that RIG-I is required, albeit partly, for the STING-dependent restriction of MNV.

Considering that the cGAS-dependent activation of STING has been implicated in restricting at least one other RNA virus[62,63], the role of cGAS during MNV infection was explored. A small-molecule inhibitor of murine cGAS, RU.521, was recently described, and was shown to inhibit IFN induction downstream of the cGAS-STING pathway, but not in cells stimulated with synthetic 5'-triphosphorylated hairpin RNA or dsRNA[180,181]. However, in our hands, doses sufficient enough to show moderate inhibition of the cGAS-STING pathway in RAW264.7 cells also inhibited the IFN response to poly (I:C) (figure 3.4h). This means that although there was a significant decrease in IFN-β induction in MNV1-infected cells pre-treated with RU.521 (figure

3.4i), it is not clear whether this was due to inhibition of cGAS alone or due to an off-target inhibition of viral RNA detection.

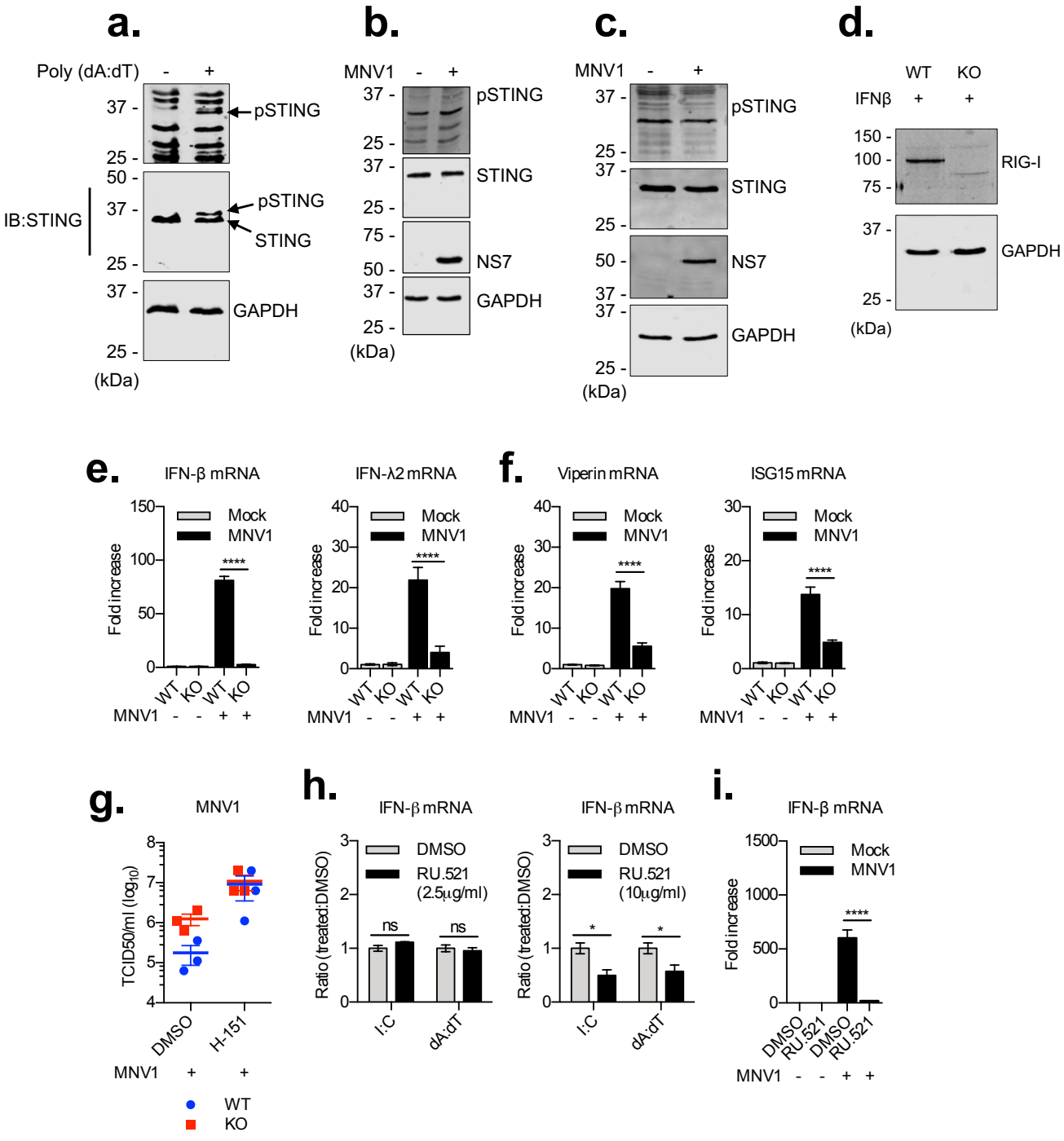

Figure 3.4. STING is non-canonically activated in MNV1 infected cells, partly in a RIG-I-dependent manner

(a) CD300lf+ HeLa M cells were either mock-transfected or transfected with 10μg/ml of poly (dA:dT). The cells were harvested 3 hrs later and assessed via western blotting using the indicated antibodies.

(b) and (c) CD300lf+ HeLa M cells (b) or BMDM cells (c) were either mock-infected or infected with wild-type MNV1 at an MOI of 10. The cells were harvested 10 hrs post-infection and assessed by western blotting for STING, pSTING, MNV NS7, and GAPDH.

(d) *Ddx58*$^{+/+}$ (WT) and *Ddx58*$^{-/-}$ (KO) BMDM cells were treated with 1000 U/ml of mouse IFN-β. The cells were harvested 4 hrs later and assessed by western blotting for RIG-I and GAPDH.

(e) and (f) *Ddx58*$^{+/+}$ (WT) and *Ddx58*$^{-/-}$ (KO) BMDM cells were either mock-infected or infected with wild-type MNV1 at an MOI of 10. The cells were harvested 12 hrs post-infection and subjected to RT-qPCR. Data represent two independent experiments each done in triplicates, and is shown relative to mock-transfected cells, and normalised to mouse *Gapdh*.

(g) *Ddx58*$^{+/+}$ (WT) and *Ddx58*$^{-/-}$ (KO) BMDM cells were either mock-infected or infected with wild-type MNV1 at an MOI of 10 following pre-treatment with DMSO or 5μM H-151. The cells were harvested 12 hrs post-infection and viral titres were assessed by TCID50 in RAW264.7 cells (n=3).

(h) RAW267.4 cells pre-treated with DMSO or indicated doses of RU.521 (2.5μg/ml and 10μg/ml for the left and right panels, respectively) for 3 hrs, were either mock-transfected, or transfected with 1μg poly (I:C) or poly (dA:dT). The cells were harvested after 2 hrs and subjected to RT-qPCR. Data is shown relative to mock-transfected cells and normalised to mouse *Gapdh* (n=3).

(i) RAW267.4 cells pre-treated with DMSO, or 10μg/ml of RU.521 for 3 hrs, were either mock-infected or infected with wild-type MNV1 at an MOI of 10. The cells were harvested 9 hrs post-infection and subjected to RT-qPCR. Data is shown relative to mock-infected cells and normalised to mouse *Gapdh* (n=3).

3.5. VF1 interacts with STING and inhibits induction of IFNs downstream of RIG-I

Having determined that the MNV VF1 protein is only able to inhibit IFN induction in the presence of STING, a literature search was performed to identify viral proteins that are known to counteract STING, in order to determine if VF1 has any previously described feature utilized in counteracting STING activation and/or function. We

found a highly conserved LXCXE motif between amino acids 158 and 162 of VF1 (figure 3.5a). The same motif was previously shown to mediate interactions between STING and the HPV E7 and AdV E1A proteins, both of which inhibit IFN induction downstream of STING[182]. In addition, the LXCXE motif is also present in human IFI16 and mouse IFI204 (p204), host proteins that interact with STING to mediate IFN induction following detection of DNA, although its role in this interaction has not been explored[183–185]. Based on this it was hypothesized that VF1 interacts with STING. To test this, HEK293T cells were co-transfected with Flag-VF1 and either HA-STING or HA-EGFP, and immunoprecipitation was carried out using agarose beads conjugated to anti-Flag M2 antibodies. As shown in figure 3.5b, VF1 strongly associated with STING, but not EGFP. Similar results were obtained with Flag-STING and HA-VF1 (figure 3.5c), indicating an interaction between VF1 and STING.

Next, the effect of VF1 over-expression on IFN induction in response to various ligands was explored. For this assay, HeLa M cells were transduced at a high MOI with lentiviruses carrying bicistronic constructs encoding either EGFP or VF1 and co-expressing mCherry (figures 3.5d and 3.5e). After a few passages, the cells were either mock-transfected or transfected with poly (I:C), poly (dA:dT), or titrated amounts of a synthetic tri-phosphorylated hairpin RNA (3p-hpRNA) that specifically activates RIG-I – it should be noted that the poly (I:C) used in this work is the longer form that specifically activates MDA5[186]. No significant difference was observed in IFN expression in the presence of either VF1 or EGFP with transfection of poly (I:C) or poly (dAdT) (figures 3.5f and 3.5g). However, there was a significant reduction in both IFN-β and IFN-λ1 with the RIG-I-specific 3p-hpRNA, with a corresponding

reduction in viperin expression (figure 3.5h). Overall, this indicates that VF1 interacts with STING and inhibits induction of IFNs downstream of RIG-I.

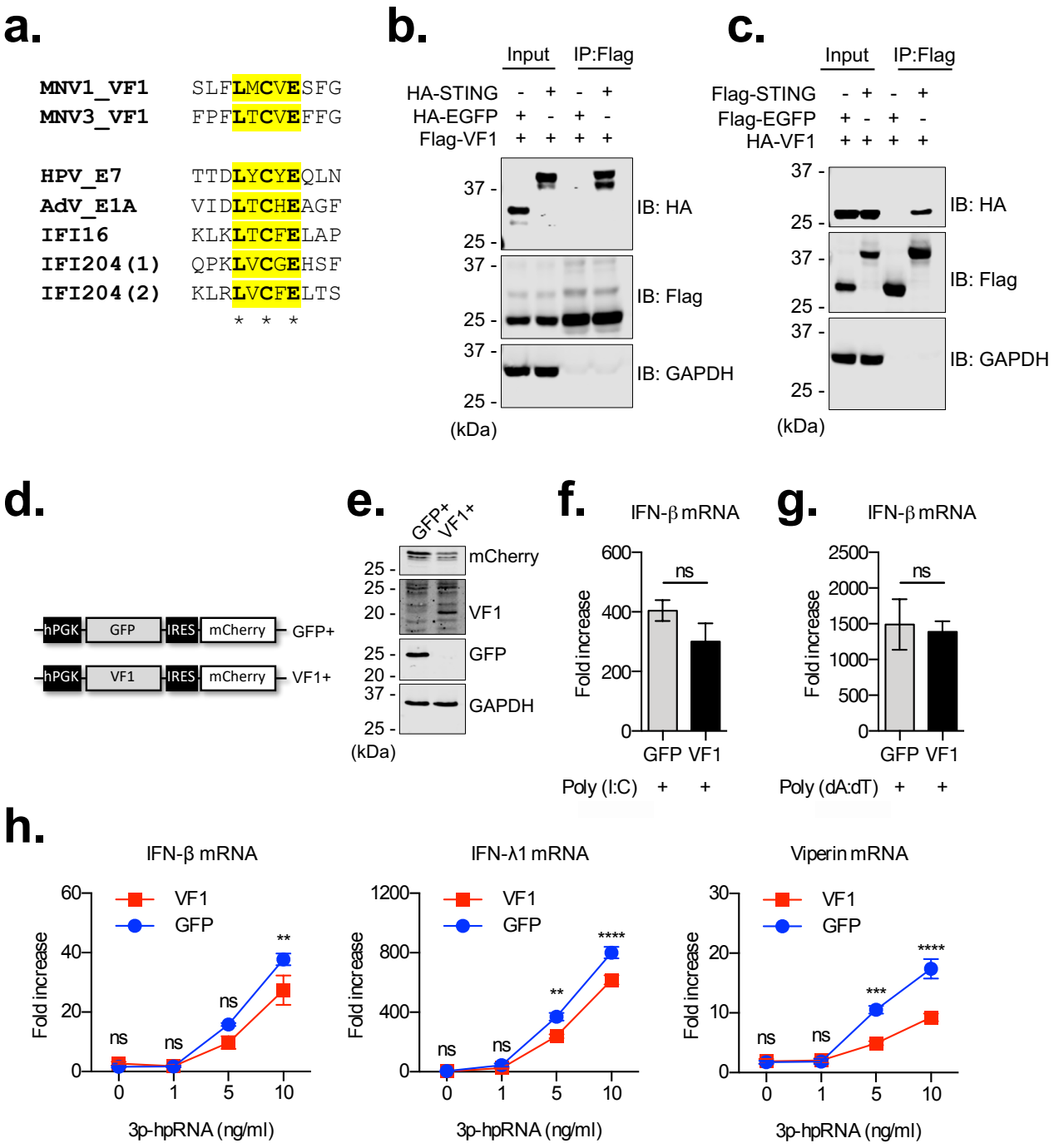

i.

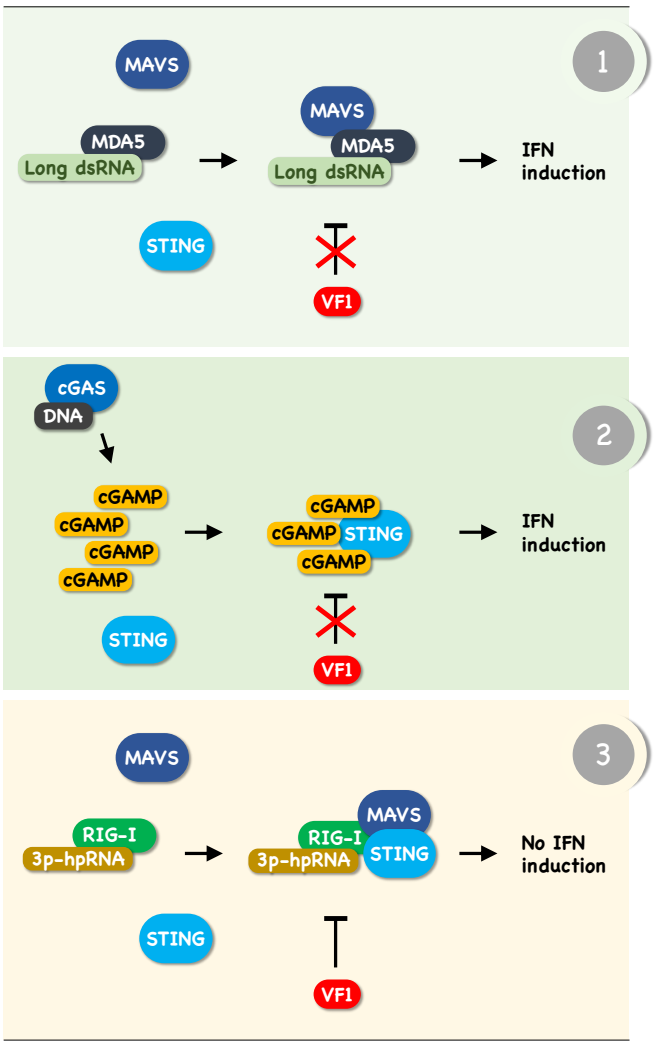

Figure 3.5. VF1 interacts with STING and inhibits induction of IFNs downstream of RIG-I

(a) An alignment of the LXCXE motifs of MNV1 VF1, MNV3 VF1, HPV E7, AdV E1A, IFI16, and IFI204.

(b) and (c) Lysates from HEK293T cells co-transfected with indicated plasmids, were subjected to co-immunoprecipitation with anti-flag M2 antibodies-conjugated agarose beads, and subsequently analysed via western blotting. Data is representative of two independent experiments.

(d) A schematic representation of the bi-cistronic plasmids packaged in the lentiviruses used.

(e) Lysates from the EGFP- and VF1-transduced HeLa M cells were assessed via western blotting.

(f) and (g) EGFP- and VF1-transduced HeLa M cells were either mock-transfected or transfected with 1μg/ml of poly (I:C) **(f)** or poly (dA:dT) **(g)**. The cells were

harvested 6 hrs later and assessed via RT-qPCR. Data is shown relative to mock-transfected cells and normalised to human β-actin (n=3).

(h) EGFP- and VF1-transduced HeLa M cells were either mock-transfected or transfected with indicated amounts of 3p-hpRNA, harvested 6 hrs later and assessed via RT-qPCR. Data represent two independent experiments each done in triplicates, and is shown relative to mock-transfected cells and normalised to human β-actin.

(i) Schematic representation of the proposed context-dependent inhibition of STING by VF1.

Discussion

Several decades after the discovery of the human norovirus, with thousands of lives and billions of dollars lost, the lack of a robust cell culture system still severely hampers development of vaccines and therapeutics. This could be in large part as a result of our limited understanding of the immune responses against an infection with the virus[128]. In this chapter, using MNV as a surrogate model, the presence of a RIG-I/STING-dependent innate response pathway that restricts the replication of noroviruses was demonstrated, and an attempt by the murine norovirus to subvert it through expression of an accessory protein was described.

RIG-I contributes to detection of MNV

Our data indicate that RIG-I contributes to host responses against MNV. Host cells detect intracellular PAMPs from RNA viruses by deploying the RIG-I-like receptors, a family of ubiquitously expressed soluble cytoplasmic receptors that include RIG-I, MDA5 and LGP2, discussed in detail in Chapter 1. While MDA5 has been established as a bona fide PRR in MNV-infected cells, other PRRs likely contribute since MNV infection is lethal in *Stat1*$^{-/-}$ mice, but not in *Ifih1*$^{-/-}$ mice. A study that explored RIG-I inhibition by a bacterial quorum-sensing molecule showed that while treating cells

with the molecule lead to a moderate increase in SeV titres in HEK293T cells, it did not appear to affect MNV titres in RAW264.7 cells[129] – although it is not clear whether there was any effect on IFN induction by the MNV infection or if the dose used was sufficient. No other study published to date has looked at the role of RIG-I in sensing MNV infections, but it has been previously demonstrated that the murine norovirus polymerase is able to transcribe RNA species that can be detected by both RIG-I and MDA5, but not TLR-3[144]. The role of RIG-I in the restriction of human norovirus was also previously explored to a limited degree. There was no significant difference in replication following transfection of viral RNA into Huh-7 and the RIG-I-deficient Huh-7.5 cells, suggesting that RIG-I is not required for norovirus restriction[130].

The initial reluctance to consider RIG-I in the sensing of MNV came about partly as a result of data from the work on human norovirus replication in Huh-7.5 cells, and partly as a result of initial seminal studies on picornaviruses as they share similarities to caliciviruses such as the presence of VPg – thought to, among other things, protect the viral genome from detection by RIG-I[122]. However, it is now clear that Huh-7.5 are not only RIG-I-deficient, but they are also deficient in STING[187,188], and our data indicates that IFN responses are severely attenuated in STING-deficient HEK293T cells. In addition, several members of the *Picornaviridae* family have recently been shown to be restricted by RIG-I, in addition to MDA5, including FMDV, Seneca valley virus, and Coxsackievirus B3[133–135].

Our finding that RIG-I is important for the restriction of noroviruses is consistent with data from a study on Tulane virus, a member of the *Caliciviridae* family[136]. There,

RIG-I-dependent restriction was shown to be particularly required early during viral replication while MDA5-dependent restriction was more critical during late stages of replication. Also, our data indicate that IFN responses are impaired to a greater extent in RIG-I deficient cells than expected, which suggests that either MDA5 and RIG-I induce IFN in a synergistic fashion, or the absence of one affects the levels or functions of the other. It is also interesting that although MDA5 depletion impairs IFN induction in cells infected with a persistent strain of MNV (CR6), there was no difference in viral titres[123]. Bearing in mind our data, it is possible that RIG-I and MDA5 display some degree of virus strain specificity or functional redundancy. The recent report about the role of HOIL1 in MNV-infected cells further adds an additional layer of complexity to this dynamic, as HOIL1 has been shown to act as a negative regulator to RIG-I activation in SeV-infected cells while also positively contributing to IFN responses to MNV[123,142]. Additional work therefore needs to be done to discern the relative contributions of the two receptors in restricting noroviruses.

There is currently no published data regarding the cognate PAMPs recognised by the PRRs in MNV-infected cells, but we can speculate on the potential ligands detected by either RIG-I or MDA5 (figure 3.6). The MNV genome is released less than 1 hr post-infection and IFN transcripts are upregulated as early as 4 hours after infection[2,124]. While it is therefore possible that the viral genome is detected by MDA5 in the cytosol, it is unlikely, as proteinase K treatment prior to transfection of viral RNA abrogates IFN induction[122], suggesting that viral replication is required for generation of PAMPs detected by the PRRs, similar to what was demonstrated for other RNA viruses such as IAV[189]. It is theoretically possible that MDA5 detects the double-stranded RNA intermediate composed of the VPg-linked positive-strand RNA

and the *de novo*-synthesized negative-stranded RNA. The negative-stranded RNA is likely not VPg-linked and thus may be able to activate RIG-I. Additionally, RIG-I can detect RNA fragments produced by RNAse L digestion of host and viral RNA[190–192]. Lastly both RIG-I and MDA5 may recognise RNA species transcribed by the RdRp from host RNA templates as already demonstrated in over-expression assays with the MNV RdRp, and in Semliki Fever Virus-infected cells (an *Alphavirus* that has a positive-sense single-stranded RNA viral genome akin to noroviruses)[144,193]. Further work is therefore warranted to identify the cognate PAMPs recognised by the PRRs in MNV-infected cells.

STING plays a central role in MNV restriction

In this chapter, we have shown that STING is required for a robust IFN response to infection with MNV1 in primary BMDMs and RAW264.7 cells, with a significant increase in viral titres in cells pre-treated with small-molecule inhibitors of STING and in STING-depleted cells. While infection of primary mouse macrophages and cell lines with the murine norovirus induces robust levels of IFNs and other cytokines[124], Huh-7 and 293FT cells do not appear to express IFNs following transfection with the human norovirus RNA[118,126]. Supernatant from Huh-7 cells transfected with poly (I:C), but not that from cells transfected with the human norovirus RNA, was able to inhibit replication of transfected viral RNA, suggesting that human norovirus replication does not trigger an IFN response[118]. Also, transfection of human norovirus RNA purified from patients' stools into 293FT cells did not induce IFNs, despite the presence of demonstrable viral replication[126]. Moreover, neutralisation of IFN using antibodies, and depletion of MAVS and IRF3 using RNA silencing, did not affect

viral replication. Also, cells transfected with the viral RNA were able to induce IFNs following infection with SeV or transfection with poly (I:C), signifying that the human norovirus replication did not interfere with the ability of the cells to express IFNs. These *in vitro* results are, however, inconsistent with data from studies in gnotobiotic pigs which show increased levels of IFNs following infection with the human norovirus[127]. One common factor in the Huh-7 and 293FT cells is that both cell lines lack the adapter protein STING[176,187,188].

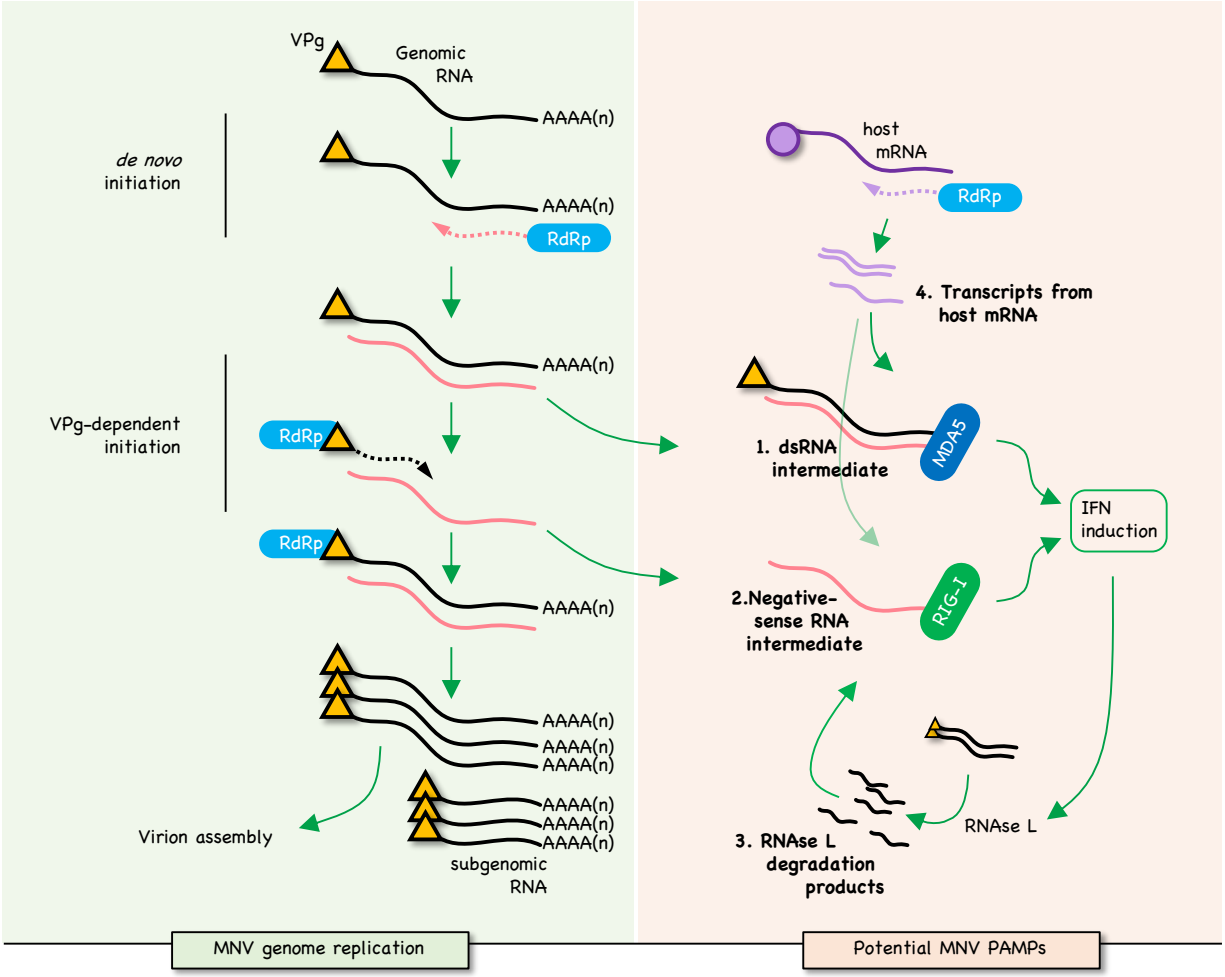

Figure 3.6. Schematic representation of genome replication in MNV, indicating potential PRR ligands.

Although STING mainly functions as an adapter protein in intracellular detection of foreign DNA, it has been shown to play important roles in the restriction of some RNA viruses through various independent mechanisms (recently reviewed by Maringer *et al.*[194], Aguirre *et al.*[63], Zevini *et al.*[57], and Ni *et al.*[56]). For example, it has been shown that STING can promote fusion-mediated IFN induction in cells infected with IAV in a manner independent of cGAS[68]. However, in cells infected with DENV, membrane recruitment to replication complexes leads to leakage of mitochondrial DNA that triggers IFN induction via STING, in a process contingent on cGAS activation[62]. Recently, it was also demonstrated that STING can inhibit host and viral translation in cells infected with a wide variety of RNA viruses in a RIG-I dependent manner[70]. In addition, at least for JEV, IFN induction is largely dependent on a RIG-I/STING-dependent pathway[69].

Data suggesting a role for STING in restricting RNA viruses are as old as the discovery of STING itself, and the first viral proteins shown to antagonize STING function are in fact encoded by RNA viruses[194]. Here, the role of STING in the IFN responses to MNV infection was explored. STING was found to be important in the restriction of MNV replication, partly in a RIG-I-dependent manner. This potentially broadens the current MDA5/IFN-dependent-centric understanding of the innate immune restriction of noroviruses to one that encompasses both IFN-dependent and independent pathways (figure 3.7). For instance, STING can inhibit replication of RNA viruses via translation shutoff[70]. Since STING is itself an ISG, this could explain a previously described ability of type I IFNs to inhibit translation of MNV proteins independent of PKR[65,108]. STING is also involved in inflammasome activation

following detection of pathogens, and this knowledge could therefore facilitate future studies of the complex relationship between noroviruses and commensal bacteria[195,196]. Importantly, this also potentially explains the discrepancy between *in vivo* and *in vitro* results from studies on IFN responses to the human norovirus.

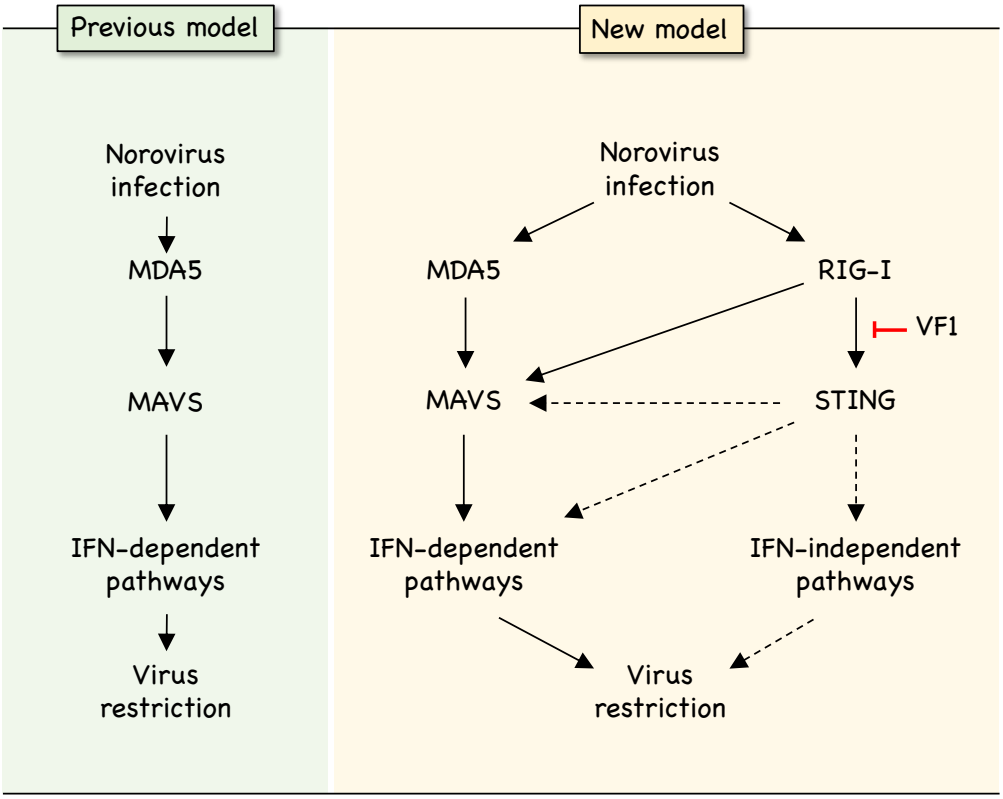

Figure 3.7. Innate immune restriction of noroviruses

A schematic representation of our current understanding of the innate immune responses against noroviruses. Dotted lines indicate areas where there is currently no direct evidence.

Previous studies on the role of STING in the innate response to RNA viruses (summarised in table 3.1) fall into two groups; (1) the ones that show canonical activation of STING and contribution to IFN responses, representing most published

studies in this area[57,69,184,197]; and (2) the recent screen of a broad range of RNA viruses that failed to observe canonical activation of STING or any reduction of IFN induction following STING depletion, while also demonstrating the contribution of STING in antiviral responses via translation inhibition[70]. Our data appear to fall in the middle, in that STING contributes to IFN responses to MNV, although there was no evidence of its canonical activation in MNV-infected cells. Nevertheless, our data contributes to this discussion, and suggest the need for further work in this area.

Table 3.1. STING activation in the innate responses to RNA viruses

sn	Receptor	Evidence of canonical activation of STING	Virus(es)	Ligand/Trigger	Outcome	Reference(s)
1.	RIG-I	??	VSV, SINV, SeV, IAV, T3D	Viral RNA	Translation shutoff	Franz et al. 2018[70]
2.		STING translocation*	SeV, VSV, NDV, JEV, HCV		IFN induction	Ishikawa et al. 2008[67], Nazmi et al. 2012[69], Nitta et al. 2013[198]
3.	LSm14A**	??	SeV			Li et al. 2012[199]
4.	cGAS	cGAMP production	DENV	Leaked mitochondrial DNA		Aguirre et al. 2017[62]
5.	??	STING dimerisation	IAV	Membrane fusion		Holm et al. 2016[68]
6.			SeV, SARS-CoV	??		Sun et al. 2012[200]

*Only shown for JEV[69]
**Functions in a RIG-I-dependent manner[199]

VF1 binds to STING and inhibits RIG-I signalling

Lastly, VF1 was found to bind to STING and inhibit IFN induction downstream of RIG-I, highlighting the relevance of the RIG-I/STING pathway in restricting

replication of noroviruses. Given that VF1 is only expressed by the murine norovirus, but not the human norovirus, further work is required to determine the existence of additional attempts by noroviruses to counteract this pathway. The presence of the LXCXE motif in VF1 is also interesting, as it potentially points to a common STING-binding motif that can be exploited by viruses and other pathogens. Although originally described as the Rb-binding motif, the nuclear and cytoplasmic localisation of STING and the Rb protein, respectively, physically compartmentalizes binding partners and possibly provides a means of functionally separating the two systems.

Chapter 4

MED23 does not localise to peroxisomes

Background

Work done by Griffiths and colleagues alluded to a role for MED23, a tail subunit of the Mediator complex, in the specific induction of type III IFNs (discussed in greater detail in chapters 1)[78]. MED23 was among the main hits obtained following genome-wide RNAi screens for host factors that inhibit replication of Herpes Simplex Virus type 1 (HSV1). Increased expression of type III IFNs was observed upon overexpression of MED23 in A549 cells, with a decrease in viral replication following infection with HSV1. Depletion of MED23 on the other hand, using a siRNA pool, lead to an increase in viral titres and a decrease in the induction of type III IFNs. Further mechanistic work demonstrated an interaction between MED23 and IRF7. Based on these findings, they concluded that MED23 specifically regulates induction of type III IFNs following infection with HSV1.

Confocal micrographs from the Human Protein Atlas (HPA)[201] and insilico analysis of the MED23 protein sequence suggest a possible presence of the human MED23 at peroxisomes, which could account for the role of MED23 in type III IFN responses. As discussed in detail in chapter 1, peroxisomal MAVS mediates a predominantly type III IFN response following infection by RNA viruses. We therefore hypothesized that MED23 localizes to both the nucleus and peroxisomes and contributes to IFN induction at peroxisomes. The aims of this chapter are to; (1) examine the possible localisation of MED23 to peroxisomes; and (2) determine the relevance of any such peroxisomal localisation on IFN induction at peroxisomes.

Results

4.1. Evidence suggesting a potential peroxisomal localization for MED23

Confocal micrographs from the Human Protein Atlas (HPA) project indicate the presence of an extranuclear MED23 in different human cell lines (figure 4.1a). This extra-nuclear MED23 has a flecked appearance within the cytoplasm that suggests localisation to small vesicular organelles such as peroxisomes.

Bioinformatic analysis of the human MED23 sequence also indicated the presence of an SKM motif, a PTS1 peroxisomal targeting signal, 30 amino acids away from the carboxyl-terminus (figure 4.1b). The SKM motif is present in 4 out the 6 MED23 isotypes, and is conserved humans, mice and rats (figures 4.1c and 4.1d). Although PTS1 motifs are typically present as the last three amino acids at the carboxyl-terminal end peroxisomal proteins, there are a few exceptions. The ATM protein, for example, was recently shown to also localize to peroxisomes, in addition to its nuclear localisation, via a PTS1 positioned 9 amino acids away from the carboxyl terminal end of the protein. Taken together, these data suggest that MED23 has a cytosolic component that potentially localizes to peroxisomes.

a.

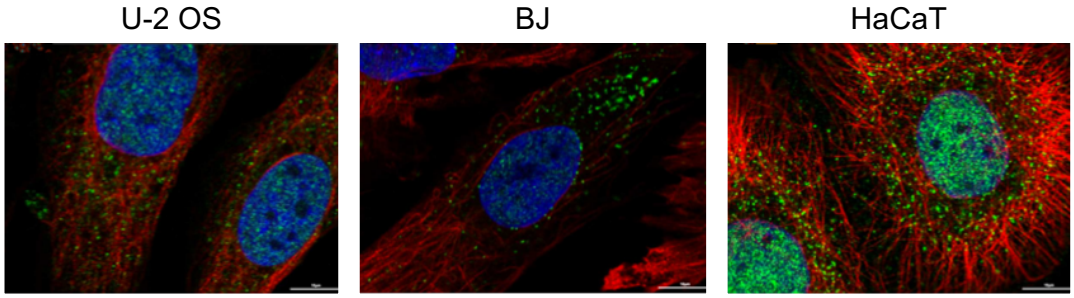

b.

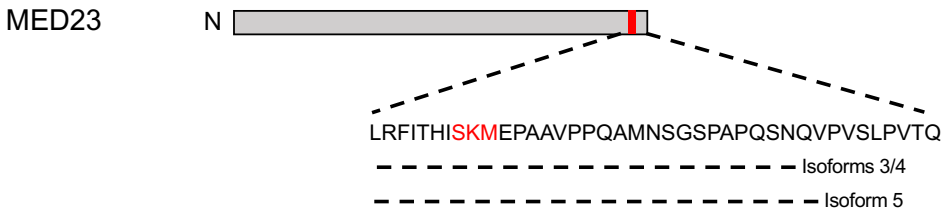

c.

```
sp|Q9ULK4-6     ----------------------------------------------------
sp|Q9ULK4-2     ----------------------------------------------------
sp|Q9ULK4-3     EKIICNLKPALKLRLRFITHISKMEPAAVPPQAMNSGSPAPQSNQ---------
sp|Q9ULK4-5     EKIICNLKPALKLRLRFITHISKMEPAAVPPQAMNSGSPAPQSNQVDTLT----
sp|Q9ULK4-1     EKIICNLKPALKLRLRFITHISKMEPAAVPPQAMNSGSPAPQSNQVPVSLPVTQ
sp|Q9ULK4-4     EKIICNLKPALKLRLRFITHISKMEPAAVPPQAMNSGSPAPQSNQ---------
```

d.

```
Arabidopsis     DILALIGRAAETLRPDVQHLLA---HLKT-NP-------NSSIYAAAH-QQNTAKTNTS-
Slime_mold      ELLRIV----KEFKPNFLSKFNQLN-----------------------------------
Fruit_fly       ESEAII----KRLRPLLQMRLRFITHLNLEDIHTEKINDNTSNNAITSQTQSPMQTQHQQ
Zebrafish       QVERII----CSLRPAMRLRLRFITHISKMEPAAVPVSNSSSVQQTSS-ASSPTAQS-TA
Frog            QVEKII----CNLRPALKLRLRHITHISTE-SAAPPPPPMNSGSPA-------PQPN-QV
Human           QVEKII----CNLKPALKLRLRFITHISKMEPAAVPPQAMNSGSPA-------PQSN-QV
Mouse           QVEKII----CNLKPALKLRLRFITHISKMEPA-VPPQALNSGSPA-------PQSN-QV
Rat             QVEKII----CNLKPALKLRLRFITHISKMEPA-VPPQALSSGSPA-------PQAN-QV
                :   ::      ::* .   :
```

Figure 4.1. Evidence suggesting a potential peroxisomal localization for MED23

a) Confocal images archived from the HPA website[201,202]. Blue represents DAPI, green represents MED23, and red represents microtubules.

[https://www.proteinatlas.org/ENSG00000112282-MED23/cell]

b) A schematic representation of human MED23, showing the last 40 c-terminal amino acids. The predicted PTS1 targeting sequence is underlined and coloured red. N, n-terminal; C, c-terminal.

c) An alignment of c-terminal sequences from the 6 MED23 isoforms available in UNIPROT. The predicted PTS1 targeting sequence is highlighted yellow.

d) An alignment of c-terminal sequences of MED23 from the indicated species. The predicted PTS1 targeting sequences are highlighted yellow.

4.2. Confocal imaging and fractionation studies

To examine the potential localisation of MED23 to peroxisomes, HeLa M cells engineered to express a peroxisome-targeted mCherry (mCherry-PTS1 HeLa) were used so that the mCherry served as a peroxisomal marker. Wild-type HeLa M cells or the mCherry-PTS1 HeLa cells were fixed, permeabilised and stained for MED23 using the HPA anti-MED23 antibody. As shown in figure 4.2a, MED23 colocalized with the peroxisomal marker, suggesting that MED23 localises to peroxisomes. Similar results were seen in HEK293T cells stably transduced with the peroxisome-targeted mCherry (figure 4.2b). However, in both HeLa and HEK293T cells the MED23 staining appeared to be mostly extra-nuclear, in contrast to previously described primarily nuclear localisation. To further clarify this, MED23 localisation was examined using a cell fractionation approach in A549 cells. For this assay, a western blot-validated antibody obtained from BD biosciences was used. GAPDH and hnRNP1 where used as controls for cytosolic and nuclear proteins, respectively. As shown in figure 4.2c, MED23 was found to be primarily nuclear, in keeping with data from previously published studies. While a small proportion is present in the cytosolic fraction, a proportion of hnRNP1 was also present in the cytoplasmic fraction, indicating a possible contamination with nuclear proteins.

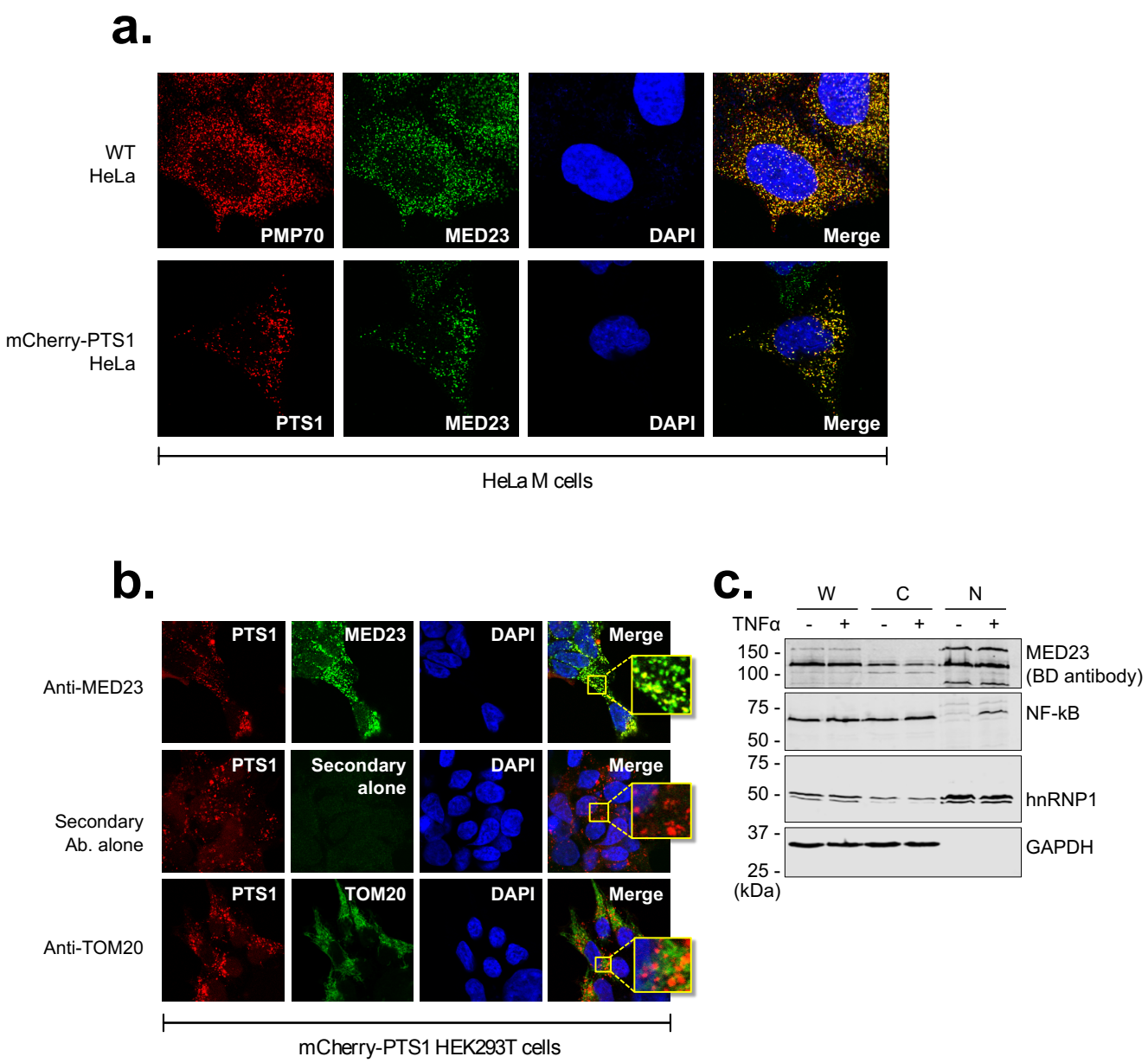

4.2. Confocal imaging and fractionation studies

a) Confocal micrographs of WT HeLa cells (top panel) or cells stably expressing a peroxisome-targeted mCherry (PTS1, bottom panel), stained with the HPA anti-MED23 primary antibody. Blue represents DAPI, green represents MED23, and red represents PTS1.

b) Confocal micrographs of HEK293T cells stably expressing a peroxisome-targeted mCherry (PTS1), stained with the an anti-TOM20 or HPA anti-MED23 primary antibody. Blue represents DAPI, green represents TOM20/MED23, and red represents PTS1.

c) REAP fractionation of A549 cells following treatment with 40ng/ml of TNFα for 6 hrs.

4.3. MED23 knockdown with siRNA

The results from figures 4.1b and 4.1c above appear to contradict each other, with confocal imaging in HeLa and HEK293T cells indicating a predominance of peroxisomal MED23 while fractionation in A549 cells shows predominant nuclear localisation. One possible explanation could be a cell line-specific difference in MED23 localisation, for instance due to a preponderance of different isotypes in the 3 cell lines. A more likely explanation is however differences in antibody specificity between the HPA and the BD anti-MED23 antibodies. To examine the latter possibility, A549 cells were transfected with either a control siRNA (siGFP) or siRNA targeting MED23. Lysates from these cells were then probed for MED23 by western blotting, using either the HPA antibody or the BD antibody. The most prominent band present on the BD antibody blot was 130kDa, similar to the reported size for MED23 (figure 4.3a). Moreover, the intensity of the 130kDa band was considerably reduced in cells transfected with the MED23-targeted siRNA, indicating that this was indeed MED23. While a similar 130kDa band was seen in the HPA antibody blot (figure 4.3b), the band with the highest intensity was seen to be about 90kDa. This 90kDa band also appears to be unaffected by siRNA targeting MED23, although the siRNA used in this work is complementary to a sequence at the carboxyl-terminus of the mRNA, and MED23 isotypes with alternate residues or truncations affecting this site will therefore not be depleted.

Confocal imaging on HeLa cells stained with the BD anti-MED23 antibody showed a primarily nuclear localisation, with no colocalization with the peroxisomal marker (figure 4.3c). Taken together, these results suggest that the HPA antibody either binds

to an artefactual target with a higher specificity than MED23, or to a 90kDa isotype of MED23 that localizes to peroxisomes.

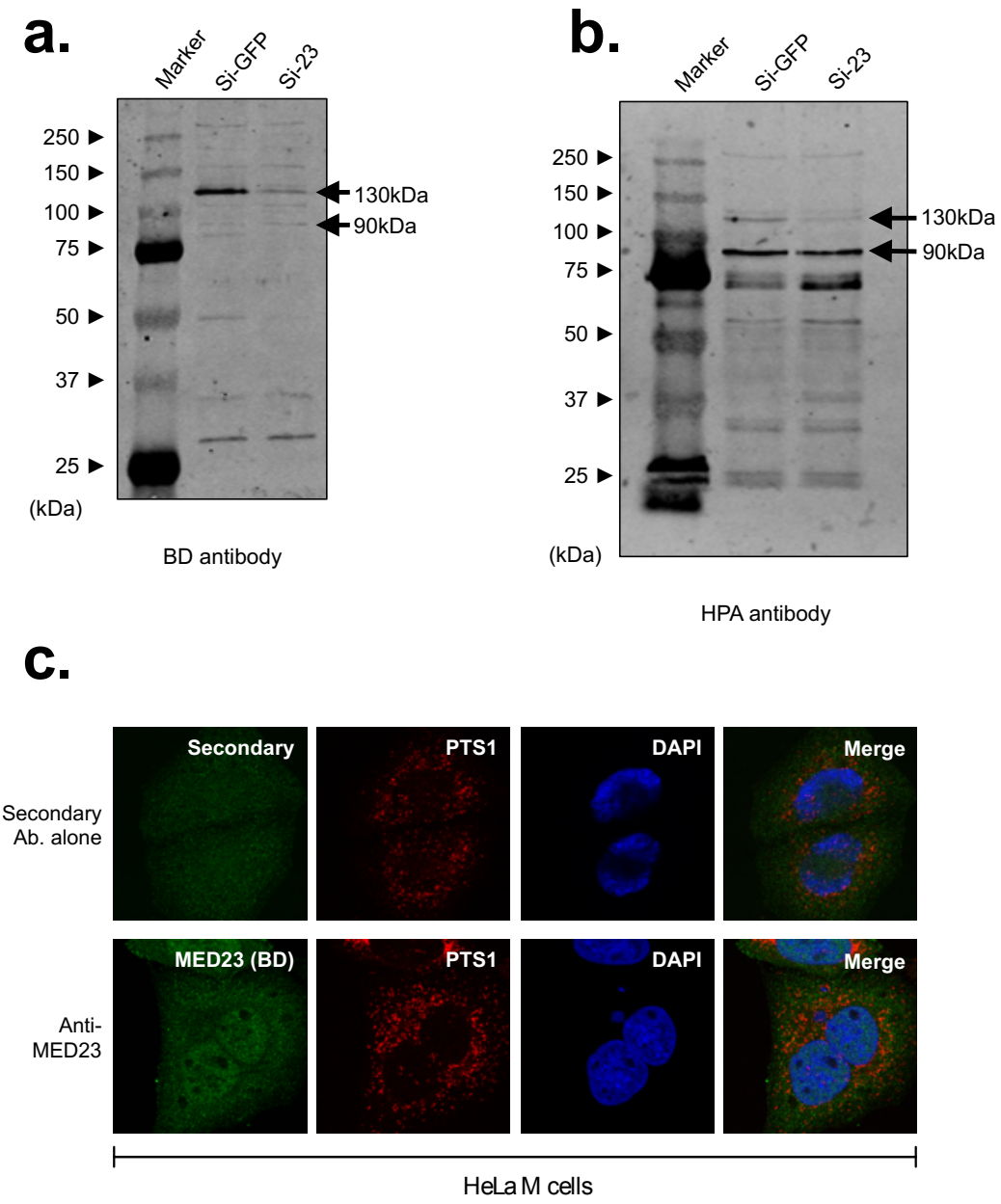

Figure 4.3. MED23 knockdown with siRNA

A549 cells were transfected with either control siRNA (siEGFP), or siRNA targeting human MED23. The cells were harvested 48 hrs later, and assessed via western blotting using the BD Biosciences anti-MED23 antibody (**a**), or the HPA antibody (**b**).

c) Confocal micrographs of HeLa cells stably expressing a peroxisome-targeted mCherry (PTS1), with either no primary antibody staining ('secondary' alone), or stained with the BD biosciences anti-MED23 primary antibody. Blue represents DAPI, green represents MED23, and red represents PTS1.

4.4. Colocalization studies with MED23 overexpression

Sequences for 6 human MED23 isotypes are currently available at Uniprot, an online database that curates protein sequences and functional data (schematically represented in figure 4.4a). Isotype 1 represents the canonical MED23 sequence and has a predicted size of 130kDa. Isotypes 3, 4 and 5 also have predicted sizes of about 130kDa but differ from each other and the main isotype (isotype 1) by the presence of alternative residues at their carboxyl-termini. In addition, isotype 3 also has an additional sequence within the site that was used as the immunogen for the HPA antibody. Both isotypes 2 and 6 appear truncated, with predicted sizes of 100kDa and 55kDa, respectively. Isotype 6 also has an SKL motif close to its carboxyl-terminus. To determine whether the prominent band seen in the HPA antibody blots represents any of these isotypes, isotypes 1, 2 and 6 were cloned into expression plasmids with EGFP tagged to their amino-termini. Isotype 2 was chosen because of its predicted size and the presence of the additional residues within the HPA antibody immunogen site that could alter its specificity. Isotype 6 was chosen because of the presence of the SKL motif near its carboxyl-terminus that could potentially increase the possibility of its localising to peroxisomes, and isotype 1 was chosen as a control. The cloned plasmids were transiently expressed in mCherry-PTS1 HeLa cells and the cells were subsequently processed for confocal microscopy. As shown in figure 4.4b, Isoform 1 mostly localized to the nucleus, while isoforms 2 and 6 both appear to have a diffused cytosolic distribution. None of the isotypes showed the characteristic punctate peroxisomal pattern, nor did they colocalize with the peroxisomal marker, indicating that MED23 is unlikely to localize to peroxisomes.

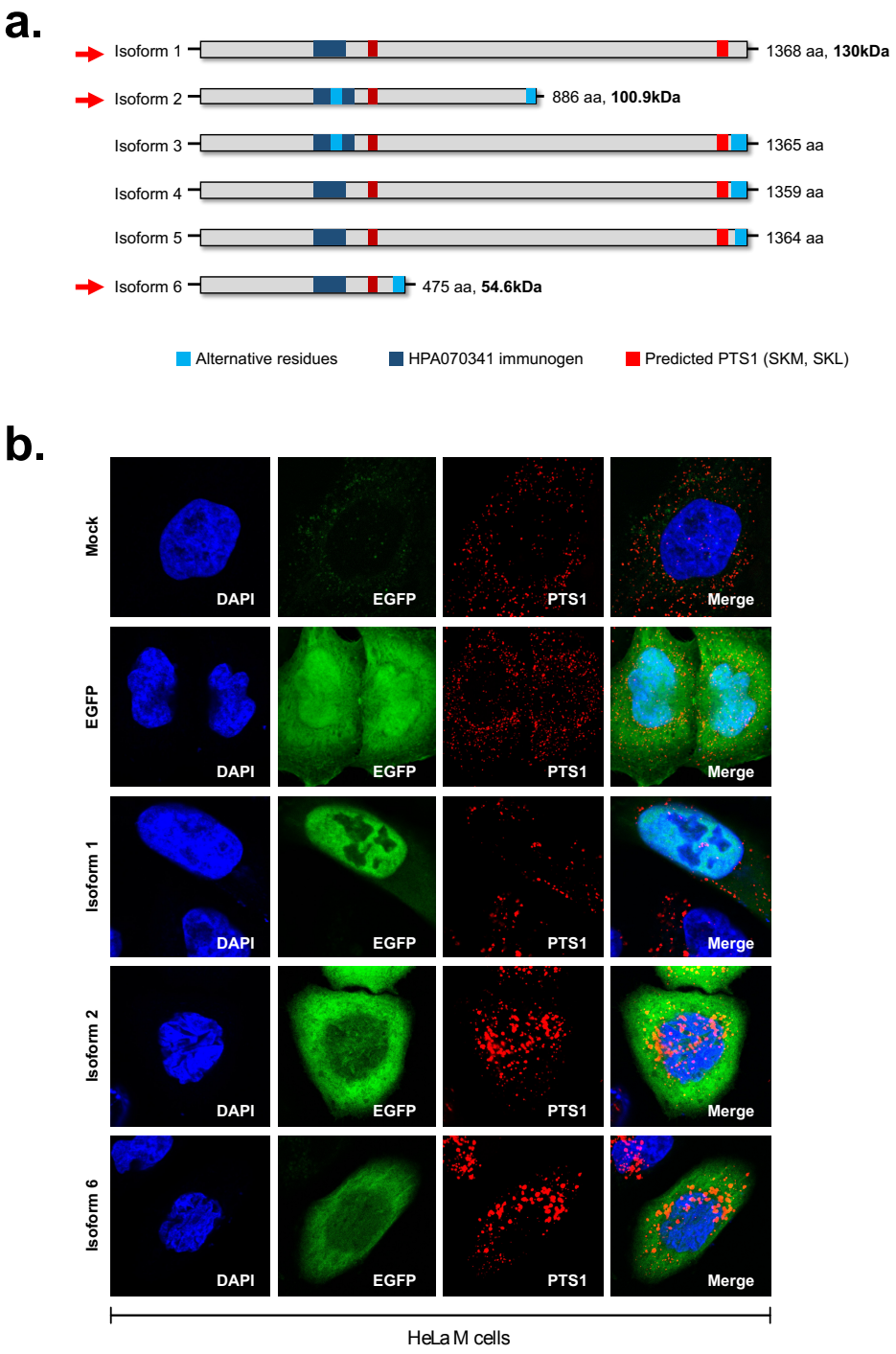

Figure 4.4. Colocalization studies with MED23 overexpression

a) A schematic representation of the six human MED23 isoforms, with color-coding indication alternative residues, predicted PTS1 targeting sites and sites of the HPA antibogy immunogen. Red arrows indicate isoforms selected for overexpression in (b).

b) Confocal micrographs of HeLa cells stably expressing a peroxisome-targeted mCherry (PTS1), and transfected with EGFP, EGFP-MED23 isoform 1, EGFP-MED23 isoform 2, EGFP-MED23 isoform 6, or none (mock). Blue represents DAPI, green represents EGFP, and red represents PTS1.

4.5. Co-expression of MED23 and differentially-localizing MAVS

MED23 has been shown to specifically promote induction of type III IFNs, likely in an IRF7-dependent manner. Interestingly, while over-expression of MED23 alone in A549 cells did not lead to induction of IFNs in our hands, co-expression with IRF7 lead to an increase in the induction of both IFN-λ1 and IFN-β compared to over-expression of IRF7 alone (figure 4.5a). Similarly, co-expression of MED23 with MAVS lead to an increase in both IFN-λ1 and IFN-β (figure 4.5b).

Activation of MAVS present on peroxisomes leads to a predominantly type III IFN response. If MED23 is present at peroxisomes and specifically augments type III IFN induction, then co-expression with a peroxisome-targeted MAVS will preferentially lead to induction of type III IFNs. To test this, an epitope-tagged MAVS localising to the peroxisomes was generated by replacing its transmembrane domain with the peroxisomal targeting sequence of Pex13 (figure 4.5c and 4.5d) and co-expressed with MED23 in A549 cells. As shown in figure 4.5e, there was a marginal increase in both IFN-λ1 and IFN-β following co-expression of MED23 and peroxisomal MAVS, similar to that seen with wild-type MAVS, indicating that MED23 does to specifically influence type III IFN induction at peroxisomes.

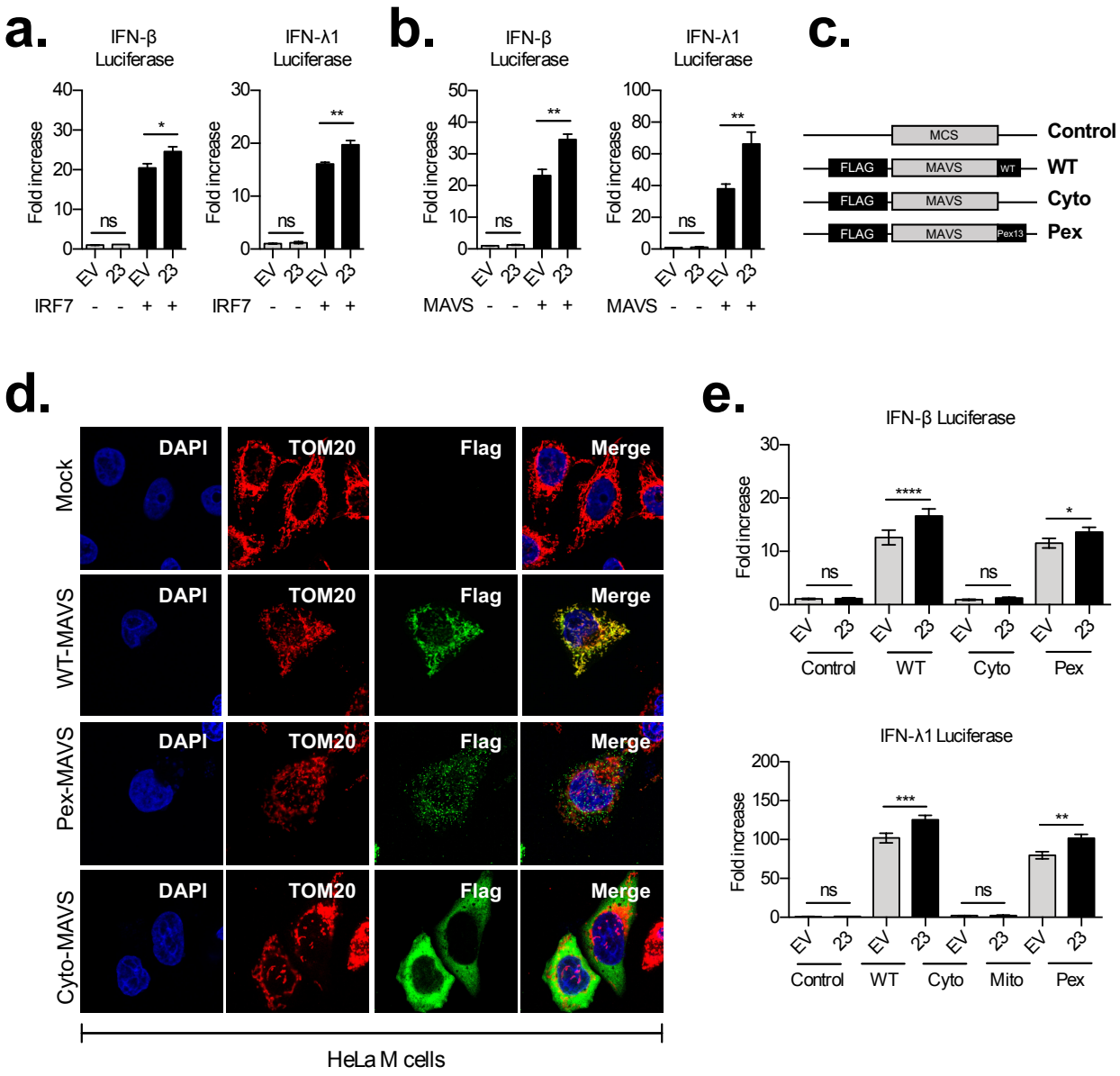

Figure 4.5. MED23 potentiates interferon induction independent of MAVS localization

a) A549 cells transiently transfected with the pRLTK plasmid, either the empty vector or mouse MED23, either a control plasmid or IRF7, and either the IFNβ-luciferase (left panel) or the IFNλ1-luciferase (right panel) plasmids. Cells were harvested after 24 hrs, and assessed for Firefly and Renilla luciferase. Data represent two independent experiments each done in triplicates, and is expressed as Firefly luciferase relative to control, normalised to Renilla luciferase.

b) Similar to (a), but with MAVS instead of IRF7.

c) A schematic representation of the plasmids encoding differentially localising MAVS mutants. EV, empty vector; WT, wild type; Cyto, cytosolic; Pex, peroxisomal.

d) Confocal micrographs of HeLa cells transiently transfected with plasmids from figure 4.5c above.

e) *Mavs*$^{-/-}$ MEF cells transiently transfected with the pRLTK plasmid, either the empty vector or mouse MED23, one of the plasmids represented in (**c**) above, and either the IFNβ-luciferase (top panel) or the IFNλ1-luciferase (bottom panel) plasmids. Cells were harvested after 24 hrs, and assessed for Firefly and Renilla luciferase. Data is pooled from three independent experiments each done in triplicates, and is expressed as Firefly luciferase relative to control, normalised to Renilla luciferase.

Discussion.

In this chapter, we have explored the possible localisation of MED23 to peroxisomes. While initial data obtained using the HPA anti-MED23 antibody indicated extra-nuclear nuclear localisation of Med23, we have failed to show that using an antibody from a different source or by over-expression of MED23 isoforms in cell lines. Moreover, functional data using peroxisome-targeted MAVS mutants did not support our hypothesis. It is therefore possible that the HPA antibody in fact detects another protein that localises to peroxisomes, in addition to MED23. This highlights the continuing need to validate antibodies prior to use for hypothesis-based scientific studies, especially since 'bad antibodies' are among the commonest causes of reproducibility problems in many labs[203–205]. Ironically, the HPA consortium was setup to tackle exactly these types of problems[201].

The overall aim of the work in this chapter was to determine how the host is able to switch between induction of one type of IFN to another are yet to be determined. Interestingly, our data suggests that MED23 may potentiate the induction of both type I and type III IFNs. In the next chapter, we examine this further and determine the relevance of this function in the restriction of an RNA virus.

Chapter 5

MED23 mediates induction of target genes

downstream of activated IRF3

Background

The interferon (IFN) response is among the earliest and most critical lines of defence against viruses[31]. Host cells have a myriad of soluble and membrane-bound pattern recognition receptors that can detect virus-specific ligands or perturbations from damage of infected cells, and are able to kickstart various molecular cascades that eventually lead to induction of interferons.[31] As both types I and III IFNs play essential non-redundant roles in host restriction of viruses, there has been considerable interest in the mechanism for the host's ability to differentially induce IFN subtypes[74,97]. Earlier studies have emphasized the requirement for activation of all three groups of transcription factors, including the IFN Regulatory Factors (IRFs), NF-kB, and AP-1 that form the 'IFN enhanceosome', in order to have a robust induction of IFNs.[206,207] While this is still largely true, recent studies have elucidated a differential requirement for transcription factor activation between type I and type III IFNs. Induction of IFN-β, for example, has been shown to depend more on activation of IRF3, while a robust induction of IFN-λ depends more on activation of NF-kB and to some extent IRF1 and IRF7, than it does on IRF3[73–77]. Additionally, activation of MAVS located on mitochondria has been shown to induce a largely type I IFN response, while activation of MAVS at peroxisomes induces a predominantly type III IFN response[50,53]. Nevertheless, the details of how the host is able to switch between induction of one type of IFN to another are yet to be determined.

Work done by Griffiths and colleagues alluded to a role for MED23, a tail subunit of the Mediator complex, in the specific induction of type III IFNs (discussed in greater detail in chapters 1 and 4)[78]. Our data from the previous chapter indicated that MED23

potentiates activation of both type I and type III IFNs. We therefore hypothesized that MED23 plays a role in the induction of not only type III IFNs as previously reported, but also in the induction of type I IFNs. The aims of this chapter are to; (1) determine the role of MED23 in type I IFN induction; and (2) examine the mechanism of any such role. We show that depletion of MED23 leads to a reduction in expression of both type I and type III IFNs in human and mouse cell lines. We also show that *Med23*$^{-/-}$ cells undergo genetic compensation, suggesting a critical role for MED23 in this pathway. Mechanistically, we show that MED23 interacts with IRF3, and is required for recruitment of the RNA polymerase (Pol) II to promoters of IRF3-dependent genes. Altogether, our data indicate that MED23 plays an essential role in antiviral responses by coupling IRF3 activation and RNA Pol II recruitment.

Results

5.1. Human and mouse cells deficient in MED23 show impaired induction of both type I and type III IFNs.

Previous work done by Griffiths *et al.* has demonstrated that MED23 plays a role in the induction of type III IFNs, likely through an interaction with IRF7.[78] However, while replicating their work, it was observed that whereas overexpressing MED23 alone in A549 cells did not lead to induction of IFN-β or IFN-λ1 promoter-driven luciferase in our hands, co-expression of MED23 with either IRF7 or MAVS lead to an increased induction of both IFN-β and IFN-λ1, compared to an empty vector, (as shown in the previous chapter, figures 4.7a and 4.7b), suggesting that MED23 potentiates induction of both type I and type III IFNs. MED23 depletion by siRNA also lead to a decrease in both IFN-β and IFN-λ1 induction (figure 5.1a). To confirm

this, 3 different shRNAs targeting human MED23 were used to stably knockdown expression in A549 cells, as shown in figure 5.1b. Using these cells, IFN induction in the absence of MED23 was examined. A549 cells lacking MED23 showed a marked reduction in their ability to induce IFN-β and all 3 IFN-λ subunits following stimulation with poly (I:C) (figure 5.1c). Compared with controls, MED23-deficient cells also showed reduced ability to induce both types I and III IFNs following infection with EMCV (Figure 5.1d) and stimulation with poly (dA:dT) (Figure 5.1e). Significantly higher levels of viral RNA were also seen in cells expressing lower levels of MED23, compared with controls (Figure 5.1d). Altogether, these data indicate that MED23 is required for the induction of both types I and III IFNs. Its worthy of note, that EMCV was used in these experiments as a model RNA virus, since the cells do not express the MNV receptor.

The mammalian Mediator complex is highly conserved.[208,209] It was therefore hypothesized that the requirement for MED23 in the induction of IFNs is conserved as well. To test this, MEF cells were stably transduced with 2 different shRNA targeting mouse MED23 (Figure 5.1f). A significant reduction was seen in the levels of IFN induced in cells lacking MED23 compared with expressing control shRNA, following stimulation with poly (I:C) (figure 5.1g). Together, this shows that MED23 is required for induction of IFNs in both human and mouse cell lines.

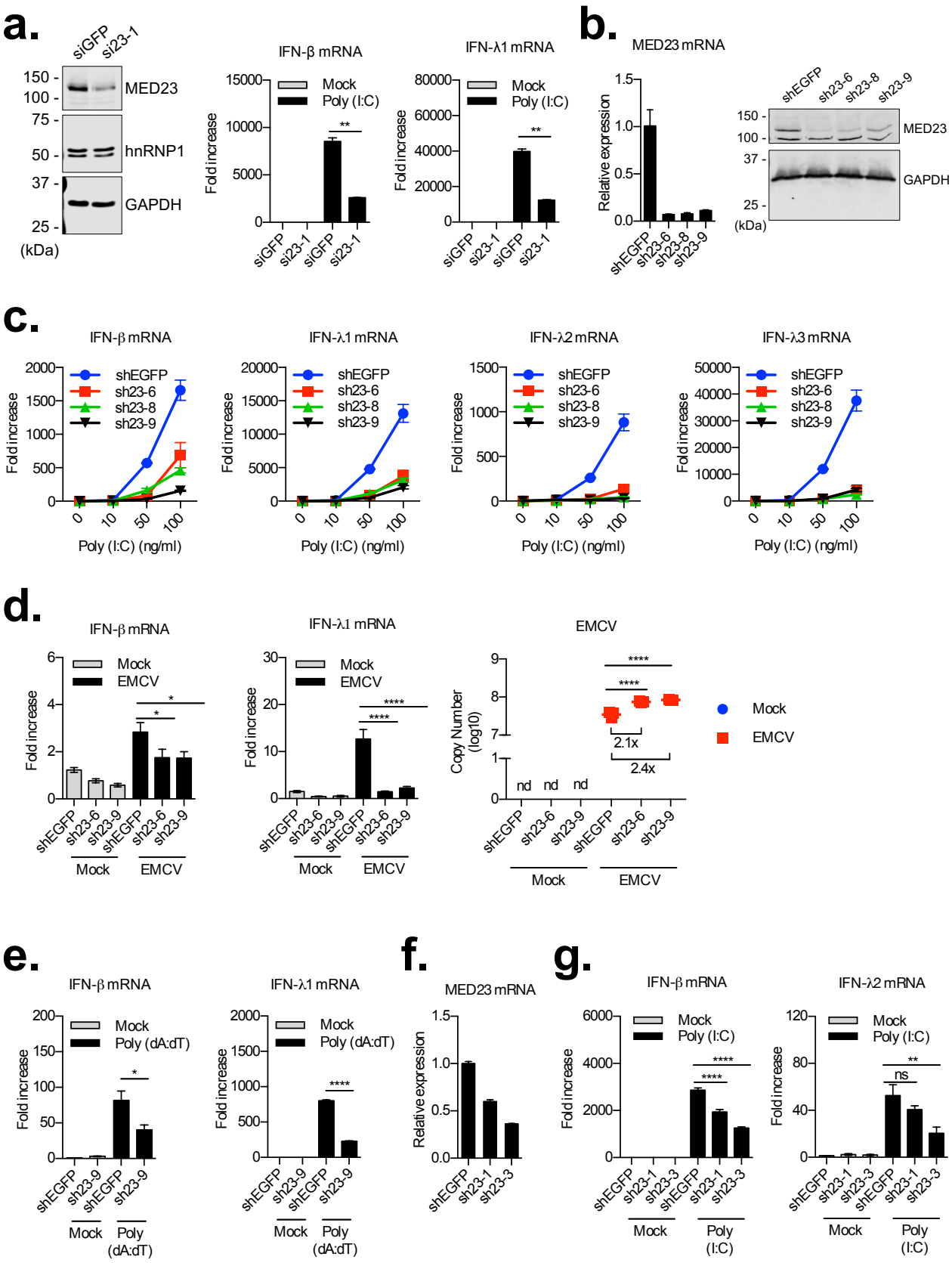
a.
siGFP
si23-1
150 -
100 -
75 -
50 -
37 -
25 -
(kDa)
MED23
hnRNP1
GAPDH
IFN-β mRNA
Fold increase
Mock
Poly (I:C)
**
siGFP
si23-1
IFN-λ1 mRNA
b.
MED23 mRNA
Relative expression
shEGFP
sh23-6
sh23-8
sh23-9
c.
IFN-β mRNA
IFN-λ1 mRNA
IFN-λ2 mRNA
IFN-λ3 mRNA
Poly (I:C) (ng/ml)
d.
EMCV
Copy Number (log10)
nd
2.1x
2.4x
****
*
Mock
EMCV
e.
Poly (dA:dT)
f.
g.
ns
Poly (I:C)

Figure 5.1 Human and mouse cells deficient in MED23 show impaired induction of both type I and type III interferons.

a) A549 cells transfected with control siRNA (siGFP) or siRNA targeting human MED23 (si23-1) were lysed and assessed for MED23 via western blotting (left panel), or transfected with 1μg/ml of poly (I:C) for 6 hrs and assessed by RT-qPCR (middle and right panels). Data in the middle and right panels are expressed relative to control and normalised to β-actin (n=3).

b) A549 cells stably transduced with control shRNA (shEGFP) or different shRNA targeting human MED23 (sh23-6, sh23-8, or sh23-9) were lysed and assessed for MED23 mRNA via RT-qPCR (left panel) or analysed via western blotting (right panel). Data in the left panel is expressed relative to control and normalised to β-actin (n=3).

c) A549 cells stably transduced with different shRNA, as indicated in (a) above, were transfected with 0, 10, 50, or 100 ng/ml of Poly (I:C) for 6hrs, and were subsequently harvested and assessed for IFN-β or IFN-λ mRNA. Data is expressed relative to control and normalised to β-actin (n=3).

d) A549 cells stably transduced with different shRNA, as indicated in (a) above, were seeded overnight and were then either mock infected or infected with EMCV at an MOI of 5. The cells were harvested 12 hrs post-infection, and assessed for IFN-β or IFN-λ1 mRNA, EMCV viral RNA. Data for IFN-β and IFN-λ1 mRNA is expressed relative to control, and normalised to β-actin. nd, not detected (n=3).

e) A549 cells stably transduced with control shRNA (shEGFP) or shRNA targeting human MED23 (sh23-9), were transfected with 50ng/ml of Poly (dA:dT) for 6hrs, and were subsequently harvested and assessed for IFN-β or IFN-λ1 mRNA. Data is expressed relative to control, and normalised to β-actin (n=3).

f) MEF cells stably transduced with control shRNA (shEGFP) or 2 different shRNA targeting mouse MED23 (sh23-1 or sh23-3) were lysed and assessed for MED23 mRNA via RT-qPCR. Data is expressed relative to control, and normalised to *Gapdh* (n=3).

g) MEF cells stably transduced with different shRNA, as indicated in (e) above, were transfected with 1 μg/ml of Poly (I:C) for 6hrs, and were subsequently harvested and assessed for IFN-β or IFN-λ1 mRNA. Data is expressed relative to control, and normalised to *Gapdh* (n=3)

5.2. MED23 knock down impairs induction of IRF3- but not NF-kB-dependent genes

Robust induction of type I IFNs is dependent upon a concerted interplay of activated transcription factors, most notably IRF3 and NF-kB[31]. We therefore hypothesized that MED23 is required for gene induction downstream of activated IRF3 and NF-kB. Indeed, A549 cells deficient in MED23 showed a marked reduction in Viperin and ISG15 induction in a dose-dependent manner, both of which are IRF3-dependent genes (Figure 5.2a). In contrast, cells lacking MED23 mostly showed higher induction of IL-6 and TNF-α (Figure 5.2a) when compared with controls, both of which are typically induced via NF-kB. A similar pattern was seen in MEF cells lacking MED23 (Figure 5.2b).

To further clarify the effect of MED23 knockdown on NF-kB-induced transcription, A549 cells and MEFs expressing shRNA targeting EGFP or MED23 were transfected with a plasmid encoding luciferase under the control of NF-kB, the control pRL-TK plasmid, and either an empty vector or FLAG-p65. As shown in figures 5.2c and 5.2d, no significant difference was seen with the shRNA targeting MED23 in A549 cells, with marginal increase seen in the MEFs, compared to the control shRNA. Together, these data suggest that MED23 is required for gene induction downstream of IRF3, but not NF-kB.

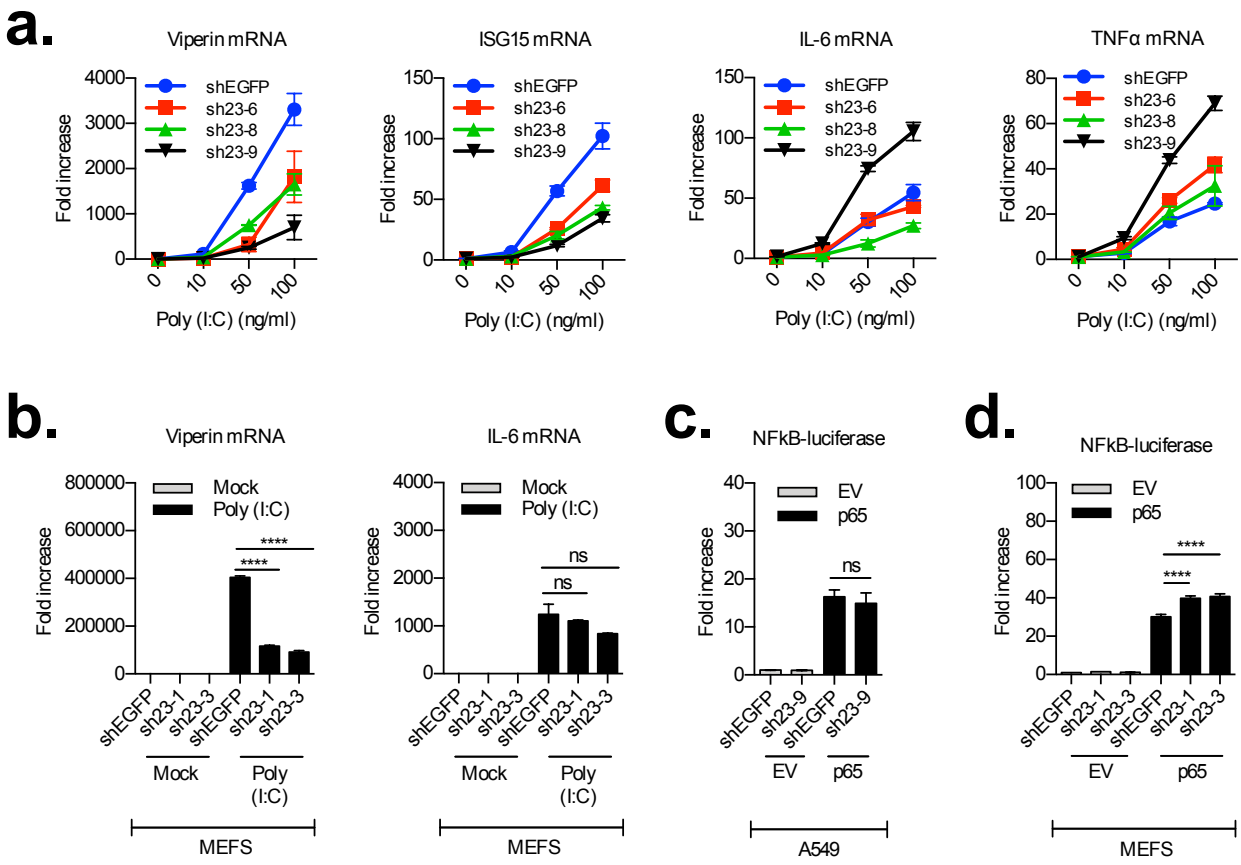

Figure 5.2 MED23 knock down impairs induction of IRF3- but not NF-kB-dependent genes

a) A549 cells stably transduced with control shRNA (shEGFP) or different shRNA targeting human MED23 (sh23-6, sh23-8, or sh23-9), were transfected with 0, 10, 50, or 100 ng/ml of Poly (I:C) for 6hrs, and were subsequently harvested and assessed for Viperin, ISG15, IL-6, or TNFα mRNA. Data is expressed relative to control and normalised to β-actin (n=3).

b) MEF cells stably transduced with control shRNA (shEGFP) or 2 different shRNA targeting mouse MED23 (sh23-1 or sh23-3), were transfected with 1 μg/ml of Poly (I:C) for 6hrs, and were subsequently harvested and assessed for Viperin and IL-6 mRNA. Data is expressed relative to control, and normalised to *Gapdh* (n=3)

c) and d) A549 cells (c) and MEFs (d) expressing shRNA targeting EGFP or MED23 were transfected with a plasmid encoding luciferase under the control of NF-kB, the control pRL-TK plasmid, and either an empty vector or FLAG-p65. The cells were harvested after 24 hrs and assessed for Firefly and Renilla luciferase. Data is expressed as Firefly luciferase relative to control and normalised to Renilla luciferase. EV, empty vector (n=3).

5.3. MED23 is not required for signalling downstream of IFNAR receptors

A previous study has suggested a role for MED23 in promoting signalling downstream of IFNAR receptors[210]. Ectopic expression of MED23 lead to a higher induction of a JAK-STAT-dependent luciferase promoter following treatment with IFN-α, compared to a control vector. Additionally, members of the IRF superfamily often have similar consensus DNA-binding sites, and activated forms of both IRF3 and IRF9 (via ISGF-3) are able to induce the same genes, such as in the case of RSAD2, ISG56 and ISG15[211–213]. To investigate whether the requirement of MED23 for gene induction is shared by IRF9, A549 cells stably expressing a control shRNA targeting EGFP or shRNA targeting human MED23 were either mock treated or treated with 500 U/ml of recombinant human IFN-α2. The cells were harvested after 6 hrs and subjected to RT-qPCR. As shown in figure 5.3a, both the cells expressing the control shRNA and those expressing shRNA targeting MED23 show induction of viperin and ISG15 to similar levels. This is further confirmed via western blotting (figure 5.3b) with knockdown of MED23 showing no impairment in either phosphorylation of STAT1 or ISG upregulation (RIG-I and ISG56) following treatment with IFN-α2, suggesting that MED23 is not required for signalling downstream of IFNAR receptors.

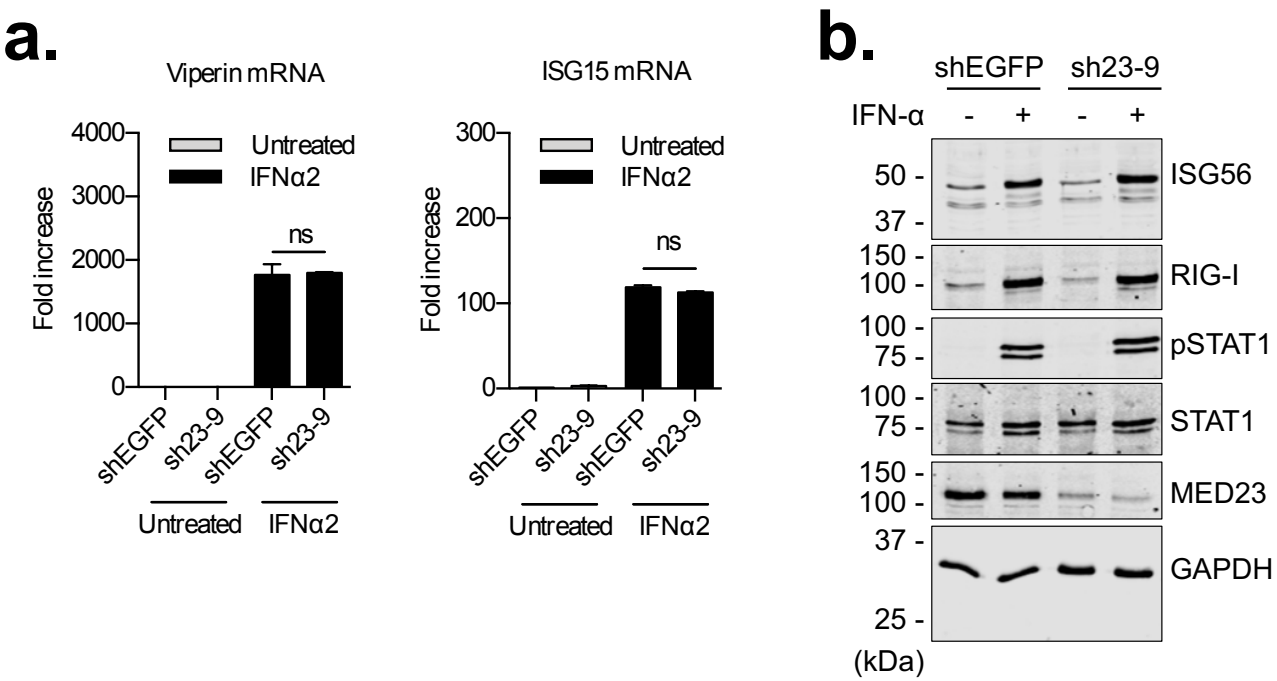

Figure 5.3 MED23 is not required for signalling downstream of IFNAR receptors

a) A549 cells stably transduced with control shRNA (shEGFP) or shRNA targeting human MED23 (sh23-9), were treated with DMEM ('untreated') or with 500 U/ml of recombinant human IFNα2 for 6hrs, and were subsequently harvested and assessed for Viperin and ISG15 mRNA. Data is expressed relative to control and normalised to β-actin (n=3).

b) A549 cells stably transduced with control shRNA (shEGFP) or shRNA targeting human MED23 (sh23-9), were treated with DMEM ('untreated') or with 1000 U/ml of recombinant human IFNα2 for 6hrs, and were subsequently harvested and assessed for indicated proteins by western blotting.

5.4. MEFs from MED23 null mice show evidence of genetic compensation

To investigate whether MED23 is essential in the induction of IFNs, wild type and *Med23*$^{-/-}$ MEF cells (figure 5.4a, previously described[160,161]) were either mock transfected or transfected with poly (I:C) over 6hrs and the IFN expression was assessed. *Med23*$^{-/-}$ MEF cells stimulated with poly (I:C) showed significantly higher induction of both type I and type III IFNs compared to wild type cells, contrary to data shown above from both siRNA and shRNA studies (figure 5.4b).

A similar mismatch between results from gene knockout and knockdown experiments has been previously described for several genes, and is thought to occur as a result of transcriptional adaptation[214,215]. This often involves upregulation of genes in other parts of a pathway, the effect of which is to restore the overall functionality of the pathway. To examine whether this is also true for MED23, RNA from unstimulated wild type and *Med23*$^{-/-}$ MEF cells where assessed via RT-qPCR for IRF3, p65, TBK1, IKKβ, and MAVS. As shown in Figure 5.4c, *Med23*$^{-/-}$ cells expressed higher levels of all the genes assessed compared to the wild type cells. The protein levels of both IRF3 and NF-kB were also higher in *Med23*$^{-/-}$ cells (Figure 5.4d). Altogether, these data suggest that MEFs from *Med23* null mice undergo genetic compensation.

The lack of correlation in the data obtained from RNA silencing and gene knockout studies could also be explained by off-target effects of the RNA silencing, although multiple shRNAs are unlikely to have a common off-target effect. Alternatively, it can be explained by the partial deletion of a gene that is able to function even in the absence of the wild type gene. To investigate these, *Med23*$^{-/-}$ MEF cells stably transduced with 2 different shRNA targeting mouse *Med23* were either mock transfected or transfected with poly (I:C) over 6hrs and the impact on IFN induction was assessed. A reduction in the levels of IFNs compared to the controls will indicate a potential off-target effect shared by all three shRNAs or a possible functional null allele. As shown in Figure 5.4f, this is not the case. Together, these data indicate that cells from *Med23* knockout mice undergo transcriptional adaptation to functionally compensate for the absence of MED23 in the IFN induction pathway.

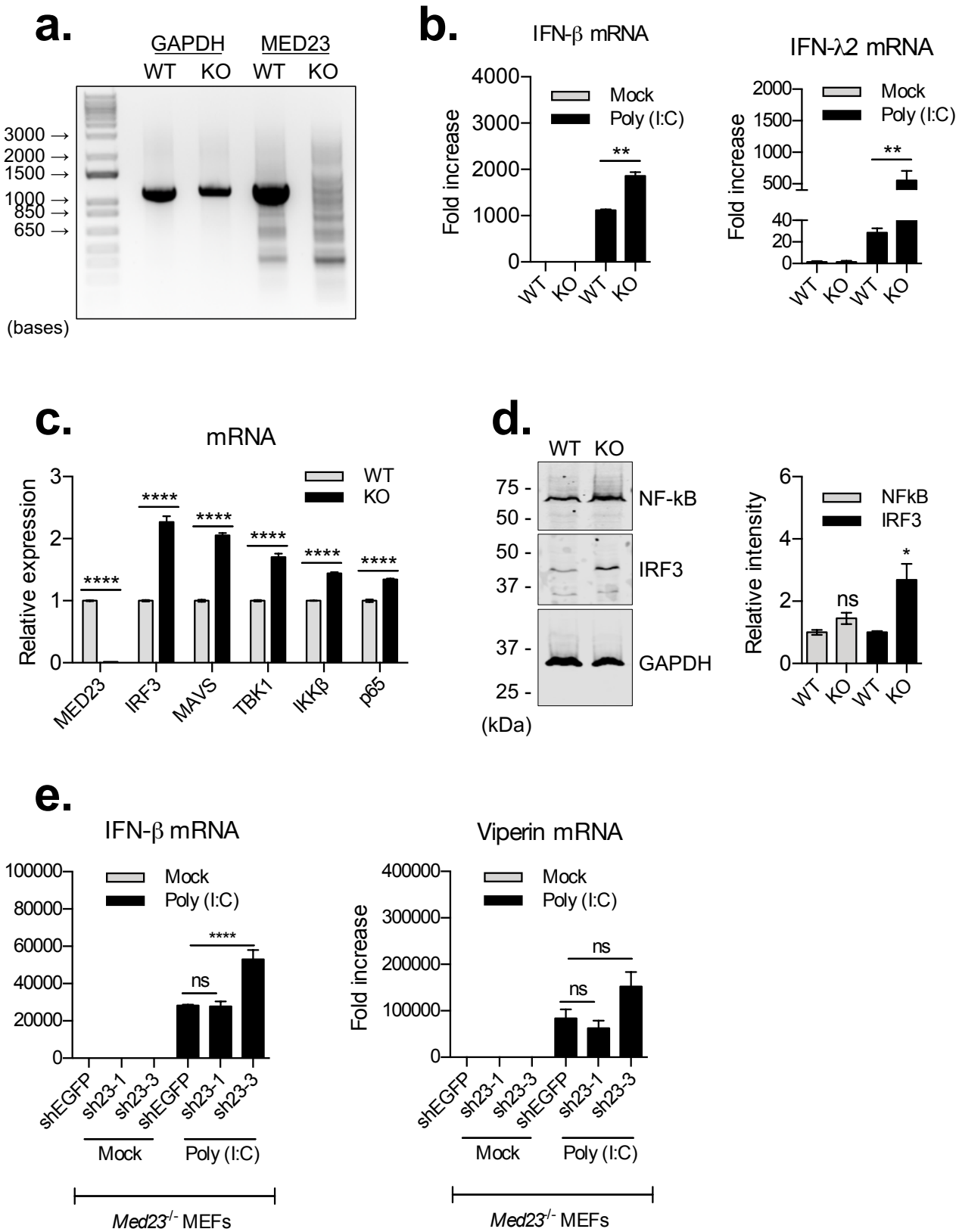
a.
GAPDH
MED23
WT KO WT KO
3000 →
2000 →
1500 →
1000 →
850 →
650 →
(bases)
b.
IFN-β mRNA
Fold increase
Mock
Poly (I:C)
**
WT KO WT KO
IFN-λ2 mRNA
Fold increase
Mock
Poly (I:C)
**
WT KO WT KO
c.
mRNA
Relative expression
WT
KO
****
MED23
IRF3
MAVS
TBK1
IKKβ
p65
d.
WT KO
75 -
50 -
NF-kB
50 -
37 -
IRF3
37 -
GAPDH
25 -
(kDa)
Relative intensity
NFkB
IRF3
ns
*
WT KO WT KO
e.
IFN-β mRNA
Fold increase
Mock
Poly (I:C)
****
ns
shEGFP
sh23-1
sh23-3
shEGFP
sh23-1
sh23-3
Mock
Poly (I:C)
Med23-/- MEFs
Viperin mRNA
Fold increase
Mock
Poly (I:C)
ns
ns
shEGFP
sh23-1
sh23-3
shEGFP
sh23-1
sh23-3
Mock
Poly (I:C)
Med23-/- MEFs

Figure 5.4 MEFs from MED23 null mice show evidence of genetic compensation

a) *Med23*$^{+/+}$ and *Med23*$^{-/-}$ MEF cells were harvested and assessed for *Gapdh* or *Med23* mRNA via end point PCR.

b) *Med23*$^{+/+}$ and *Med23*$^{-/-}$ MEF cells were transfected with 1 μg/ml of Poly (I:C) for 6hrs, and were subsequently harvested and assessed for IFN-β or IFN-λ2 mRNA. Data is expressed relative to control, and normalised to *Gapdh* (n=3)

c) *Med23*$^{+/+}$ and *Med23*$^{-/-}$ MEF cells were harvested and assessed for *Med23*, *Irf3*, *p65*, *Tbk1*, *Ikkb*, or *Mavs* mRNA via RT-qPCR. Data is expressed relative to WT cells and normalised to *Gapdh* (n=3).

d) Lysates from *Med23*$^{+/+}$ and *Med23*$^{-/-}$ MEF cells were blotted for IRF3, p65 and GAPDH (left panel). Data in the left panel is representative of 3 independent experiments, and those in the right panel represent quantification from 3 different blots each.

e) *Med23*$^{-/-}$ MEF cells stably transduced with control shRNA (shEGFP) or 2 different shRNA targeting mouse *Med23* (sh23-1 or sh23-3), were transfected with 1 μg/ml of Poly (I:C) for 6hrs, and were subsequently harvested and assessed for IFNβ and Viperin mRNA. Data is expressed relative to control and normalised to *Gapdh* (n=3).

5.5. MED23 is not required for activation of IRF3

Following detection of viral RNA or DNA in the cytosol, IRF3 is recruited to and is phosphorylated by TBK1/IKKε, after which it dimerises and translocates into the nucleus to induce IFN expression[216]. Activation of NF-kB instead requires phosphorylation (and eventual degradation) of IkB, allowing the NF-kB heterodimer to translocate into the nucleus and effect gene expression. To determine whether MED23 is involved in activation of IRF3 and/or NF-kB, A549 cells expressing either shEGFP or shMED23 were transfected poly (I:C), harvested 6 hrs later and assessed for phosphorylation of IRF3 and degradation of IkBα by western blotting. As shown in Figure 5.5a, there was no difference observed in the level of phosphorylated IRF3 between cells expressing MED23-targeting shRNA compared to the control shRNA. Similar results were obtained with siRNA knockdown of MED23, as shown in figures

5.5b and 5.5c. Translocation of IRF3 and NF-kB also appear to occur unhindered by MED23 depletion in cells transfected with poly (I:C) (figure 5.5d), indicating that MED23 is not required for activation of IRF3 or NF-kB.

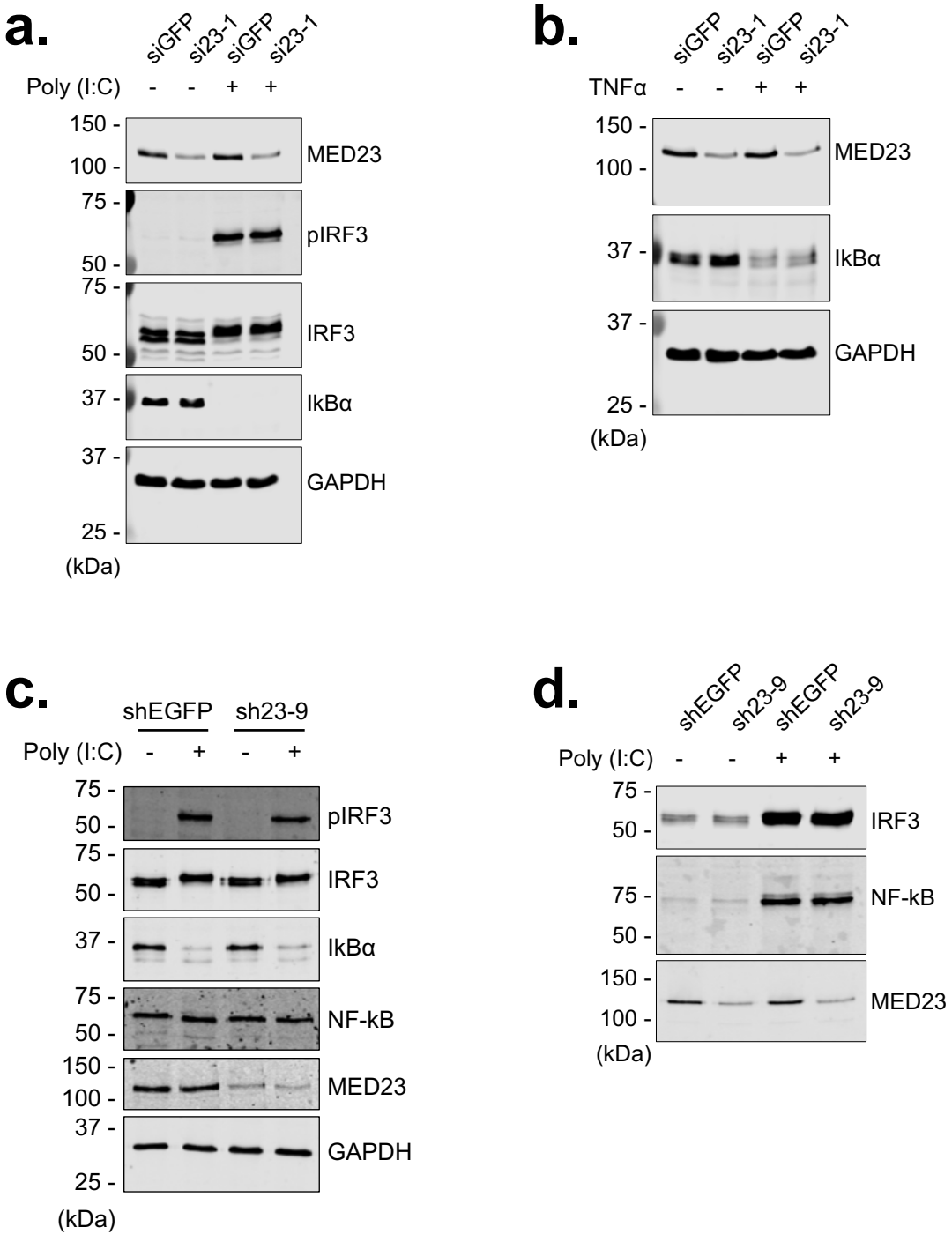

Figure 5.5 MED23 is not required for activation of IRF3

a) A549 cells stably transduced with control shRNA (shEGFP) or shRNA targeting human MED23 (sh23-9), were either mock transfected, or transfected with 1 μg/ml of poly (I:C), harvested 6 hrs later, and assessed via western blotting.

b) A549 cells were transfected with either control siRNA (siEGFP), or siRNA targeting human MED23. Forty-eight hrs later, the cells were either mock transfected, or transfected with 10 μg/ml of poly (I:C), harvested 6 hrs later, and assessed via western blotting.

c) A549 cells were transfected with either control siRNA (siEGFP), or siRNA targeting human MED23. Forty-eight hrs later, the cells were treated with either DMEM or 40 ng/ml recombinant human TNFα, harvested 6 hrs later, and assessed via western blotting.

d) A549 cells stably transduced with control shRNA (shEGFP) or shRNA targeting human MED23 (sh23-9), were either mock transfected, or transfected with 1 μg/ml of poly (I:C) and harvested 6 hrs later. Nuclear fractions were then assessed via western blotting.

5.6. MED23 interacts with activated IRF3 and is required for recruitment of RNA Pol II to promoters of IRF3-dependent genes

Gene-specific transcription factors often recruit the Mediator complex to gene enhancer regions via an interaction with a tail subunit of the complex[79]. It was therefore hypothesized that IRF3 interacts with MED23. To test this, HEK293T cells were co-transfected with HA-MED23 and either FLAG-EGFP or a FLAG-tagged constitutively-active IRF3 (IRF3-5D). The cells were then either mock-transfected or transfected with poly (I:C) 48 hrs later. The cells were harvested 6hrs later and co-immunoprecipitated using anti-FLAG antibodies-conjugated agarose beads and analysed by western blotting. As shown in Figure 5.6a, MED23 strongly associates with IRF3 but not EGFP, suggesting an interaction between MED23 and IRF3.

Next, the role of MED23 in the recruitment of RNA Pol II to transcription sites of IRF3-dependent genes was explored. A549 cells expressing either control shRNA or shRNA targeting MED23 were transfected with poly (I:C) and subjected to chromatin immunoprecipitation using anti-RNA Pol II antibodies. Immunoprecipitated DNA was then assessed by RT-qPCR. As shown in figure 5.6b, there was a significant reduction in RNA Pol II enrichment at the IFN-β promoter in MED23-depleted cells, indicating that MED23 is required for RNA Pol II recruitment downstream of activated IRF3.

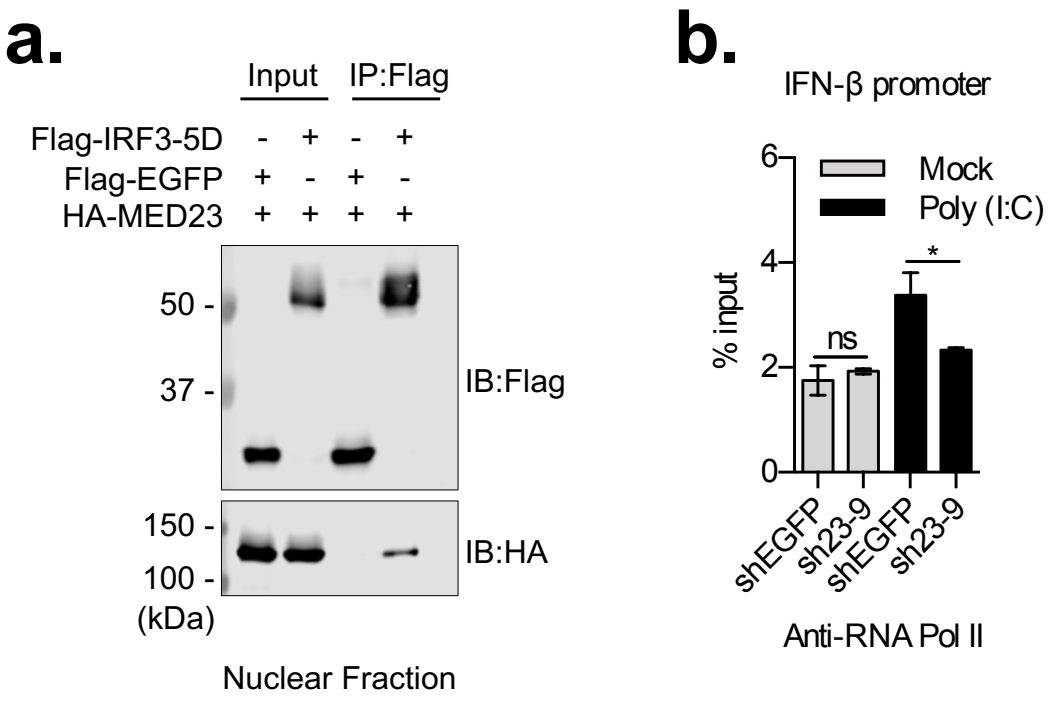

Figure 5.6 MED23 interacts with activated IRF3 and is required for recruitment of RNA Pol II to promoters of IRF3-dependent genes

a) HEK293T cells were co-transfected with HA-MED23 and either Flag-EGFP or Flag-IRF3-5D, and after 48 hrs nuclear fractions were subjected to co-immunoprecipitation with anti-flag M2 antibodies-conjugated agarose beads, and subsequently analysed via western blotting. Data represent three independent repeats.

b) A549 cells stably transduced with control shRNA (shEGFP) or shRNA targeting human MED23 (sh23-9), were either mock transfected, or transfected with 1 μg/ml of poly (I:C) and harvested 2 hrs later. Chromatin immunoprecipitation was carried out using anti-RNA Pol II and isotype control antibodies, immunoprecipitated DNA was assessed by RT-qPCR. Data represent three technical replicates, and is presented as amount of DNA relative to total input.

Discussion

A previous paper has shown that MED23 is required for induction of type III IFNs, likely through an interaction with IRF7[78]. Our data indicate that MED23 is required for induction of both type I and type III IFNs. While we did not observe IFN induction with overexpression of MED23 alone, MED23 appeared to increase IFN induction when co-expressed with either IRF7 or MAVS. Cells depleted of MED23 also showed reduced ability to express both type I and type III IFNs in response to cytoplasmic synthetic dsRNA and dsDNA analogues, as well as infection with an RNA virus. This critical role in innate immune responses is consistent with previous findings in *Drosophila*, where MED23 was shown to be required for heat-shock-specific gene expression via an interaction with Dif – a functional homologue of mammalian NF-kB – and the Heat shock transcription factor (*Hsf*)[217]. The heat shock response was recently shown to be vital in controlling infection by RNA viruses in *Drosophila*[218].

The observation that *Med23*$^{-/-}$ cells undergo genetic compensation is interesting, albeit a rather surprising one. MED23 has been shown to be required for induction of the *Egfr1* gene in embryonic stem cells downstream of phosphorylated ternary complex factor ELK1[160]. Using the same *Med23*$^{-/-}$ murine embryonic fibroblasts used in our experiments, Balamotis *et. al.* showed that *Egfr1* transcription still occurred in these

cells despite the lack of MED23[161]. While the authors, using transcriptome analyses and chromatin immunoprecipitation assays, showed that different ternary complex factors bound to the same regions as ELK1 to induce transcription of *Egfr1* in the fibroblasts, it will be interesting to see if transcriptional adaptation played a role there as well.

Our data indicate that MED23 is required for Mediator recruitment and induction of genes downstream of activated IRF3, but not those dependent on NF-kB activation. This is consistent with published data that shows MED17 as the critical Mediator subunit required for recruitment of Mediator to transcription sites of NF-kB-dependent genes[168]. Although both IRF3 and NF-kB extensively cooperate following activation to promote transcription of the same genes, IRF3 was shown to be partial towards *de novo* recruitment of RNA Pol II while NF-kB showed a greater tendency to mediate release of RNA Pol II paused at target sites[169]. As the Mediator is critical for both RNA Pol II recruitment and commencement of transcription elongation[79], it will be interesting to see if, and how, this is affected by the difference in the mechanism of Mediator recruitment.

MED23 depletion did not affect signalling downstream of IFNAR receptors, indicating that it is not required for Mediator recruitment by IRF9. This is understandable, considering that STAT2 – a component of ISGF-3 together with STAT1 and IRF9 – is likely able to recruit the Mediator via an interaction with MED14[210]. Given that IRF7 and IRF3 require MED23 for transcriptional activation,

it is possible that other positive regulatory IRFs such as IRF1 and IRF5 will also share this property.

The events taking place in the nucleus during type I IFN induction have been studied extensively. However, much of these studies precede the discovery of the Mediator complex, and therefore do not take it into account[71]. To the best of our knowledge, this is the first description of the mechanism of Mediator recruitment downstream of activated IRF3. Further work is required to gain more insight into this process, including the nature of the interaction between IRF3 and MED23, as well as the role of post-translational modifications, especially considering the recent resolution of the structure of MED23[219]. Additionally, further work is still required to determine the details of how the host is able to switch between induction of one type of IFN to another.

Chapter 6

Conclusion

Conclusion and future work

The first two aims of this thesis were to define additional innate immune mechanisms employed in the detection of MNV1 and clarify the mechanism of VF1 antagonism of host IFN responses. We described the presence of a RIG-I/STING-dependent innate response pathway that restricts the replication of noroviruses, and demonstrated an attempt by the murine norovirus to subvert it through expression of VF1. Our data largely agree with, and contribute to the current body of work on IFN responses to noroviruses, while also exposing the need for future work to understand the interplay between MDA5 and RIG-I in norovirus-infected hosts, as well as the cognate PAMPs recognised during infection with noroviruses. Future studies are also needed to further understand the function(s) of VF1 (including its ability to inhibit apoptosis), and other potential strategies used by noroviruses to evade host innate immune responses.

The last aim of this thesis was to explore other innate immune mechanisms at play in the restriction of RNA viruses. While we were unable to show peroxisomal localisation of MED23, we observed that it promotes the induction of both types I and III IFNs. We showed that depletion of MED23 leads to a reduction in expression of both type I and type III IFNs in human and mouse cell lines transfected with synthetic dsRNA. We also showed that *Med23*$^{-/-}$ cells undergo genetic compensation, suggesting a critical role for MED23 in this pathway. Mechanistically, we showed that MED23 interacts with IRF3, and is required for recruitment of RNA Pol II to promoters of IRF3-dependent genes. Altogether, our data indicate that MED23 plays an important role in antiviral responses by coupling IRF3 activation and RNA Pol II recruitment. Further work is required to gain more insight into this process, including

the nature of the interaction between IRF3 and MED23, as well as the role of post-translational modifications. Additionally, further work is still required to determine the details of how the host is able to switch between induction of one type of IFN to another.

References

1. Thiel HJ, König M. Caliciviruses: an overview. *Vet Microbiol*. 1999;69(1-2):55-62. http://www.ncbi.nlm.nih.gov/pubmed/10515270. Accessed January 10, 2019.

2. GREEN, KY. Caliciviridae: The Noroviruses. In: Knipe DM, Howley PM, eds. *Fields Virology*. 6th ed. Philadelphia: Lippincott Williams & Wilkins; 2013:582-608.

3. Karst SM, Wobus CE, Goodfellow IG, Green KY, Virgin HW. Advances in Norovirus Biology. *Cell Host Microbe*. 2014;15(6):668-680. doi:10.1016/j.chom.2014.05.015

4. Bányai K, Estes MK, Martella V, Parashar UD. Viral gastroenteritis. *Lancet*. 2018;392(10142):175-186. doi:10.1016/S0140-6736(18)31128-0

5. Patel MM, Hall AJ, Vinjé J, Parashar UD. Noroviruses: A comprehensive review. *J Clin Virol*. 2009;44(1):1-8. doi:10.1016/j.jcv.2008.10.009

6. Ramani S, Kang G. Viruses causing childhood diarrhoea in the developing world. *Curr Opin Infect Dis*. 2009;22(5):477-482. doi:10.1097/QCO.0b013e328330662f

7. Katpally U, Smith TJ. The Caliciviruses. In: *Current Topics in Microbiology and Immunology*. Vol 343. ; 2010:23-41. doi:10.1007/82_2010_36

8. Clarke IN, Lambden PR. Organization and Expression of Calicivirus Genes. *J Infect Dis*. 2000;181(s2):S309-S316. doi:10.1086/315575

9. Oka T, Wang Q, Katayama K, Saif LJ. Comprehensive review of human sapoviruses. *Clin Microbiol Rev*. 2015;28(1):32-53. doi:10.1128/CMR.00011-

10. McFadden N, Bailey D, Carrara G, et al. Norovirus regulation of the innate immune response and apoptosis occurs via the product of the alternative open reading frame 4. *PLoS Pathog*. 2011;7(12):e1002413. doi:10.1371/journal.ppat.1002413

11. Zhu S, Regev D, Watanabe M, et al. Identification of Immune and Viral Correlates of Norovirus Protective Immunity through Comparative Study of Intra-Cluster Norovirus Strains. Heise MT, ed. *PLoS Pathog*. 2013;9(9):e1003592. doi:10.1371/journal.ppat.1003592

12. Zhu S, Jones MK, Hickman D, Han S, Reeves W, Karst SM. Norovirus antagonism of B-cell antigen presentation results in impaired control of acute infection. *Mucosal Immunol*. 2016;9(6):1559-1570. doi:10.1038/mi.2016.15

13. Lopman BA, Steele D, Kirkwood CD, Parashar UD. The Vast and Varied Global Burden of Norovirus: Prospects for Prevention and Control. *PLOS Med*. 2016;13(4):e1001999. doi:10.1371/journal.pmed.1001999

14. Glass RI, Parashar UD, Estes MK. Norovirus Gastroenteritis. *N Engl J Med*. 2009;361(18):1776-1785. doi:10.1056/NEJMra0804575

15. Bartsch SM, Lopman BA, Ozawa S, Hall AJ, Lee BY. Global Economic Burden of Norovirus Gastroenteritis. Olson DR, ed. *PLoS One*. 2016;11(4):e0151219. doi:10.1371/journal.pone.0151219

16. Takanashi S, Saif LJ, Hughes JH, et al. Failure of propagation of human norovirus in intestinal epithelial cells with microvilli grown in three-dimensional cultures. *Arch Virol*. 2014;159(2):257-266. doi:10.1007/s00705-

013-1806-4

17. Oka T, Stoltzfus GT, Zhu C, Jung K, Wang Q, Saif LJ. Attempts to grow human noroviruses, a sapovirus, and a bovine norovirus in vitro. Wobus CE, ed. *PLoS One*. 2018;13(2):e0178157. doi:10.1371/journal.pone.0178157

18. Ettayebi K, Crawford SE, Murakami K, et al. Replication of human noroviruses in stem cell-derived human enteroids. *Science (80-)*. 2016;353(6306):1387-1393. doi:10.1126/science.aaf5211

19. Karst SM, Wobus CE, Lay M, Davidson J, Virgin HW. STAT1-Dependent Innate Immunity to a Norwalk-Like Virus. *Science*. 2003;299(5612):1575-1578. doi:10.1126/science.1077905

20. Mumphrey SM, Changotra H, Moore TN, et al. Murine norovirus 1 infection is associated with histopathological changes in immunocompetent hosts, but clinical disease is prevented by STAT1-dependent interferon responses. *J Virol*. 2007;81(7):3251-3263. doi:10.1128/JVI.02096-06

21. Thorne LG, Goodfellow IG. Norovirus gene expression and replication. *J Gen Virol*. 2014;95(Pt_2):278-291. doi:10.1099/vir.0.059634-0

22. Perry JW, Wobus CE. Endocytosis of murine norovirus 1 into murine macrophages is dependent on dynamin II and cholesterol. *J Virol*. 2010;84(12):6163-6176. doi:10.1128/JVI.00331-10

23. Wobus CE, Karst SM, Thackray LB, et al. Replication of Norovirus in cell culture reveals a tropism for dendritic cells and macrophages. Michael Emerman, ed. *PLoS Biol*. 2004;2(12):e432. doi:10.1371/journal.pbio.0020432

24. Haga K, Fujimoto A, Takai-Todaka R, et al. Functional receptor molecules

CD300lf and CD300ld within the CD300 family enable murine noroviruses to infect cells. *Proc Natl Acad Sci*. 2016;113(41):E6248-E6255. doi:10.1073/pnas.1605575113

25. Orchard RC, Wilen CB, Doench JG, et al. Discovery of a proteinaceous cellular receptor for a norovirus. *Science (80-)*. 2016;353(6302):933-936. doi:10.1126/science.aaf1220

26. Grau KR, Roth AN, Zhu S, et al. The major targets of acute norovirus infection are immune cells in the gut-associated lymphoid tissue. *Nat Microbiol*. 2017;2(12):1586-1591. doi:10.1038/s41564-017-0057-7

27. Lee S, Wilen CB, Orvedahl A, et al. Norovirus Cell Tropism Is Determined by Combinatorial Action of a Viral Non-structural Protein and Host Cytokine. *Cell Host Microbe*. 2017;22(4):449-459.e4. doi:10.1016/j.chom.2017.08.021

28. Wilen CB, Lee S, Hsieh LL, et al. Tropism for tuft cells determines immune promotion of norovirus pathogenesis. *Science (80-)*. 2018;360(6385):204-208. doi:10.1126/science.aar3799

29. Jones MK, Grau KR, Costantini V, et al. Human norovirus culture in B cells. *Nat Protoc*. 2015;10(12):1939-1947. doi:10.1038/nprot.2015.121

30. Fensterl V, Chattopadhyay S, Sen GC. No Love Lost Between Viruses and Interferons. *Annu Rev Virol*. 2015;2(1):549-572. doi:10.1146/annurev-virology-100114-055249

31. Hoffmann H-H, Schneider WM, Rice CM. Interferons and viruses: an evolutionary arms race of molecular interactions. *Trends Immunol*. 2015;36(3):124-138. doi:10.1016/j.it.2015.01.004

32. Netea MG, Balkwill F, Chonchol M, et al. A guiding map for inflammation. *Nat Immunol*. 2017;18(8):826-831. doi:10.1038/ni.3790

33. Taniguchi K, Karin M. NF-κB, inflammation, immunity and cancer: coming of age. *Nat Rev Immunol*. 2018;18(5):309-324. doi:10.1038/nri.2017.142

34. Iwasaki A. A Virological View of Innate Immune Recognition. *Annu Rev Microbiol*. 2012;66(1):177-196. doi:10.1146/annurev-micro-092611-150203

35. Brubaker SW, Bonham KS, Zanoni I, Kagan JC. Innate Immune Pattern Recognition: A Cell Biological Perspective. *Annu Rev Immunol*. 2015;33(1):257-290. doi:10.1146/annurev-immunol-032414-112240

36. Yoneyama M, Kikuchi M, Natsukawa T, et al. The RNA helicase RIG-I has an essential function in double-stranded RNA-induced innate antiviral responses. *Nat Immunol*. 2004;5(7):730-737. doi:10.1038/ni1087

37. Andrejeva J, Childs KS, Young DF, et al. The V proteins of paramyxoviruses bind the IFN-inducible RNA helicase, mda-5, and inhibit its activation of the IFN-beta promoter. *Proc Natl Acad Sci U S A*. 2004;101(49):17264-17269. doi:10.1073/pnas.0407639101

38. Gürtler C, Bowie AG. Innate immune detection of microbial nucleic acids. *Trends Microbiol*. 2013;21(8):413-420. doi:10.1016/j.tim.2013.04.004

39. Bruns AM, Horvath CM. Antiviral RNA recognition and assembly by RLR family innate immune sensors. *Cytokine Growth Factor Rev*. 2014;25(5):507-512. doi:10.1016/j.cytogfr.2014.07.006

40. West AP, Shadel GS, Ghosh S. Mitochondria in innate immune responses. *Nat Rev Immunol*. 2011;11(6):389-402. doi:10.1038/nri2975

41. Rodriguez KR, Bruns AM, Horvath CM. MDA5 and LGP2: Accomplices and Antagonists of Antiviral Signal Transduction. *J Virol*. 2014;88(15):8194-8200. doi:10.1128/JVI.00640-14

42. Xu L-G, Wang Y-Y, Han K-J, Li L-Y, Zhai Z, Shu H-B. VISA is an adapter protein required for virus-triggered IFN-beta signaling. *Mol Cell*. 2005;19(6):727-740. doi:10.1016/j.molcel.2005.08.014

43. Meylan E, Curran J, Hofmann K, et al. Cardif is an adaptor protein in the RIG-I antiviral pathway and is targeted by hepatitis C virus. *Nature*. 2005;437(7062):1167-1172. doi:10.1038/nature04193

44. Kawai T, Takahashi K, Sato S, et al. IPS-1, an adaptor triggering RIG-I- and Mda5-mediated type I interferon induction. *Nat Immunol*. 2005;6(10):981-988. doi:10.1038/ni1243

45. Seth RB, Sun L, Ea C-K, Chen ZJ. Identification and characterization of MAVS, a mitochondrial antiviral signaling protein that activates NF-kappaB and IRF 3. *Cell*. 2005;122(5):669-682. doi:10.1016/j.cell.2005.08.012

46. Brubaker SW, Gauthier AE, Mills EW, Ingolia NT, Kagan JC. A bicistronic MAVS transcript highlights a class of truncated variants in antiviral immunity. *Cell*. 2014;156(4):800-811. doi:10.1016/j.cell.2014.01.021

47. Belgnaoui SM, Paz S, Hiscott J. Orchestrating the interferon antiviral response through the mitochondrial antiviral signaling (MAVS) adapter. *Curr Opin Immunol*. 2011;23(5):564-572. doi:10.1016/j.coi.2011.08.001

48. Vazquez C, Horner SM. MAVS coordination of antiviral innate immunity. *J Virol*. May 2015. doi:10.1128/JVI.01918-14

49. Horner SM, Liu HM, Park HS, Briley J, Gale M. Mitochondrial-associated endoplasmic reticulum membranes (MAM) form innate immune synapses and are targeted by hepatitis C virus. *Proc Natl Acad Sci U S A*. 2011;108(35):14590-14595. doi:10.1073/pnas.1110133108

50. Dixit E, Boulant S, Zhang Y, et al. Peroxisomes are signaling platforms for antiviral innate immunity. *Cell*. 2010;141(4):668-681. doi:10.1016/j.cell.2010.04.018

51. Sun Q, Sun L, Liu H-H, et al. The specific and essential role of MAVS in antiviral innate immune responses. *Immunity*. 2006;24(5):633-642. doi:10.1016/j.immuni.2006.04.004

52. Kumar H, Kawai T, Kato H, et al. Essential role of IPS-1 in innate immune responses against RNA viruses. *J Exp Med*. 2006;203(7):1795-1803. doi:10.1084/jem.20060792

53. Odendall C, Dixit E, Stavru F, et al. Diverse intracellular pathogens activate type III interferon expression from peroxisomes. *Nat Immunol*. 2014;15(8):717-726. doi:10.1038/ni.2915

54. Bender S, Reuter A, Eberle F, Einhorn E, Binder M, Bartenschlager R. Activation of Type I and III Interferon Response by Mitochondrial and Peroxisomal MAVS and Inhibition by Hepatitis C Virus. Randall G, ed. *PLoS Pathog*. 2015;11(11):e1005264. doi:10.1371/journal.ppat.1005264

55. Ma Z, Ni G, Damania B. Innate Sensing of DNA Virus Genomes. *Annu Rev Virol*. 2018;5(1):341-362. doi:10.1146/annurev-virology-092917-043244

56. Ni G, Ma Z, Damania B. cGAS and STING: At the intersection of DNA and

RNA virus-sensing networks. Evans MJ, ed. *PLOS Pathog*. 2018;14(8):e1007148. doi:10.1371/journal.ppat.1007148

57. Zevini A, Olagnier D, Hiscott J. Crosstalk between Cytoplasmic RIG-I and STING Sensing Pathways. *Trends Immunol*. 2017;38(3):194-205. doi:10.1016/j.it.2016.12.004

58. Chiu Y-H, MacMillan JB, Chen ZJ. RNA Polymerase III Detects Cytosolic DNA and Induces Type I Interferons through the RIG-I Pathway. *Cell*. 2009;138(3):576-591. doi:10.1016/j.cell.2009.06.015

59. Ablasser A, Bauernfeind F, Hartmann G, Latz E, Fitzgerald KA, Hornung V. RIG-I-dependent sensing of poly(dA:dT) through the induction of an RNA polymerase III-transcribed RNA intermediate. *Nat Immunol*. 2009;10(10):1065-1072. doi:10.1038/ni.1779

60. Mankan AK, Schmidt T, Chauhan D, et al. Cytosolic RNA:DNA hybrids activate the cGAS-STING axis. *EMBO J*. 2014;33(24):2937-2946. doi:10.15252/embj.201488726

61. Herzner A-M, Hagmann CA, Goldeck M, et al. Sequence-specific activation of the DNA sensor cGAS by Y-form DNA structures as found in primary HIV-1 cDNA. *Nat Immunol*. 2015;16(10):1025-1033. doi:10.1038/ni.3267

62. Aguirre S, Luthra P, Sanchez-Aparicio MT, et al. Dengue virus NS2B protein targets cGAS for degradation and prevents mitochondrial DNA sensing during infection. *Nat Microbiol*. 2017;2(5):17037. doi:10.1038/nmicrobiol.2017.37

63. Aguirre S, Fernandez-Sesma A. Collateral Damage during Dengue Virus

Infection: Making Sense of DNA by cGAS. Gack MU, ed. *J Virol*. 2017;91(14). doi:10.1128/JVI.01081-16

64. Schoggins JW, MacDuff DA, Imanaka N, et al. Pan-viral specificity of IFN-induced genes reveals new roles for cGAS in innate immunity. *Nature*. 2014;505(7485):691-695. doi:10.1038/nature12862

65. Ma F, Li B, Yu Y, Iyer SS, Sun M, Cheng G. Positive feedback regulation of type I interferon by the interferon-stimulated gene STING. *EMBO Rep*. 2015;16(2):202-212. doi:10.15252/embr.201439366

66. Zhong B, Yang Y, Li S, et al. The Adaptor Protein MITA Links Virus-Sensing Receptors to IRF3 Transcription Factor Activation. *Immunity*. 2008;29(4):538-550. doi:10.1016/j.immuni.2008.09.003

67. Ishikawa H, Barber GN. STING is an endoplasmic reticulum adaptor that facilitates innate immune signalling. *Nature*. 2008;455(7213):674-678. doi:10.1038/nature07317

68. Holm CK, Rahbek SH, Gad HH, et al. Influenza A virus targets a cGAS-independent STING pathway that controls enveloped RNA viruses. *Nat Commun*. 2016;7(1):10680. doi:10.1038/ncomms10680

69. Nazmi A, Mukhopadhyay R, Dutta K, Basu A. STING Mediates Neuronal Innate Immune Response Following Japanese Encephalitis Virus Infection. *Sci Rep*. 2012;2(1):347. doi:10.1038/srep00347

70. Franz KM, Neidermyer WJ, Tan Y-J, Whelan SPJ, Kagan JC. STING-dependent translation inhibition restricts RNA virus replication. *Proc Natl Acad Sci*. 2018;115(9):E2058-E2067. doi:10.1073/pnas.1716937115

71. Ford E, Thanos D. The transcriptional code of human IFN-β gene expression. *Biochim Biophys Acta - Gene Regul Mech*. 2010;1799(3-4):328-336. doi:10.1016/j.bbagrm.2010.01.010

72. Au-Yeung N, Horvath CM. Transcriptional and chromatin regulation in interferon and innate antiviral gene expression. *Cytokine Growth Factor Rev*. 2018;44:11-17. doi:10.1016/j.cytogfr.2018.10.003

73. Kotenko S V., Durbin JE. Contribution of type III interferons to antiviral immunity: location, location, location. *J Biol Chem*. 2017;292(18):7295-7303. doi:10.1074/jbc.R117.777102

74. Lazear HM, Nice TJ, Diamond MS. Interferon-λ: Immune Functions at Barrier Surfaces and Beyond. *Immunity*. 2015;43(1):15-28. doi:10.1016/j.immuni.2015.07.001

75. Osterlund PI, Pietilä TE, Veckman V, Kotenko S V, Julkunen I. IFN regulatory factor family members differentially regulate the expression of type III IFN (IFN-lambda) genes. *J Immunol*. 2007;179(6):3434-3442. http://www.ncbi.nlm.nih.gov/pubmed/17785777. Accessed September 25, 2018.

76. Iversen MB, Ank N, Melchjorsen J, Paludan SR. Expression of type III interferon (IFN) in the vaginal mucosa is mediated primarily by dendritic cells and displays stronger dependence on NF-kappaB than type I IFNs. *J Virol*. 2010;84(9):4579-4586. doi:10.1128/JVI.02591-09

77. Thomson SJP, Goh FG, Banks H, et al. The role of transposable elements in the regulation of IFN-λ1 gene expression. *Proc Natl Acad Sci*. 2009;106(28):11564-11569. doi:10.1073/pnas.0904477106

78. Griffiths SJ, Koegl M, Boutell C, et al. A Systematic Analysis of Host Factors Reveals a Med23-Interferon-λ Regulatory Axis against Herpes Simplex Virus Type 1 Replication. Gao S-J, ed. *PLoS Pathog*. 2013;9(8):e1003514. doi:10.1371/journal.ppat.1003514

79. Soutourina J. Transcription regulation by the Mediator complex. *Nat Rev Mol Cell Biol*. 2017;19(4):262-274. doi:10.1038/nrm.2017.115

80. Jeronimo C, Robert F. The Mediator Complex: At the Nexus of RNA Polymerase II Transcription. *Trends Cell Biol*. 2017;27(10):765-783. doi:10.1016/j.tcb.2017.07.001

81. Poss ZC, Ebmeier CC, Taatjes DJ. The Mediator complex and transcription regulation. *Crit Rev Biochem Mol Biol*. 2013;48(6):575-608. doi:10.3109/10409238.2013.840259

82. Ansari SA, Morse RH. Mechanisms of Mediator complex action in transcriptional activation. *Cell Mol Life Sci*. 2013;70(15):2743-2756. doi:10.1007/s00018-013-1265-9

83. Schoggins JW. Recent advances in antiviral interferon-stimulated gene biology. *F1000Research*. 2018;7:309. doi:10.12688/f1000research.12450.1

84. Au WC, Moore PA, LaFleur DW, Tombal B, Pitha PM. Characterization of the interferon regulatory factor-7 and its potential role in the transcription activation of interferon A genes. *J Biol Chem*. 1998;273(44):29210-29217. http://www.ncbi.nlm.nih.gov/pubmed/9786932. Accessed January 9, 2019.

85. Marie I, Durbin JE, Levy DE. Differential viral induction of distinct interferon-alpha genes by positive feedback through interferon regulatory

factor-7. *EMBO J*. 1998;17(22):6660-6669. doi:10.1093/emboj/17.22.6660

86. de Weerd NA, Samarajiwa SA, Hertzog PJ. Type I interferon receptors: biochemistry and biological functions. *J Biol Chem*. 2007;282(28):20053-20057. doi:10.1074/jbc.R700006200

87. Wack A, Terczyńska-Dyla E, Hartmann R. Guarding the frontiers: the biology of type III interferons. *Nat Immunol*. 2015;16(8):802-809. doi:10.1038/ni.3212

88. Sommereyns C, Paul S, Staeheli P, Michiels T. IFN-Lambda (IFN-λ) Is Expressed in a Tissue-Dependent Fashion and Primarily Acts on Epithelial Cells In Vivo. Buchmeier MJ, ed. *PLoS Pathog*. 2008;4(3):e1000017. doi:10.1371/journal.ppat.1000017

89. Pott J, Mahlakoiv T, Mordstein M, et al. IFN- determines the intestinal epithelial antiviral host defense. *Proc Natl Acad Sci*. 2011;108(19):7944-7949. doi:10.1073/pnas.1100552108

90. Mordstein M, Neugebauer E, Ditt V, et al. Lambda Interferon Renders Epithelial Cells of the Respiratory and Gastrointestinal Tracts Resistant to Viral Infections. *J Virol*. 2010;84(11):5670-5677. doi:10.1128/JVI.00272-10

91. Lin J-D, Feng N, Sen A, et al. Distinct Roles of Type I and Type III Interferons in Intestinal Immunity to Homologous and Heterologous Rotavirus Infections. Staeheli P, ed. *PLOS Pathog*. 2016;12(4):e1005600. doi:10.1371/journal.ppat.1005600

92. Ivashkiv LB, Donlin LT. Regulation of type I interferon responses. *Nat Rev Immunol*. 2014;14(1):36-49. doi:10.1038/nri3581

93. Odendall C, Kagan JC. The unique regulation and functions of type III interferons in antiviral immunity. *Curr Opin Virol*. 2015;12:47-52. doi:10.1016/j.coviro.2015.02.003

94. Nice TJ, Baldridge MT, McCune BT, et al. Interferon-λ cures persistent murine norovirus infection in the absence of adaptive immunity. *Science*. 2015;347(6219):269-273. doi:10.1126/science.1258100

95. Pott J, Mahlakõiv T, Mordstein M, et al. IFN-lambda determines the intestinal epithelial antiviral host defense. *Proc Natl Acad Sci U S A*. 2011;108(19):7944-7949. doi:10.1073/pnas.1100552108

96. Galani IE, Triantafyllia V, Eleminiadou E-E, et al. Interferon-λ Mediates Non-redundant Front-Line Antiviral Protection against Influenza Virus Infection without Compromising Host Fitness. *Immunity*. 2017;46(5):875-890.e6. doi:10.1016/j.immuni.2017.04.025

97. Andreakos E, Salagianni M, Galani IE, Koltsida O. Interferon-λs: Front-Line Guardians of Immunity and Homeostasis in the Respiratory Tract. *Front Immunol*. 2017;8:1232. doi:10.3389/fimmu.2017.01232

98. Schneider WM, Chevillotte MD, Rice CM. Interferon-Stimulated Genes: A Complex Web of Host Defenses. *Annu Rev Immunol*. 2014;32(1):513-545. doi:10.1146/annurev-immunol-032713-120231

99. Gizzi AS, Grove TL, Arnold JJ, et al. A naturally occurring antiviral ribonucleotide encoded by the human genome. *Nature*. 2018;558(7711):610-614. doi:10.1038/s41586-018-0238-4

100. Fensterl V, Sen GC. Interferon-Induced Ifit Proteins: Their Role in Viral

Pathogenesis. Goff SP, ed. *J Virol*. 2015;89(5):2462-2468. doi:10.1128/JVI.02744-14

101. Schoggins JW, Rice CM. Interferon-stimulated genes and their antiviral effector functions. *Curr Opin Virol*. 2011;1(6):519-525. doi:10.1016/j.coviro.2011.10.008

102. Castanier C, Zemirli N, Portier A, et al. MAVS ubiquitination by the E3 ligase TRIM25 and degradation by the proteasome is involved in type I interferon production after activation of the antiviral RIG-I-like receptors. *BMC Biol*. 2012;10:44. doi:10.1186/1741-7007-10-44

103. You F, Sun H, Zhou X, et al. PCBP2 mediates degradation of the adaptor MAVS via the HECT ubiquitin ligase AIP4. *Nat Immunol*. 2009;10(12):1300-1308. doi:10.1038/ni.1815

104. Zhong B, Zhang Y, Tan B, Liu T-T, Wang Y-Y, Shu H-B. The E3 ubiquitin ligase RNF5 targets virus-induced signaling adaptor for ubiquitination and degradation. *J Immunol*. 2010;184(11):6249-6255. doi:10.4049/jimmunol.0903748

105. Arimoto K, Takahashi H, Hishiki T, Konishi H, Fujita T, Shimotohno K. Negative regulation of the RIG-I signaling by the ubiquitin ligase RNF125. *Proc Natl Acad Sci U S A*. 2007;104(18):7500-7505. doi:10.1073/pnas.0611551104

106. Vitour D, Dabo S, Ahmadi Pour M, et al. Polo-like kinase 1 (PLK1) regulates interferon (IFN) induction by MAVS. *J Biol Chem*. 2009;284(33):21797-21809. doi:10.1074/jbc.M109.018275

107. Rocha-Pereira J, Jacobs S, Noppen S, Verbeken E, Michiels T, Neyts J. Interferon lambda (IFN-λ) efficiently blocks norovirus transmission in a mouse model. *Antiviral Res*. 2018;149:7-15. doi:10.1016/j.antiviral.2017.10.017

108. Changotra H, Jia Y, Moore TN, et al. Type I and type II interferons inhibit the translation of murine norovirus proteins. *J Virol*. 2009;83(11):5683-5692. doi:10.1128/JVI.00231-09

109. Rodriguez MR, Monte K, Thackray LB, Lenschow DJ. ISG15 Functions as an Interferon-Mediated Antiviral Effector Early in the Murine Norovirus Life Cycle. *J Virol*. 2014;88(16):9277-9286. doi:10.1128/JVI.01422-14

110. Ng YC, Kim YW, Lee J-S, Lee SJ, Jung Song M. Antiviral activity of Schizonepeta tenuifolia Briquet against noroviruses via induction of antiviral interferons. *J Microbiol*. 2018;56(9):683-689. doi:10.1007/s12275-018-8228-7

111. Enosi Tuipulotu D, Netzler NE, Lun JH, Mackenzie JM, White PA. TLR7 Agonists Display Potent Antiviral Effects against Norovirus Infection via Innate Stimulation. *Antimicrob Agents Chemother*. 2018;62(5). doi:10.1128/AAC.02417-17

112. Dang W, Xu L, Yin Y, et al. IRF-1, RIG-I and MDA5 display potent antiviral activities against norovirus coordinately induced by different types of interferons. *Antiviral Res*. 2018;155:48-59. doi:10.1016/j.antiviral.2018.05.004

113. Nice TJ, Osborne LC, Tomov VT, Artis D, Wherry EJ, Virgin HW. Type I Interferon Receptor Deficiency in Dendritic Cells Facilitates Systemic Murine

Norovirus Persistence Despite Enhanced Adaptive Immunity. Coyne CB, ed. *PLOS Pathog*. 2016;12(6):e1005684. doi:10.1371/journal.ppat.1005684

114. Van Winkle JA, Robinson BA, Peters AM, et al. Persistence of Systemic Murine Norovirus Is Maintained by Inflammatory Recruitment of Susceptible Myeloid Cells. *Cell Host Microbe*. 2018;24(5):665-676.e4. doi:10.1016/j.chom.2018.10.003

115. Jung K, Wang Q, Kim Y, et al. The Effects of Simvastatin or Interferon-α on Infectivity of Human Norovirus Using a Gnotobiotic Pig Model for the Study of Antivirals. Guan Y, ed. *PLoS One*. 2012;7(7):e41619. doi:10.1371/journal.pone.0041619

116. Chang K-O, Sosnovtsev S V, Belliot G, King AD, Green KY. Stable expression of a Norwalk virus RNA replicon in a human hepatoma cell line. *Virology*. 2006;353(2):463-473. doi:10.1016/j.virol.2006.06.006

117. Chang K-O, George DW. Interferons and Ribavirin Effectively Inhibit Norwalk Virus Replication in Replicon-Bearing Cells. *J Virol*. 2007;81(22):12111-12118. doi:10.1128/JVI.00560-07

118. Susanna G, Estes MK. Caliciviridae and Astroviridae. In: Brasier AR, García-Sastre A, Lemon SM, eds. *Cellular Signaling and Innate Immune Responses to RNA Virus Infections*. 1st ed. Washington D.C.: ASM Press; 2009:389-402.

119. Li MMH, MacDonald MR, Rice CM. To translate, or not to translate: viral and host mRNA regulation by interferon-stimulated genes. *Trends Cell Biol*. 2015;25(6):320-329. doi:10.1016/j.tcb.2015.02.001

120. Baldridge MT, Turula H, Wobus CE. Norovirus Regulation by Host and

Microbe. *Trends Mol Med*. 2016;22(12):1047-1059. doi:10.1016/j.molmed.2016.10.003

121. Emmott E, Sorgeloos F, Caddy SL, et al. Norovirus-Mediated Modification of the Translational Landscape via Virus and Host-Induced Cleavage of Translation Initiation Factors. *Mol Cell Proteomics*. 2017;16(4 suppl 1):S215-S229. doi:10.1074/mcp.M116.062448

122. McCartney SA, Thackray LB, Gitlin L, et al. MDA-5 Recognition of a Murine Norovirus. Baric RS, ed. *PLoS Pathog*. 2008;4(7):e1000108. doi:10.1371/journal.ppat.1000108

123. MacDuff DA, Baldridge MT, Qaqish AM, et al. HOIL1 Is Essential for the Induction of Type I and III Interferons by MDA5 and Regulates Persistent Murine Norovirus Infection. Pfeiffer JK, ed. *J Virol*. 2018;92(23). doi:10.1128/JVI.01368-18

124. Levenson EA, Martens C, Kanakabandi K, et al. Comparative Transcriptomic Response of Primary and Immortalized Macrophages to Murine Norovirus Infection. *J Immunol*. 2018;200(12):4157-4169. doi:10.4049/jimmunol.1700384

125. Baldridge MT, Lee S, Brown JJ, et al. Expression of *Ifnlr1* on Intestinal Epithelial Cells Is Critical to the Antiviral Effects of Interferon Lambda against Norovirus and Reovirus. López S, ed. *J Virol*. 2017;91(7). doi:10.1128/JVI.02079-16

126. Qu L, Murakami K, Broughman JR, et al. Replication of Human Norovirus RNA in Mammalian Cells Reveals Lack of Interferon Response. López S, ed. *J Virol*. 2016;90(19):8906-8923. doi:10.1128/JVI.01425-16

127. Souza M, Cheetham SM, Azevedo MSP, Costantini V, Saif LJ. Cytokine and Antibody Responses in Gnotobiotic Pigs after Infection with Human Norovirus Genogroup II.4 (HS66 Strain). *J Virol*. 2007;81(17):9183-9192. doi:10.1128/JVI.00558-07

128. Karst SM. The Role of Type I Interferon in Regulating Norovirus Infections. *J Clin Cell Immunol*. August 2011:1-5. doi:10.4172/2155-9899.S1-001

129. Lee W, Lee S-H, Kim M, et al. Vibrio vulnificus quorum-sensing molecule cyclo(Phe-Pro) inhibits RIG-I-mediated antiviral innate immunity. *Nat Commun*. 2018;9(1):1606. doi:10.1038/s41467-018-04075-1

130. Guix S, Asanaka M, Katayama K, et al. Norwalk Virus RNA Is Infectious in Mammalian Cells. *J Virol*. 2007;81(22):12238-12248. doi:10.1128/JVI.01489-07

131. Wang P, Zhu S, Yang L, et al. Nlrp6 regulates intestinal antiviral innate immunity. *Science*. 2015;350(6262):826-830. doi:10.1126/science.aab3145

132. Sarvestani ST, Cotton B, Fritzlar S, O'Donnell TB, Mackenzie JM. Norovirus Infection: Replication, Manipulation of Host, and Interaction with the Host Immune Response. *J Interf Cytokine Res*. 2016;36(4):215-225. doi:10.1089/jir.2015.0124

133. Zhu Z, Wang G, Yang F, et al. Foot-and-Mouth Disease Virus Viroporin 2B Antagonizes RIG-I-Mediated Antiviral Effects by Inhibition of Its Protein Expression. *J Virol*. 2016;90(24):11106-11121. doi:10.1128/JVI.01310-16

134. Li P, Zhang X, Cao W, et al. RIG-I is responsible for activation of type I interferon pathway in Seneca Valley virus-infected porcine cells to suppress

viral replication. *Virol J*. 2018;15(1):162. doi:10.1186/s12985-018-1080-x

135. Francisco E, Suthar M, Gale M, Rosenfeld AB, Racaniello VR. Cell-type specificity and functional redundancy of RIG-I-like receptors in innate immune sensing of Coxsackievirus B3 and encephalomyocarditis virus. *Virology*. 2019;528:7-18. doi:10.1016/j.virol.2018.12.003

136. Chhabra P, Ranjan P, Cromeans T, Sambhara S, Vinjé J. Critical role of RIG-I and MDA5 in early and late stages of Tulane virus infection. *J Gen Virol*. 2017;98(5):1016-1026. doi:10.1099/jgv.0.000769

137. Aarreberg LD, Esser-Nobis K, Driscoll C, Shuvarikov A, Roby JA, Gale M. Interleukin-1β Induces mtDNA Release to Activate Innate Immune Signaling via cGAS-STING. *Mol Cell*. 2019;74(4):801-815.e6. doi:10.1016/j.molcel.2019.02.038

138. Dubois H, Sorgeloos F, Sarvestani ST, et al. Nlrp3 inflammasome activation and Gasdermin D-driven pyroptosis are immunopathogenic upon gastrointestinal norovirus infection. Baldridge M, ed. *PLOS Pathog*. 2019;15(4):e1007709. doi:10.1371/journal.ppat.1007709

139. Ponterio E, Mariotti S, Tabolacci C, Ruggeri FM, Nisini R. Virus Like Particles of GII.4 norovirus bind Toll Like Receptors 2 and 5. *Immunol Lett*. May 2019. doi:10.1016/j.imlet.2019.05.016

140. Lee SM-Y, Yip T-F, Yan S, et al. Recognition of Double-Stranded RNA and Regulation of Interferon Pathway by Toll-Like Receptor 10. *Front Immunol*. 2018;9:516. doi:10.3389/fimmu.2018.00516

141. Khan M, Syed GH, Kim S-J, Siddiqui A. Hepatitis B Virus-Induced Parkin-

Dependent Recruitment of Linear Ubiquitin Assembly Complex (LUBAC) to Mitochondria and Attenuation of Innate Immunity. Feng P, ed. *PLoS Pathog*. 2016;12(6):e1005693. doi:10.1371/journal.ppat.1005693

142. Inn K-S, Gack MU, Tokunaga F, et al. Linear Ubiquitin Assembly Complex Negatively Regulates RIG-I- and TRIM25-Mediated Type I Interferon Induction. *Mol Cell*. 2011;41(3):354-365. doi:10.1016/j.molcel.2010.12.029

143. Chattopadhyay S, Kuzmanovic T, Zhang Y, Wetzel JL, Sen GC. Ubiquitination of the Transcription Factor IRF-3 Activates RIPA, the Apoptotic Pathway that Protects Mice from Viral Pathogenesis. *Immunity*. 2016;44(5):1151-1161. doi:10.1016/j.immuni.2016.04.009

144. Subba-Reddy C V, Goodfellow I, Kao CC. VPg-primed RNA synthesis of norovirus RNA-dependent RNA polymerases by using a novel cell-based assay. *J Virol*. 2011;85(24):13027-13037. doi:10.1128/JVI.06191-11

145. Hwang S, Alhatlani B, Arias A, et al. Murine norovirus: propagation, quantification, and genetic manipulation. *Curr Protoc Microbiol*. 2014;33:15K.2.1-61. doi:10.1002/9780471729259.mc15k02s33

146. Roth AN, Karst SM. Norovirus mechanisms of immune antagonism. *Curr Opin Virol*. 2015;16:24-30. doi:10.1016/j.coviro.2015.11.005

147. Kuyumcu-Martinez M, Belliot G, Sosnovtsev S V, Chang K-O, Green KY, Lloyd RE. Calicivirus 3C-like proteinase inhibits cellular translation by cleavage of poly(A)-binding protein. *J Virol*. 2004;78(15):8172-8182. doi:10.1128/JVI.78.15.8172-8182.2004

148. Chaudhry Y, Nayak A, Bordeleau M-E, et al. Caliciviruses Differ in Their

Functional Requirements for eIF4F Components. *J Biol Chem*. 2006;281(35):25315-25325. doi:10.1074/jbc.M602230200

149. Chung L, Bailey D, Leen EN, et al. Norovirus translation requires an interaction between the C Terminus of the genome-linked viral protein VPg and eukaryotic translation initiation factor 4G. *J Biol Chem*. 2014;289(31):21738-21750. doi:10.1074/jbc.M114.550657

150. Nice TJ, Strong DW, McCune BT, Pohl CS, Virgin HW. A Single-Amino-Acid Change in Murine Norovirus NS1/2 Is Sufficient for Colonic Tropism and Persistence. *J Virol*. 2013;87(1):327-334. doi:10.1128/JVI.01864-12

151. Borin BN, Tang W, Nice TJ, McCune BT, Virgin HW, Krezel AM. Murine norovirus protein NS1/2 aspartate to glutamate mutation, sufficient for persistence, reorients side chain of surface exposed tryptophan within a novel structured domain. *Proteins Struct Funct Bioinforma*. 2014;82(7):1200-1209. doi:10.1002/prot.24484

152. Nice TJ, Robinson BA, Van Winkle JA. The Role of Interferon in Persistent Viral Infection: Insights from Murine Norovirus. *Trends Microbiol*. 2018;26(6):510-524. doi:10.1016/j.tim.2017.10.010

153. Mahlakõiv T, Hernandez P, Gronke K, Diefenbach A, Staeheli P. Leukocyte-derived IFN-α/β and epithelial IFN-λ constitute a compartmentalized mucosal defense system that restricts enteric virus infections. Greenberg HB, ed. *PLoS Pathog*. 2015;11(4):e1004782. doi:10.1371/journal.ppat.1004782

154. Oh S-W, Onomoto K, Wakimoto M, et al. Leader-Containing Uncapped Viral Transcript Activates RIG-I in Antiviral Stress Granules. Weber F, ed. *PLOS Pathog*. 2016;12(2):e1005444. doi:10.1371/journal.ppat.1005444

155. Langereis MA, Feng Q, van Kuppeveld FJ. MDA5 localizes to stress granules, but this localization is not required for the induction of type I interferon. *J Virol*. 2013;87(11):6314-6325. doi:10.1128/JVI.03213-12

156. Poblete-Durán N, Prades-Pérez Y, Vera-Otarola J, Soto-Rifo R, Valiente-Echeverría F. Who Regulates Whom? An Overview of RNA Granules and Viral Infections. *Viruses*. 2016;8(7). doi:10.3390/v8070180

157. Liu X-Y, Wei B, Shi H-X, Shan Y-F, Wang C. Tom70 mediates activation of interferon regulatory factor 3 on mitochondria. *Cell Res*. 2010;20(9):994-1011. doi:10.1038/cr.2010.103

158. Wei B, Cui Y, Huang Y, et al. Tom70 Mediates Sendai Virus-Induced Apoptosis on Mitochondria. Sandri-Goldin RM, ed. *J Virol*. 2015;89(7):3804-3818. doi:10.1128/JVI.02959-14

159. Walther DM, Rapaport D. Biogenesis of mitochondrial outer membrane proteins. *Biochim Biophys Acta - Mol Cell Res*. 2009;1793(1):42-51. doi:10.1016/J.BBAMCR.2008.04.013

160. Stevens JL, Cantin GT, Wang G, Shevchenko A, Shevchenko A, Berk AJ. Transcription Control by E1A and MAP Kinase Pathway via Sur2 Mediator Subunit. *Science (80-)*. 2002;296(5568):755-758. doi:10.1126/science.1068943

161. Balamotis MA, Pennella MA, Stevens JL, Wasylyk B, Belmont AS, Berk AJ. Complexity in Transcription Control at the Activation Domain-Mediator Interface. *Sci Signal*. 2009;2(69):ra20-ra20. doi:10.1126/scisignal.1164302

162. Thorne L, Lu J, Chaudhry Y, Goodfellow I. miR-155 induction is a marker of

murine norovirus infection but does not contribute to control of replication in vivo. *Wellcome open Res*. 2018;3:42. doi:10.12688/wellcomeopenres.14188.1

163. Chaudhry Y, Skinner MA, Goodfellow IG. Recovery of genetically defined murine norovirus in tissue culture by using a fowlpox virus expressing T7 RNA polymerase. *J Gen Virol*. 2007;88(8):2091-2100. doi:10.1099/vir.0.82940-0

164. Yang X, Zhao M, Xia M, et al. Selective requirement for Mediator MED23 in Ras-active lung cancer. *Proc Natl Acad Sci*. 2012;109(41):E2813-E2822. doi:10.1073/pnas.1204311109

165. Yao X, Tang Z, Fu X, et al. The Mediator subunit MED23 couples H2B mono-ubiquitination to transcriptional control and cell fate determination. *EMBO J*. 2015;34(23):2885-2902. doi:10.15252/embj.201591279

166. Hierholzer J, Killington RA. Virus isolation and quantitation. In: Mahy BW, Kangro HO, eds. *Virology Methods Manual*. San Diego, Calif.: Academic Press; 1996:374. https://www.elsevier.com/books/virology-methods-manual/kangro/978-0-12-465330-6.

167. Suzuki K, Bose P, Leong-Quong RY, Fujita DJ, Riabowol K. REAP: A two minute cell fractionation method. *BMC Res Notes*. 2010;3(1):294. doi:10.1186/1756-0500-3-294

168. van Essen D, Engist B, Natoli G, Saccani S. Two modes of transcriptional activation at native promoters by NF-kappaB p65. Ashwell JD, ed. *PLoS Biol*. 2009;7(3):e73. doi:10.1371/journal.pbio.1000073

169. Freaney JE, Kim R, Mandhana R, Horvath CM. Extensive cooperation of

immune master regulators IRF3 and NFκB in RNA Pol II recruitment and pause release in human innate antiviral transcription. *Cell Rep*. 2013;4(5):959-973. doi:10.1016/j.celrep.2013.07.043

170. Lee H-C, Narayanan S, Park S-J, Seong S-Y, Hahn YS. Transcriptional regulation of IFN-λ genes in hepatitis C virus-infected hepatocytes via IRF-3·IRF-7·NF-κB complex. *J Biol Chem*. 2014;289(8):5310-5319. doi:10.1074/jbc.M113.536102

171. Atianand MK, Hu W, Satpathy AT, et al. A Long Noncoding RNA lincRNA-EPS Acts as a Transcriptional Brake to Restrain Inflammation. *Cell*. 2016;165(7):1672-1685. doi:10.1016/j.cell.2016.05.075

172. Livak KJ, Schmittgen TD. Analysis of relative gene expression data using real-time quantitative PCR and the 2(-Delta Delta C(T)) Method. *Methods*. 2001;25(4):402-408. doi:10.1006/meth.2001.1262

173. Petro TM. ERK-MAP-kinases differentially regulate expression of IL-23 p19 compared with p40 and IFN-β in Theiler's virus-infected RAW264.7 cells. *Immunol Lett*. 2005;97(1):47-53. doi:10.1016/j.imlet.2004.09.013

174. Zhang X, Edwards JP, Mosser DM. The expression of exogenous genes in macrophages: obstacles and opportunities. *Methods Mol Biol*. 2009;531:123-143. doi:10.1007/978-1-59745-396-7_9

175. Keller A-A, Maeß MB, Schnoor M, Scheiding B, Lorkowski S. Transfecting Macrophages. In: *Methods in Molecular Biology (Clifton, N.J.)*. Vol 1784. ; 2018:187-195. doi:10.1007/978-1-4939-7837-3_18

176. Burdette DL, Monroe KM, Sotelo-Troha K, et al. STING is a direct innate

immune sensor of cyclic di-GMP. *Nature*. 2011;478(7370):515-518. doi:10.1038/nature10429

177. Haag SM, Gulen MF, Reymond L, et al. Targeting STING with covalent small-molecule inhibitors. *Nature*. 2018;559(7713):269-273. doi:10.1038/s41586-018-0287-8

178. Liu S, Cai X, Wu J, et al. Phosphorylation of innate immune adaptor proteins MAVS, STING, and TRIF induces IRF3 activation. *Science*. 2015;347(6227):aaa2630. doi:10.1126/science.aaa2630

179. Dunphy G, Flannery SM, Almine JF, et al. Non-canonical Activation of the DNA Sensing Adaptor STING by ATM and IFI16 Mediates NF-κB Signaling after Nuclear DNA Damage. *Mol Cell*. 2018;71(5):745-760.e5. doi:10.1016/j.molcel.2018.07.034

180. Vincent J, Adura C, Gao P, et al. Small molecule inhibition of cGAS reduces interferon expression in primary macrophages from autoimmune mice. *Nat Commun*. 2017;8(1):750. doi:10.1038/s41467-017-00833-9

181. Zhou W, Whiteley AT, de Oliveira Mann CC, et al. Structure of the Human cGAS–DNA Complex Reveals Enhanced Control of Immune Surveillance. *Cell*. 2018;174(2):300-311.e11. doi:10.1016/j.cell.2018.06.026

182. Lau L, Gray EE, Brunette RL, Stetson DB. DNA tumor virus oncogenes antagonize the cGAS-STING DNA-sensing pathway. *Science (80-)*. 2015;350(6260):568-571. doi:10.1126/science.aab3291

183. Almine JF, O'Hare CAJ, Dunphy G, et al. IFI16 and cGAS cooperate in the activation of STING during DNA sensing in human keratinocytes. *Nat*

Commun. 2017;8:14392. doi:10.1038/ncomms14392

184. Jønsson KL, Laustsen A, Krapp C, et al. IFI16 is required for DNA sensing in human macrophages by promoting production and function of cGAMP. *Nat Commun*. 2017;8:14391. doi:10.1038/ncomms14391

185. Chunfa L, Xin S, Qiang L, et al. The Central Role of IFI204 in IFN-β Release and Autophagy Activation during Mycobacterium bovis Infection. *Front Cell Infect Microbiol*. 2017;7:169. doi:10.3389/fcimb.2017.00169

186. Lincez PJ, Shanina I, Horwitz MS. Reduced expression of the MDA5 Gene IFIH1 prevents autoimmune diabetes. *Diabetes*. 2015;64(6):2184-2193. doi:10.2337/db14-1223

187. Thomsen MK, Nandakumar R, Stadler D, et al. Lack of immunological DNA sensing in hepatocytes facilitates hepatitis B virus infection. *Hepatology*. 2016;64(3):746-759. doi:10.1002/hep.28685

188. Ding Q, Cao X, Lu J, et al. Hepatitis C virus NS4B blocks the interaction of STING and TBK1 to evade host innate immunity. *J Hepatol*. 2013;59(1):52-58. doi:10.1016/j.jhep.2013.03.019

189. Rehwinkel J, Tan CP, Goubau D, et al. RIG-I Detects Viral Genomic RNA during Negative-Strand RNA Virus Infection. *Cell*. 2010;140(3):397-408. doi:10.1016/j.cell.2010.01.020

190. Malathi K, Dong B, Gale M, Silverman RH. Small self-RNA generated by RNase L amplifies antiviral innate immunity. *Nature*. 2007;448(7155):816-819. doi:10.1038/nature06042

191. Samanta M, Iwakiri D, Kanda T, Imaizumi T, Takada K. EB virus-encoded

RNAs are recognized by RIG-I and activate signaling to induce type I IFN. *EMBO J*. 2006;25(18):4207-4214. doi:10.1038/sj.emboj.7601314

192. Plumet S, Herschke F, Bourhis J-M, Valentin H, Longhi S, Gerlier D. Cytosolic 5'-triphosphate ended viral leader transcript of measles virus as activator of the RIG I-mediated interferon response. *PLoS One*. 2007;2(3):e279. doi:10.1371/journal.pone.0000279

193. Nikonov A, Mölder T, Sikut R, et al. RIG-I and MDA-5 Detection of Viral RNA-dependent RNA Polymerase Activity Restricts Positive-Strand RNA Virus Replication. Sherry B, ed. *PLoS Pathog*. 2013;9(9):e1003610. doi:10.1371/journal.ppat.1003610

194. Maringer K, Fernandez-Sesma A. Message in a bottle: lessons learned from antagonism of STING signalling during RNA virus infection. *Cytokine Growth Factor Rev*. 2014;25(6):669-679. doi:10.1016/j.cytogfr.2014.08.004

195. Gaidt MM, Ebert TS, Chauhan D, et al. The DNA Inflammasome in Human Myeloid Cells Is Initiated by a STING-Cell Death Program Upstream of NLRP3. *Cell*. 2017;171(5):1110-1124.e18. doi:10.1016/j.cell.2017.09.039

196. Sullender ME, Baldridge MT. Norovirus interactions with the commensal microbiota. Condit RC, ed. *PLOS Pathog*. 2018;14(9):e1007183. doi:10.1371/journal.ppat.1007183

197. Zhong B, Yang Y, Li S, et al. The Adaptor Protein MITA Links Virus-Sensing Receptors to IRF3 Transcription Factor Activation. *Immunity*. 2008;29(4):538-550. doi:10.1016/j.immuni.2008.09.003

198. Nitta S, Sakamoto N, Nakagawa M, et al. Hepatitis C virus NS4B protein

targets STING and abrogates RIG-I-mediated type I interferon-dependent innate immunity. *Hepatology*. 2013;57(1):46-58. doi:10.1002/hep.26017

199. Li Y, Chen R, Zhou Q, et al. LSm14A is a processing body-associated sensor of viral nucleic acids that initiates cellular antiviral response in the early phase of viral infection. *Proc Natl Acad Sci*. 2012;109(29):11770-11775. doi:10.1073/pnas.1203405109

200. Sun L, Xing Y, Chen X, et al. Coronavirus papain-like proteases negatively regulate antiviral innate immune response through disruption of STING-mediated signaling. *PLoS One*. 2012;7(2):e30802. doi:10.1371/journal.pone.0030802

201. Berglund L, Björling E, Oksvold P, et al. A Genecentric Human Protein Atlas for Expression Profiles Based on Antibodies. *Mol Cell Proteomics*. 2008;7(10):2019-2027. doi:10.1074/mcp.R800013-MCP200

202. Cell atlas - MED23 - The Human Protein Atlas. https://www.proteinatlas.org/ENSG00000112282-MED23/cell. Accessed January 11, 2019.

203. Baker M. Reproducibility crisis: Blame it on the antibodies. *Nature*. 2015;521(7552):274-276. doi:10.1038/521274a

204. Bradbury A, Plückthun A. Reproducibility: Standardize antibodies used in research. *Nature*. 2015;518(7537):27-29. doi:10.1038/518027a

205. Bordeaux J, Welsh AW, Agarwal S, et al. Antibody validation. *Biotechniques*. 2010;48(3):197-209. doi:10.2144/000113382

206. Merika M, Thanos D. Enhanceosomes. *Curr Opin Genet Dev*.

2001;11(2):205-208. http://www.ncbi.nlm.nih.gov/pubmed/11250145. Accessed October 22, 2018.

207. Panne D, Maniatis T, Harrison SC. An Atomic Model of the Interferon-β Enhanceosome. *Cell*. 2007;129(6):1111-1123. doi:10.1016/j.cell.2007.05.019

208. Bourbon H-M. Comparative genomics supports a deep evolutionary origin for the large, four-module transcriptional mediator complex. *Nucleic Acids Res*. 2008;36(12):3993-4008. doi:10.1093/nar/gkn349

209. Conaway RC, Conaway JW. Origins and activity of the Mediator complex. *Semin Cell Dev Biol*. 2011;22(7):729-734. doi:10.1016/j.semcdb.2011.07.021

210. Lau JF, Nusinzon I, Burakov D, Freedman LP, Horvath CM. Role of metazoan mediator proteins in interferon-responsive transcription. *Mol Cell Biol*. 2003;23(2):620-628. http://www.ncbi.nlm.nih.gov/pubmed/12509459. Accessed September 22, 2018.

211. Ourthiague DR, Birnbaum H, Ortenlöf N, Vargas JD, Wollman R, Hoffmann A. Limited specificity of IRF3 and ISGF3 in the transcriptional innate-immune response to double-stranded RNA. *J Leukoc Biol*. 2015;98(1):119-128. doi:10.1189/jlb.4A1014-483RR

212. Andersen J, VanScoy S, Cheng T-F, Gomez D, Reich NC. IRF-3-dependent and augmented target genes during viral infection. *Genes Immun*. 2008;9(2):168-175. doi:10.1038/sj.gene.6364449

213. Grandvaux N, Servant MJ, TenOever B, et al. Transcriptional profiling of interferon regulatory factor 3 target genes: direct involvement in the regulation of interferon-stimulated genes. *J Virol*. 2002;76(11):5532-5539.

http://www.ncbi.nlm.nih.gov/pubmed/11991981. Accessed September 22, 2018.

214. Rossi A, Kontarakis Z, Gerri C, et al. Genetic compensation induced by deleterious mutations but not gene knockdowns. *Nature*. 2015;524(7564):230-233. doi:10.1038/nature14580

215. El-Brolosy MA, Stainier DYR. Genetic compensation: A phenomenon in search of mechanisms. Moens C, ed. *PLOS Genet*. 2017;13(7):e1006780. doi:10.1371/journal.pgen.1006780

216. Wu J, Chen ZJ. Innate Immune Sensing and Signaling of Cytosolic Nucleic Acids. *Annu Rev Immunol*. 2014;32(1):461-488. doi:10.1146/annurev-immunol-032713-120156

217. Kim TW, Kwon Y-J, Kim JM, Song Y-H, Kim SN, Kim Y-J. MED16 and MED23 of Mediator are coactivators of lipopolysaccharide- and heat-shock-induced transcriptional activators. *Proc Natl Acad Sci*. 2004;101(33):12153-12158. doi:10.1073/pnas.0401985101

218. Merkling SH, Overheul GJ, van Mierlo JT, Arends D, Gilissen C, van Rij RP. The heat shock response restricts virus infection in Drosophila. *Sci Rep*. 2015;5(1):12758. doi:10.1038/srep12758

219. Monté D, Clantin B, Dewitte F, et al. Crystal structure of human Mediator subunit MED23. *Nat Commun*. 2018;9(1):3389. doi:10.1038/s41467-018-05967-y